



# Durham E-Theses

---

## *Resonance production and decays*

Vlassopoulos, Spyridon Demetres

### How to cite:

---

Vlassopoulos, Spyridon Demetres (1974) *Resonance production and decays*, Durham theses, Durham University. Available at Durham E-Theses Online: <http://etheses.dur.ac.uk/8166/>

### Use policy

---

The full-text may be used and/or reproduced, and given to third parties in any format or medium, without prior permission or charge, for personal research or study, educational, or not-for-profit purposes provided that:

- a full bibliographic reference is made to the original source
- a [link](#) is made to the metadata record in Durham E-Theses
- the full-text is not changed in any way

The full-text must not be sold in any format or medium without the formal permission of the copyright holders.

Please consult the [full Durham E-Theses policy](#) for further details.

# RESONANCE PRODUCTION AND DECAYS

by

Spyridon Demetres P. Vlassopoulos

A thesis presented for the degree of  
Doctor of Philosophy  
of the University of Durham

July 1974

Mathematics Department,  
University of Durham, U.K.



# CONTENTS

	<u>Page</u>
PREFACE	
ABSTRACT	
CHAPTER I	INTRODUCTION
I-1	Physics Today 1
I-2	Strong Interactions 3
I-3	What is this Thesis about ? 8
CHAPTER II	CHARGE ASYMMETRY IN $\omega(\eta) \rightarrow \pi^+ \eta^- \eta^0$ DECAY
II-1	Introduction 12
II-2	The $\eta \rightarrow 3\pi$ decay and the Yuta-Okubo mechanism 15
II-3	Charge asymmetry in $\omega \rightarrow 3\pi$ decay 18
II-4	Model for $\omega$ -signal - background interference in $\eta^+ p \rightarrow \omega \Delta^+$ 24
CHAPTER III	THE $KN \rightarrow KN, K\Delta, K^*N$ PROCESSES
III-1	Introduction 46
III-2	The $KN \rightarrow K\Delta$ channel 48
III-3	Model for the $KN \rightarrow K^*N$ process 63
III-4	Simple model for elastic $K^*N \rightarrow KN$ scattering 81
III-5	Conclusions 86
CHAPTER IV	LOW ENERGY ISOSCALAR $KN$ SCATTERING
IV-1	Introduction 88
IV-2	Philosophy 93
IV-3	Model for the $K^*N \rightarrow K^*N$ channel 98
IV-4	Phase shifts 101
IV-5	An alternative unitarization technique 107
IV-6	Conclusions 109

	<u>Page</u>	
APPENDIX A	CHARGE ASYMMETRY AND THE YUTA-OKUBO FORMULA	111
APPENDIX B	PARTIAL WAVE ANALYSIS OF A $2 \rightarrow 3$ PROCESS AND INTERFERING $2 \rightarrow 4$ AMPLITUDES	115
APPENDIX C	CALCULATION OF SOME FEYNMAN DIAGRAMS	
C-1	Vector meson exchange in $0^{-\frac{1}{2}+} \rightarrow 0^{-\frac{3}{2}+}$	121
C-2	Pseudoscalar meson exchange in $0^{-}(1^{-})\frac{1}{2}^{+} \rightarrow 1^{-}\frac{1}{2}^{+}$	130
C-3	Vector meson exchange in $0^{-\frac{1}{2}+} \rightarrow 1^{-}\frac{1}{2}^{+}$	134
APPENDIX D	SOME USEFUL RELATIONS	
D-1	Dirac spinors	139
D-2	An identity	141
D-3	Isospin conservation in KN scattering	143
APPENDIX E	CROSSING RELATIONS AND PARTIAL WAVE AMPLITUDES FOR THE $KN \rightarrow K^*N$ AND $K^*N \rightarrow K^*N$ PROCESSES	146
APPENDIX F	NOTATION AND NORMALIZATION CONVENTIONS	153
REFERENCES		159

# PREFACE

Most of the work presented in this thesis was carried out in the Department of Mathematics, at the University of Durham, U.K. , during the period from October 1971 to June 1974 , under the supervision of Dr. R.C. Johnson. Some of the work (mainly computational) contained in chapter II was done at the Rutherford High Energy Laboratory, U.K. , during two short visits of the author in May and July 1972, and the financial support for those visits, by the Rutherford Laboratory, is gratefully acknowledged. Also, most of the work in chapter IV was done while the author was visiting CERN , Geneva , during the period from January to April 1974, and a partial financial support for this visit by the Department of Mathematics, University of Durham, U.K. , is gratefully acknowledged.

The material in this thesis has not been submitted for any other degree in this or any other University, and it is claimed to be original, except chapter I and where referenced. Chapter II is based on unpublished work by the author. Chapter III is based on a Durham preprint (May 1974) by the author. Chapter IV is based on a CERN preprint (TH-1861, April 1974) by the author in collaboration with R.C. Johnson, together with some unpublished material by the author.

I wish to express my sincere thanks to Dr. R.C. Johnson for his continuous guidance, patience and encouragement during all stages of the present work. Several discussions with Dr. G.A. Ringland concerning the work in chapter II are gratefully

acknowledged. I have also benefited from discussions with my colleagues A.B. Lahanas, D. Martin, D.M. Webber, and S.K.A.S. Yagoobi. Finally, I wish to thank Professor E.J. Squires for a critical reading of the manuscript, J.R. Havil, M.Sc. for carefully reading the manuscript and pointing out several spelling mistakes, and Miss Mary Sideris for her skilful typing of this thesis.

# ABSTRACT

This thesis deals with some phenomena connected with resonance production or formation, at low energies, and/or their subsequent decay. It is subdivided into two almost independent parts :

The first part (chapter II) is concerned with  $\omega/\eta$  production in  $\eta$ -N scattering and a possible charge asymmetry in their decay. We explicitly calculate the asymmetry for the reaction  $\eta^+ p \rightarrow \eta^+ \eta^- \eta^0 \Delta^{++}$  caused by interference of  $\omega$  production with uncorrelated  $3\eta$  production. Assuming C-invariance for the  $\omega$ -decay, we find that interference terms with a coherent  $3\eta$  background cannot explain the whole of the asymmetry experimentally observed.

The second part (chapters III and IV), deals with K-N scattering. In chapter III, examining the possible Lorentz-invariant, parity-conserving couplings of the t-channel exchanges to the external particles, and afterwards reggeizing them, we are able to construct simple models for the processes  $KN \rightarrow K\Delta$  and  $KN \rightarrow K^*N$ , which are capable of giving a satisfactory fit to the data over a wide range of energies. For completeness, a simple model for elastic KN scattering is also presented. In chapter IV we use the results of chapter III as input into a K-matrix machinery, from which we get a unitary isoscalar KN scattering model, analytically solvable, which reproduces several basic features of recent phase shift analyses, in particular a wide  $J^P = \frac{1}{2}^+$  exotic resonance  $Z_0^*$  (1780).

# CHAPTER I

## INTRODUCTION

### I-1 Physics Today.

Despite the number and the efforts of the present day physicists working on Elementary Particles, the abundance of published work, and the large amount of the experimental data becoming available every day, our theoretical understanding of this field of physics has been progressing rather slowly during the past, two decades. A few isolated successes should be mentioned, such as the invention of Regge parametrization, the discovery of  $SU(3)$  symmetry of strong interactions, and the construction of renormalizable unified Field Theories of weak and electromagnetic interactions. Nevertheless, the present state of affairs in Elementary Particle Physics is rather confusing, and no one can claim to have a clear understanding of the situation. Perhaps the most awkward point about our time (energy) Physics, is the belief in various, distinct, fundamentally different in nature interactions (strong, electromagnetic, weak, superweak, gravitational )\*

---

\* Had this thesis been written, say, two hundred years ago, this parenthesis could had been replaced by (electric, magnetic, gravitational).





between all the known particles. Hadrons (plenty of them) enjoy all of them, but leptons (which are only a few), are not allowed the luxury of strong interactions \*. There is also the photon, which has only electromagnetic interactions.

Although there is a total lack of any complete, unified theory of Elementary Particles, some fundamental principles and some general properties (exact or approximate), that such a theory - if existing - should enjoy have been realized (e.g. symmetries - conservation laws, asymptotic behaviours, e.t.c. ). The Theorist of our time, proceeds to make "models" of limited validity which obey such principles and have such properties, and by means of these models he tries to "understand" what is going on in the exciting world of Elementary Particles. He becomes temporarily happy when he thinks that his model may "explain" something (= may be a limiting or a special case of The Theory ); then some new data or new models may emerge which are in contradiction with his model, and he becomes sad. Whether we live in the eve of great revolutions, or we have reached the asymptotic abilities of the human mind - for its present biological age - remains to be seen.

---

\* But see also reference 43), and references therein, where the possibility that, at very high energies, leptons may exhibit "strong" interactions is discussed.

I-2 Strong Interactions.

In this work, we concentrate on the strong interaction, and we now outline very briefly some very basic concepts, which we shall rely upon ; for a full treatment of them, we refer to the standard textbooks (see, e.g. references 2),22),58),59),60) ). To start, we list a few established properties which the strong interaction is believed to obey :

- (1) Lorentz invariance.
- (2) Causality .
- (3) Unitarity (conservation of probability).
- (4) Analyticity (only singularities demanded by unitarity, are allowed to the scattering amplitude ) .
- (5) Crossing symmetry.
- (6) Conservation of charge.
- (7) SU(2) symmetry (exact in the absence of electromagnetism)
- (8) SU(3) symmetry (approximate)
- (9) S,B,L conservation (Strangeness, Baryon and Lepton number conservation )
- (10) P,C,T conservation.
- (11) Regge asymptotic behaviour.
- (12) Duality (very approximate).

The projection\* of any unified theory of microphysics onto what we now call strong interaction physics, should have these properties ; the more of them a present time "model" allows for, the nicer and more realistic it is thought to be.

---

\* This projection may be thought of either as a "low energy limit", or as a subgroup of a more general group, or ...

Although the Lagrangian Field Theory has proved to be the approach to electromagnetism, and a useful tool in treating weak interactions, the magnitude of the strong interaction coupling constant, does not allow any sort of simple perturbative approach to strong interaction physics. The S-matrix (Heisenberg) approach has proved much more fruitful as far as the strong interaction is concerned. Because of its short range, the probability for a strong transition from an initial state  $|i\rangle$  to a final state  $|f\rangle$ , may be written as :

$$S_{fi} = \langle f|S|i\rangle \quad (\text{I-1})$$

where the states  $|i\rangle$ ,  $|f\rangle$ , may be thought of, as being non-interacting. Conservation of probability requires the S-matrix to be unitary :

$$S^\dagger S = I = S S^\dagger \quad (\text{I-2})$$

Any conservation law may be built into the S-matrix which directly links theory with experiment.

It is customary to separate the probability amplitude for no interaction by defining the T-matrix :

$$S = I + iT \quad (\text{I-3})$$

which we relate to directly measurable quantities in Appendix F, where our kinematics and normalization conventions are defined. Mandelstam analyticity requires the T-matrix elements to have only isolated singularities in the form of poles or cuts, only where and when they are required by unitarity.

Unitarity and Analyticity, supplemented with crossing symmetry (Field Theory's substitution law) are the three most

fundamental principles reigning in strong interactions\*, which if combined together, lead to powerful links between theory and experimentally measurable quantities (e.g. Dispersion Relations) ; at one time they were even thought of as capable of providing the solution to Physics. They also lead to asymptotic bounds, such as the Froissart bound :

$$|T(t, z=1)| < \text{constant} \times t(\log t)^2 \quad \text{as } t \rightarrow \infty \quad (\text{I-4})$$

(z = cos  $\theta_t$ )

which cannot, obviously, be satisfied by any "elementary particle" exchange with spin  $\ell > 1$  :

$$T(s, z) = \beta \frac{P_\ell(z)}{m^2 - t} \quad (\text{I-5})$$

Regge Theory provides the way out of this difficulty : the amplitude is expressed in terms of its singularities in the complex  $\ell$ -plane. E.g. if only a pole in the position  $\ell = \alpha(t)$ , with signature  $\beta$  is allowed, we have :

$$T(s, z) = \beta(t) \frac{P_{\alpha(t)}(-z) + \beta P_{\alpha(t)}(z)}{2 \sin \pi \alpha(t)} \quad (\text{I-6})$$

As  $t$  varies, the pole moves on the trajectory  $\alpha(t)$  on the  $\ell$ -plane, and when it passes from any integral physical values of  $\ell$ , we have bound state poles. This idea (Mandelstam, Chew, Frautschi), originally produced and heavily used for  $2 \rightarrow 2$  reactions, has been employed for multihadron physics as well.

---

\* Of course, they are true in all physics ; but it is the strong interactions where they have proved to be so useful.



Hence, the easiest way to satisfy equation (I-7a) with the left hand side exactly zero, would be to require that

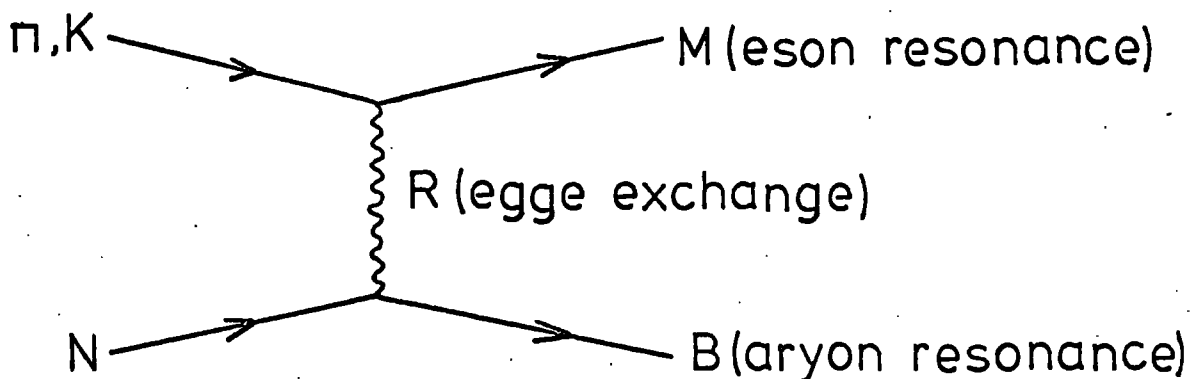
$$\alpha_p(t) = \alpha_{A_2}(t) \quad ; \quad \beta_p(t) = \beta_{A_2}(t) \quad (\text{I-9})$$

Veneziano has written down, an analytic expression for the  $2 \rightarrow 2$  amplitude, which obeys crossing symmetry, duality and Regge asymptotic behaviour at the same time. This idea is being made sophisticated to a large extent, in the ambitious Dual Resonance Models.

I-3 What is this Thesis about ?

There are one hundred and forty five entries in the latest particle tables <sup>64)</sup> of the Particle Data Group ( $\sim 55$  of them are mesonic and  $\sim 90$  baryonic ; there are also the leptons  $\gamma, \nu, e, \mu$ ). One hundred and thirty four of them decay strongly and they are called resonances. Although, theoretically, a resonance is defined as a pole in the unphysical  $s$  sheet, experimentally, it is recognised in formation as a counterclockwise loop in the Argand plot of a particular partial wave, or even more loosely as a bump in a total cross-section if it is not caused by apparently kinematical effects. In production, a resonance may be seen as a bump in the invariant mass plot of the particles in which it decays, but again, such bumps may be of kinematic origin.

In this thesis, dealing with low energy strong interaction phenomenology, we attempt to understand some awkward phenomena connected with resonance production and/or formation, and/or their decay, and/or resonances which are awkward themselves. The diagrams which we are going to play with, will be of the general form :



That is, our primitive underlying dynamics, responsible for scattering is the exchange of a certain object, and scattering occurs as a consequence of momentum conservation. As implied by this picture, we will find it convenient, most of the times, to parametrize our amplitudes in terms of Regge poles. But this description may correspond, approximately, via duality to s-channel resonance formation.

In the first part of this work (chapter II) we deal with the intriguing question of whether any charge asymmetry in the  $\omega$  or  $\eta$  decay Dalitz plot should be interpreted as a result of C-violation in substrong interactions. <sup>8)</sup> These resonances are produced in  $\pi$ -N interactions, and interference with coherent production of their decay products may be responsible for some charge asymmetry <sup>11)</sup>; but how much? We make a simple explicit model to calculate the  $\omega \rightarrow \pi^+ \pi^- \pi^0$  charge asymmetry ( $\omega$  produced in  $\eta N \rightarrow \omega \Delta$ ) caused by interference of the  $\omega$ -signal with uncorrelated  $3\pi$  background, produced coherently under the  $\omega$ -signal. We start with a very simple Regge model for  $\omega$  production via  $\eta^+ p \rightarrow \omega \Delta^{++}$ ; and for the  $\omega \rightarrow \pi^+ \pi^- \pi^0$  decay we employ the standard C-invariant amplitude <sup>28)</sup>; we then calculate our principal background amplitudes in terms of an equally simple Regge model for  $\pi N \rightarrow \pi \Delta$ , and the known  $\pi\pi$  phase shifts <sup>30)</sup>. We are always careful about the phases of our amplitudes, since they are so important as far as interference terms are concerned. In all cases, we come to the conclusion that the signal - background interference mechanism, although capable of producing asymmetry of the correct sign, it cannot quantitatively account for the whole of the asymmetry experimentally <sup>14), 15)</sup>



observed. But before being tempted to look for any exotic explanations of the excess asymmetry, we are of the opinion that we should await for more accurate experimental data (high statistics experiments <sup>10)</sup> in  $\pi N \rightarrow \eta N'$  did not confirm a substantial charge asymmetry in  $\eta \rightarrow \pi^+ \pi^- \pi^0$  which had been found earlier <sup>9)</sup> ).

In chapter III we turn to K-N scattering ; we make high energy models for  $KN \rightarrow K\Delta$  and  $KN \rightarrow K^*N$ , that is, the dominant inelastic channels in low energy KN scattering. We start with elementary t-channel exchanges, and write down the amplitudes which are allowed to be non-zero by our Lagrangians, obtaining information about their residue structure. We then alter our dynamics, replacing the Feynman propagator by the Regge propagator. Thus, we succeed in having a concise picture of the exchanges which are important in each amplitude and our work in chapter IV is greatly facilitated. Despite their simplicity, the success of our models, in fitting the dif. cross-sections and production density matrix elements <sup>40) \rightarrow 42), 45) \rightarrow 51)</sup> over a wide range of energies, is remarkable <sup>32)</sup>. We also make a very simple, purely phenomenological model for KN elastic scattering ( $P$ -dominated). Its main use is to show quantitatively that the non-diffractive, elastic KN amplitudes are very small compared with the  $\pi$ -exchange amplitude in  $KN \rightarrow K^*N$ , as well as the vector and tensor meson exchange amplitudes in  $KN \rightarrow K^*N$ , for the  $I = 0$  channel. This fact, greatly simplifies our approach in chapter IV, where we input these purely non-diffractive pole amplitudes, after extrapolation to very low energy, crossing into the s-channel, and partial wave projection, into a K-matrix model <sup>74)</sup>. Amplitudes for the awkward channel  $K^*N \rightarrow K^*N$  are also required, which we are able to model,

via SU(6), in terms of those for  $KN \rightarrow K^*N$ . We get out a unitary, corrected for cuts, mainly diffractive isoscalar KN scattering model <sup>62)</sup>, which despite its simplicity (it is analytically solvable), can account for the qualitative features of the favoured solutions of a recent BGRT, I = 0 KN phase shift analysis <sup>70)</sup>; in particular, it contains a  $Z_0^*$  (1780) "exotic" resonance <sup>63),64)</sup> with  $J^P = \frac{1}{2}^+$ , and it strongly favours negative  $S_{\frac{1}{2}}$  and  $P_{\frac{3}{2}}$  scattering lengths. Although we had assumed exact duality and strong exchange degeneracy - at the input level - we got output t-channel structure, which should be considered to be dual, via unitarity, to  $\pi$ -exchange in  $KN \rightarrow K^*N$ .

## CHAPTER II

### CHARGE ASYMMETRY IN $\omega(\eta) \rightarrow \eta^+ \eta^- \pi^0$ DECAY .

#### II-1 Introduction

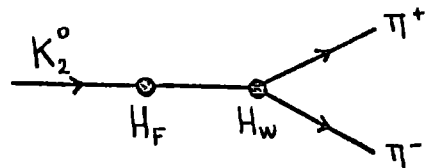
The measurement <sup>1)</sup>  $\Gamma(K_2^0 \rightarrow \eta^+ \eta^-) / \Gamma(K_1^0 \rightarrow \eta^+ \eta^-) \simeq 10^{-6} \neq 0$  reveals an apparent CP non-conservation in  $K \rightarrow 2\eta$  decays. This is because the system  $\eta^+ \eta^-$  has a definite CP, and since out of the  $K^0, \bar{K}^0$  we can construct the two  $K_1^0, K_2^0$  with  $CP = \pm 1$ , then, both decays  $K_2^0 \rightarrow \eta^+ \eta^-$  and  $K_1^0 \rightarrow \eta^+ \eta^-$ , cannot simultaneously conserve CP. Conventionally, we assign  $CP = +1$  to  $\eta^+ \eta^-$  s-state,  $CP = +1$  to  $K_1^0$ , and  $CP = -1$  to  $K_2^0$ , so,  $K_2^0 \rightarrow \eta^+ \eta^-$  is the CP non-conserving decay (reference 2), page 117 ).

If one insists on considering CP conservation as part of the definition of the weak Hamiltonian  $H_W$ , then, one is led to the conclusion that  $K_2^0 \rightarrow \eta^+ \eta^-$  is due to the possible existence <sup>3),4)</sup> of a new, CP non-invariant, interaction  $H_F$ , the strength of which depends <sup>3)</sup> on its behaviour with respect to strangeness. If  $H_F$  is assumed to conserve strangeness, then, for the coupling constants (c.c.) it is estimated <sup>3)</sup>  $g_F \sim 10^3 g_W$  (or  $m^2 g_F \sim 10^{-2}$ , the dimensionless c.c. ) ; if only  $|\Delta S| = 1$  is allowed,

then  $g_F \sim 10^{-2} g_W - 10^{-3} g_W$ , while if  $|\Delta S| = 2$  is allowed as well,

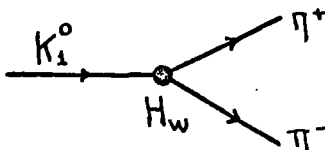
then  $g_F \sim 10^{-9} g_W$ . The usual weak Hamiltonian  $H_W$  violates C and P, but it is invariant under T and CP, while  $H_F$  would violate C and T but be invariant under CT and P. Now,  $K_2^0 \rightarrow \pi^+ \pi^-$  can

proceed via the second order term  $H_W H_F$  :



and so it is much slower than  $K_1^0 \rightarrow \pi^+ \pi^-$  which proceeds via

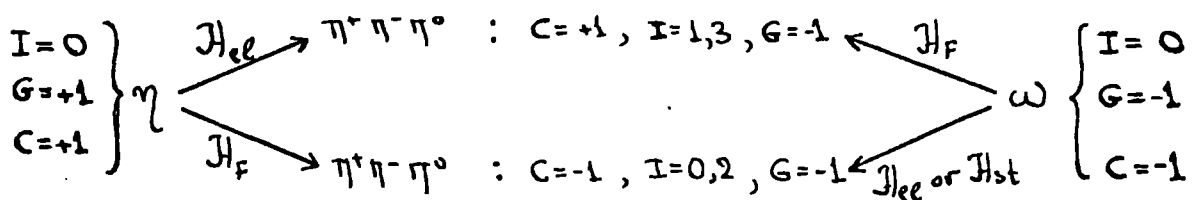
$H_W$  alone :



. It is also remarked 5)

that, since the electromagnetic Hamiltonian of the strongly interacting particles may violate C and T, this "new" interaction  $H_F$ , might be of electromagnetic origin, entering as a second order effect, in agreement with the estimation  $m_p^2 g_F \sim 10^{-2}$ , being of the order of the fine structure constant.

The decays  $\eta \rightarrow \pi^+ \pi^- \pi^0$  and  $\omega \rightarrow \pi^+ \pi^- \pi^0$  (also  $\rho \rightarrow \pi^+ \pi^- \pi^0$  via  $\rho - \omega$  interference 6), see below) would provide a nice test 7), 8) of the existence of such a relatively strong C non-invariant interaction. We can have the transitions :  
( a neutral  $3\pi$  state with isospin I, has  $C = -(-1)^I$  )



So, the interference between the  $C = +1$  and  $C = -1$  amplitudes,

could possibly result in an asymmetry in the energy distribution of  $\eta^+$  and  $\eta^-$ . The detection of such an asymmetry would be an absolute proof of C non-invariance in  $\omega$  or  $\eta$  decay. Lee (in reference 8) ) gives the direct experimental implications, on the Dalitz plot of such a C violation. Also, according to the change in isospin  $H_F$  can do (  $|\Delta I| = 0, 2$  or  $|\Delta I| = 1, 3$  ) it will be present in  $\eta$  decay,  $\omega$  decay, or in both.

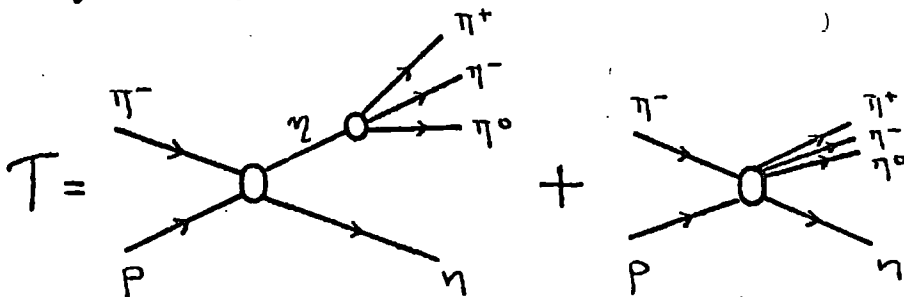
II-2 The  $\eta \rightarrow 3\pi$  decay and the Yuta-Okubo mechanism

Numerous experiments have been performed (exhaustive lists may be found in references 11) and 13) ), to detect any asymmetry in the  $\eta \rightarrow \pi^+ \pi^- \pi^0$  decay. From the analysis in reference 8), one expects the  $\Delta I = 0$  piece of the C-violating transition to the  $J^{PC} = 0^{--} \pi^+ \pi^- \pi^0$  final state, to produce a sextant asymmetry on the Dalitz plot, while its  $\Delta I = 2$  piece to lead to a charge asymmetry. But since the  $\Delta I = 0$  transition is considerably suppressed <sup>8)</sup> by angular momentum-like barrier factors, an  $\eta$ -decay asymmetry study is primarily a probe for the  $\Delta I = 2$  C-violating transition.

The experimental situation is somewhat controversial. For example, some time ago, Gormley et. al. <sup>9)</sup> found evidence for a charge asymmetry,  $\alpha = (1.5 \pm 0.5)\%$  (for the definition of the charge asymmetry and other relevant quantities, see Appendix A ), and no evidence for sextant asymmetry ( $0.5 \pm 0.5\%$ ) in  $\eta \rightarrow \pi^+ \pi^- \pi^0$  decay with  $\eta$ 's produced in the reaction  $\pi^- p \rightarrow \eta n$  ( $p_L = 0.72$  GeV/c , 36,800  $\eta$ 's ), in line with the expectations from the previous section. On the other hand, more recently, Jane et. al. <sup>10)</sup> in a high statistics experiment with  $\eta$ 's from the same reaction, ( $p_L = 0.718$  GeV/c, 165311  $\eta$ 's) found no evidence for either charge ( $\alpha = 0.28 \pm 0.26\%$ ), or sextant ( $0.2 \pm 0.25\%$ ) asymmetries.

Even if we believe that some charge asymmetry is experimentally possible, it is not straightforward to conclude

that it is directly associated with C-violation in the  $\eta \rightarrow \pi^+ \pi^- \pi^0$  decay. Since we cannot have  $\eta$ 's available independently of a certain production mechanism, Yuta and Okubo<sup>11)</sup> suggested that the charge asymmetry, if any, observed in their decay, might be caused by interference between  $\eta$  production and subsequent decay, with some  $3\pi$  background, coherently added to the  $\eta$  signal. They write :

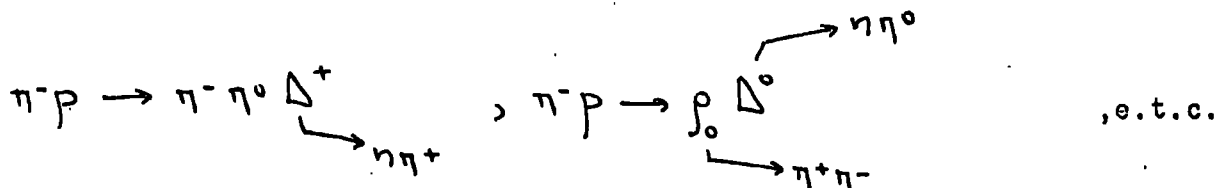


and find ( for a quick derivation of the Yuta-Okubo formula see Appendix A ), that the upper limit of the asymmetry which may be produced via this mechanism is :

$$\alpha_{max} = \left[ \frac{2\eta \Gamma_{\eta}}{\Delta m_{\eta}} \frac{\sigma_B}{\sigma_{\eta}} \right]^{1/2} \quad (A-12)$$

where  $\Gamma_{\eta}$  ( $\Delta m_{\eta}$ ) is the intrinsic (experimental) width of the  $\eta$ , and  $\sigma_B$  ( $\sigma_{\eta}$ ) is the cross-section associated with the background ( $\eta$ -signal). To get the upper limit (A-12), two assumptions are made (see Appendix A) about the background, namely that all of it is in a (i)  $J^{PC} = 0^{--}$ , (ii) charge asymmetric state. If this is the mechanism responsible for any charge asymmetry in  $\eta$ -decay, this asymmetry should presumably vary with energy, and should depend upon the production mechanism; so, if it persists as we vary the energy and change the production mechanism,

then one could start talking about possible C-violation. Possible background mechanisms would be :



Note, that it is possible to have small asymmetry in the background, as it is experimentally observed <sup>9)</sup>, and at the same time, most of it being in a charge asymmetric state (see Appendix A ).

Applying (A-12) for the  $\eta$  parameters (  $\Gamma_\eta \simeq 4$  KeV,  $\Delta m_\eta \simeq 10$  MeV ,  $\sigma_B/\sigma_\eta \simeq 1/10$  ) we get  $\alpha_{\max} \simeq 1.6$  % , so it would seem possible to explain some charge asymmetry in  $\eta \rightarrow \eta^+ \eta^- \eta^0$  decay via the Yuta-Okubo mechanism. But of course, what we have estimated here, is the maximum allowed asymmetry, and the assumptions (i) and (ii) which we made above in order to derive (A-12), are very difficult to accept without further discussion. In fact, Gormley et al <sup>12)</sup> parametrizing the background in a consistent with their experiment way, find no more than  $\alpha_{\max} = 0.23$  % asymmetry being possible by the Yuta-Okubo mechanism. On the other hand, Taggart <sup>13)</sup> does a simple, explicit calculation, taking into account the most important charge asymmetric and charge symmetric background diagrams, and finds no more than  $\alpha_{\max} \simeq 10^{-3}$  % .

To conclude this short review, the present situation with the  $\eta \rightarrow \eta^+ \eta^- \eta^0$  decay is that interference of the  $\eta$ -signal with a coherently added background can only explain a very small charge asymmetry (of the same sign as it had been experimentally observed <sup>9)</sup> some time ago ) , but the most recent experimental results <sup>10)</sup> are consistent with no asymmetry in this decay.



II-3 Charge asymmetry in  $\omega \rightarrow 3\pi$  decay.

The decay  $\omega \rightarrow \pi^+ \pi^- \pi^0$  is tested <sup>14), 15)</sup> with about 4000  $\omega$ 's, from the reaction  $\pi^+ p \rightarrow \omega \pi^+ p$  at 3.7 GeV/c. A significant charge asymmetry,  $\alpha = 18 \pm 5\%$ , is observed in the  $\omega$  Dalitz plot for the channel  $\pi^+ p \rightarrow \omega \Delta^{++}$  (see figure II-1, from reference <sup>14)</sup>). This large effect is localized in  $t'$  ( $t' = |t - t_{\min}|$ , where  $t$  is the momentum transfer for  $p$  to  $\Delta$ ), being most prominent for  $0.08 \leq t' \leq 0.20 \text{ GeV}^2$ ; outside this region, the asymmetry is consistent with zero (see fig. II-2, from reference <sup>14)</sup>). The asymmetry is observed strictly on the  $\omega$  signal and not in the background (see fig. II-3, from ref. <sup>14)</sup>). Note, that in a previous experiment <sup>16)</sup>, with 4,200  $\omega$ 's from  $K^- p \rightarrow \omega \Lambda$ , no evidence for charge asymmetry in the  $\omega \rightarrow \pi^+ \pi^- \pi^0$  decay had been found.

As analysed by Abrams, Goldhaber, and Hall <sup>17)</sup> the observation of a charge asymmetry on the  $\omega$ -Dalitz plot provides unambiguous evidence for the presence, in the region of  $\omega$ -mass, of a coherent  $3\pi$  production amplitude with  $I^G = 1^-$  and  $J^{PC} = 1^{-+}$  (see also Appendix B for an explicit proof that this coherent amplitude should necessarily have  $J^P = 1^-$ , if it is going to interfere with  $\omega$  production). At least four different possible dynamical interpretations of this interfering amplitude have been suggested <sup>14), 15), 17), 18)</sup>:

(1) The  $\Delta I = 1$ , C-violating decay of  $\omega$  <sup>8)</sup>, as discussed in section II-1. But this mechanism may be ruled out, since it would presumably affect all  $\omega$  events, rather than a restricted subsample,

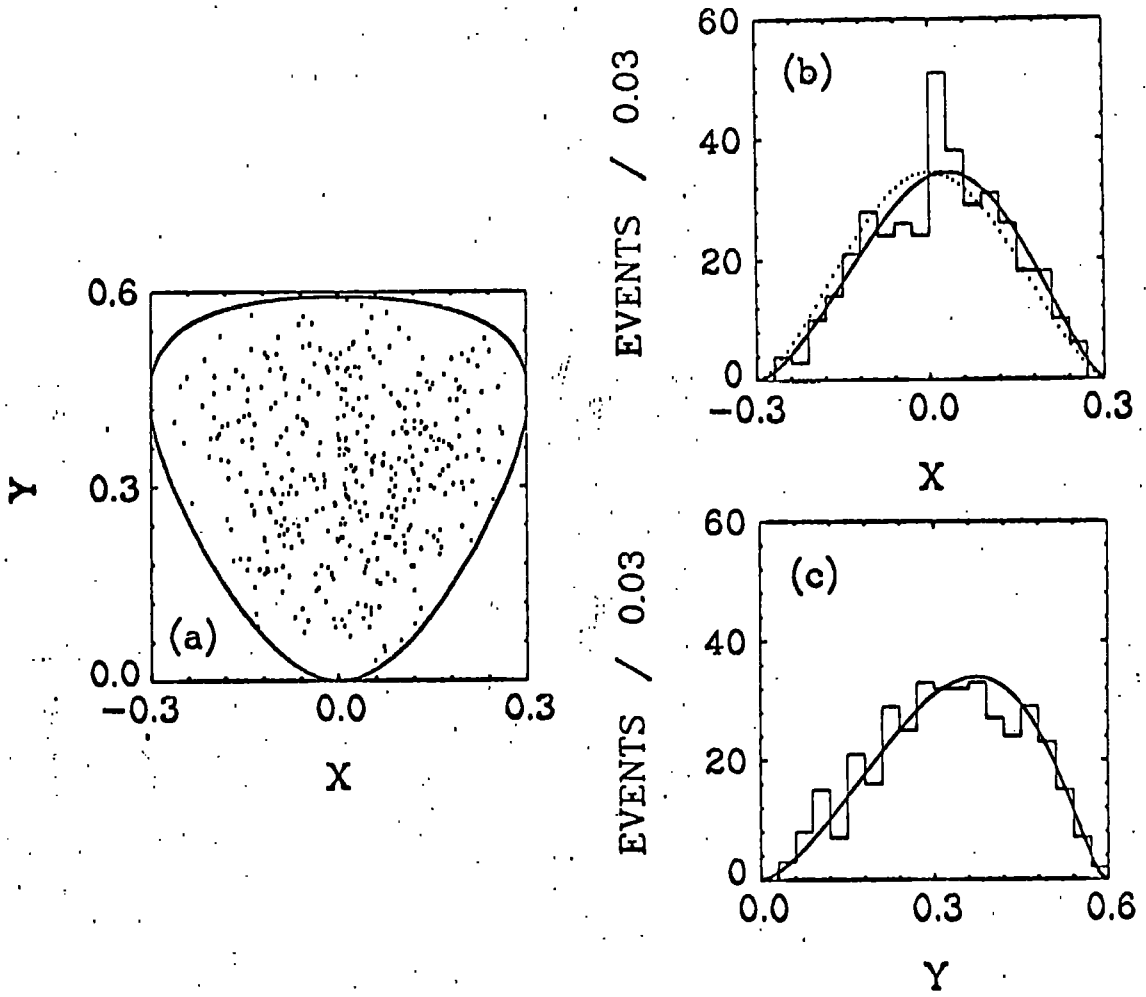


FIG. II-1 From reference 14).

Decay Dalitz-plot for 380  $\omega \rightarrow \pi^+ \pi^- \pi^0$  events  
with  $0.08 \leq t \leq 0.20 \text{ GeV}^2$  :

(a) Two-dimensional distribution.

(b) x-distribution ;  $x = (T_+ - T_-) / Q\sqrt{3}$

(c) y-distribution ;  $y = T_0 / Q$

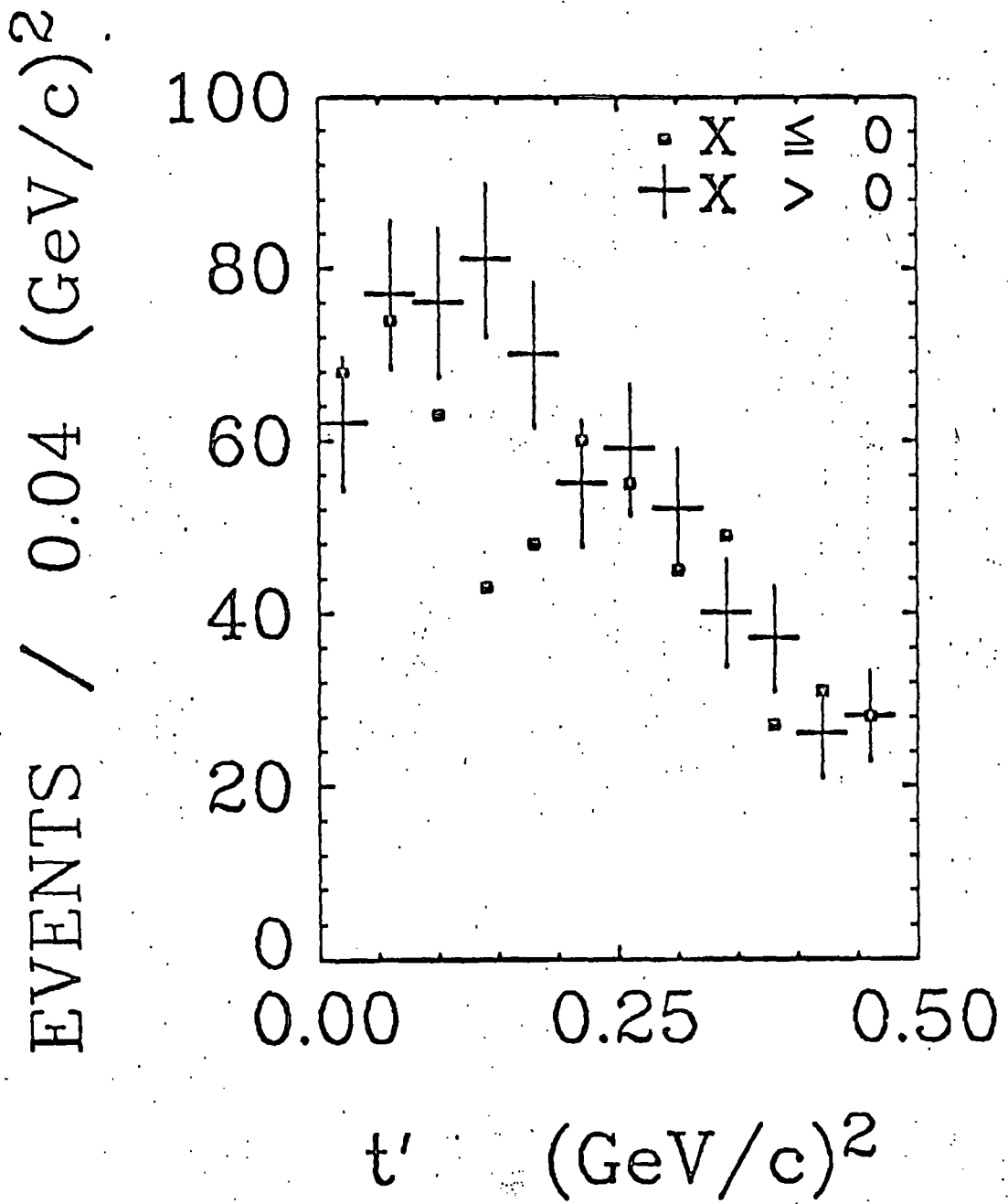


FIG. II-2 From reference 14).  
Production angular distribution for each half  
of the  $\omega$  Dalitz-plot.

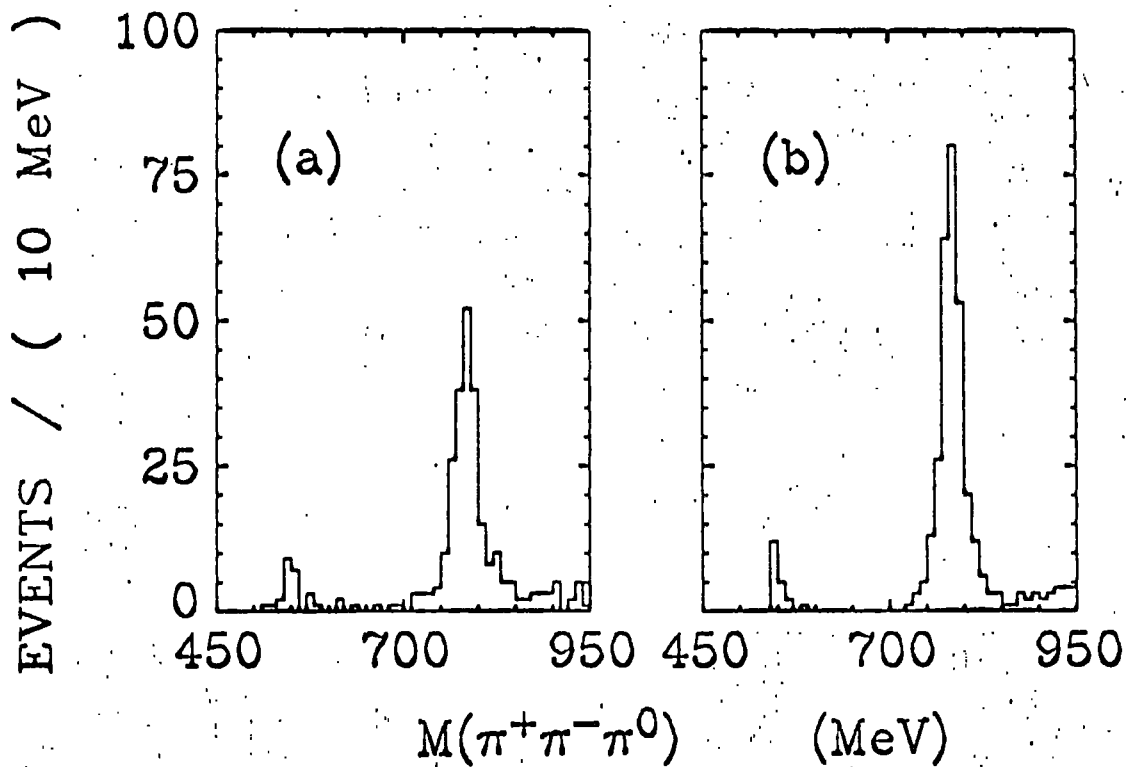


FIG. II-3 From reference 14).  
Distribution of the  $\pi^+\pi^-\pi^0$  effective mass near the  $\omega$  region  
for events with  $0.08 \leq t \leq 0.20 \text{ GeV}^2$ .  
(a)  $x \leq 0$  ; (b)  $x > 0$  .

as observed.

(ii) The  $\Delta I = 0$  decay of the  $\rho^0$ , produced coherently with the  $\omega$  (C-violation in electromagnetic interactions <sup>5)</sup>, as briefly mentioned in section II-1 ); but notice that the  $t'$  region in which the asymmetry is observed, does not completely overlap with the region  $0 \leq t' \leq 0.14 \text{ GeV}^2$ , of the known  $\rho - \omega$  coherence <sup>6),19)</sup>

(iii) A Yuta-Okubo interference mechanism, of the type examined in the previous section.

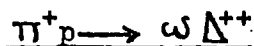
(iv) A possible exotic resonance,  $\tilde{\rho}$ , with  $I^G = 1^-$ ,  $J^{PC} = 1^{-+}$  and mass near the mass of the  $\omega$ .

In the remainder of this chapter, we concentrate on mechanism (iii) (for a discussion of (ii) and (iv) see e.g. reference 18) ); applying (A-12) for the  $\omega$  parameters (  $\Gamma_\omega \approx 12 \text{ MeV}$ ,  $\Delta m_\omega \approx 100 \text{ MeV}$ ,  $\sigma_B / \sigma_\omega \approx 1/20$  ), we get  $\alpha_{\text{max}} \approx 20\%$  ! But some care is required at this point : Apart from the fact that the Yuta-Okubo formula is a worse approximation for the  $\omega \rightarrow 3\pi$  decay ( $\omega$  is much broader than the  $\eta$  ), putting  $\sin \phi \approx 1$  in (A-8) is not justified . Because, as discussed in Appendix A,  $\sin \phi$  essentially measures the mean strength of the interference between the charge asymmetric part of the background and the resonance production amplitude. Even if the whole of the background is in a charge asymmetric state, only that part of it which is in an  $J^P = 1^-$  state is going to interfere with  $\omega$  production (see Appendix B ) to give asymmetry, if any . But the lowest  $3\pi$   $1^-$  state has two pions in a  $J^P = 1^-$  state, and the third, with a relative ang. momentum 1, with respect to them (see Appendix B, table B-1 ) so it is rather unlikely that this high ang. momentum configuration will contribute significantly at such

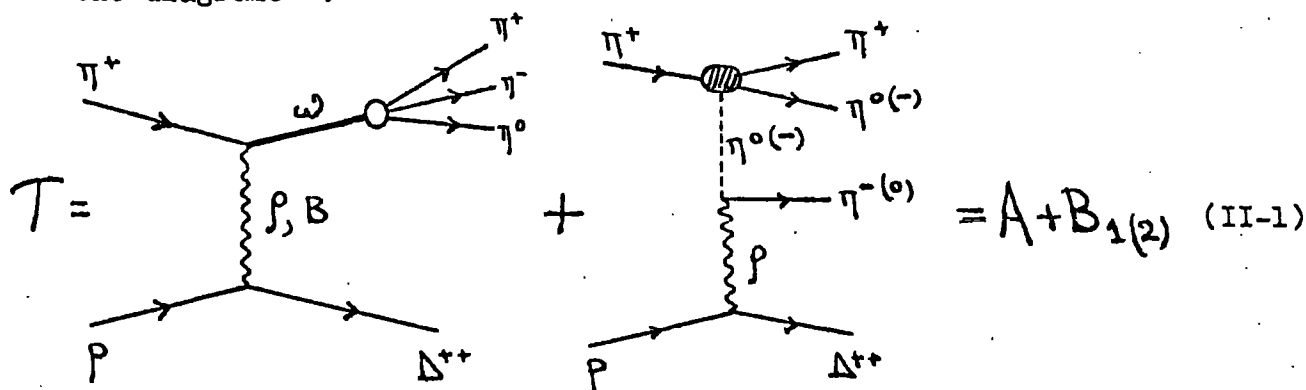
low energies as the mass of the  $\omega$  <sup>20)</sup> (unless the exotic  $\tilde{\rho}$  particle exists, as mentioned above ).

In view of the above argument, it is not straightforward to draw any definite conclusions from the Yuta-Okubo formula (A-12), as it stands. In the following section we proceed to make an explicit simple model for  $\omega$  -production and background, contributing to  $\pi^+ p \rightarrow \eta^+ \eta^- \eta^0 \Delta^{++}$ , and calculate the charge asymmetry which may arise by a Yuta-Okubo type mechanism.

II-4 Model for  $\omega$ -signal - background interference in



As first suggested by Berger in 14), we coherently add the diagrams :



the first of which represents peripheral production of  $\omega$  via  $\rho$  and B exchanges (which subsequently decays into  $\pi^+ \pi^- \pi^0$ ), while the second is the assumed principal background mechanism, the blob representing the full  $\pi - \pi$  scattering amplitude, while in its lower part we have  $\pi p \rightarrow \pi \Delta^{++}$  scattering, which goes via  $\rho$  exchange. The  $3\pi$  system in  $B_{1(2)}$  may, of course, be found in any  $J^P$  state, but by calculating integrals of the form e.g.

$$\int dF_{\{x,y\}} |T|^2 \equiv \frac{d^2\sigma}{dx dy} \quad (\text{II-2})$$

we leave the  $\omega$  production amplitude to choose that piece of the background it wants to interfere with. In figure II-4 we plot the dif. cross-section for  $\pi^+ p \rightarrow \omega \Delta^{++}$  at 3.7 GeV/c<sup>24)</sup> (a) and  $\pi^+ p \rightarrow \pi^0 \Delta^{++}$  at 3.84 GeV/c<sup>25)</sup> (b), together with their geometrical mean (c). Looking at this figure one could hope to explain, with diagrams (II-1), even the  $t'$ -dependence of the asymmetry in

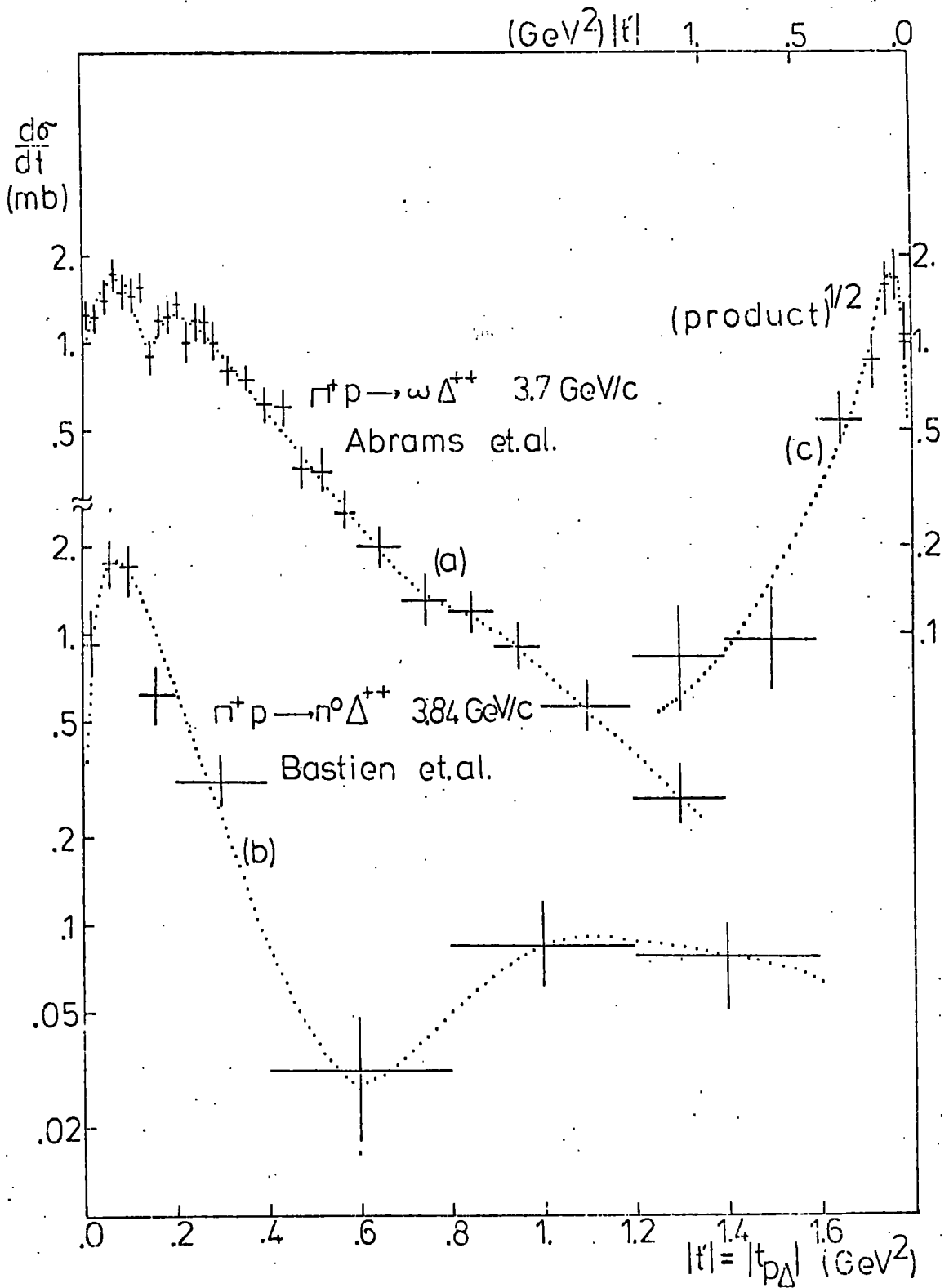


FIG. II-4 Dif. cross-section for  $\pi^+ p \rightarrow \omega \Delta^{++}$ , at 3.7 GeV/c (a), for  $\pi^+ p \rightarrow \pi^0 \Delta^{++}$ , at 3.84 GeV/c (b), together with their geometrical mean (c); dotted curves to guide the eye.



the experiment by Abrams et. al. <sup>15)</sup>, discussed in the previous section, although the  $t'$  interval in which the said geometrical mean is largest does not completely coincide with the region of maximum charge asymmetry ( $0.08 \leq t' \leq 0.20 \text{ GeV}^2$ ). We now discuss in some detail every separate piece of our diagrams A and  $B_1(2)$  :

The  $\pi^+ p \rightarrow \omega \Delta^{++}$  process.

For the  $t$ -channel centre of mass ( $t$ -CM) helicity amplitudes we write (we label the helicities with the name of the corresponding particle) :

$$\widehat{\Omega}_{p\omega\Delta} = \beta_{p\omega\Delta}^p \rho_{p\omega\Delta}^p \left(\frac{s}{s_0}\right)^{\alpha_p(t)} + \beta_{p\omega\Delta}^B \rho_{p\omega\Delta}^B \left(\frac{s}{s_0}\right)^{\alpha_B(t)} \quad (\text{II-3})$$

where :

$$\rho_{p,B}^p(t) = -1 + e^{-i\pi\alpha_{p,B}(t)} \quad (\text{II-4})$$

the  $\rho, B$  signature factors, and for the Regge trajectories we have, approximately :

$$\alpha_p(t) \approx \frac{1}{2} + t, \quad \alpha_B(t) \approx t \quad (\text{II-5})$$

The residues  $\beta_{p\omega\Delta}^{p,B}(t)$  are smooth functions of  $t$ ; assuming that

we are at energies asymptotic enough, so that the separation of t-channel helicity amplitudes into natural/unnatural parity exchange pieces <sup>26)</sup> may be justified, we can have some information about them by looking at the  $\omega$  decay density matrix elements, in the Jackson frame, at 3.7 GeV/c <sup>24)</sup> :

We have  $\beta_{p_0\Delta}^{\rho}(t) \approx 0$  (identically),  $\beta_{p_0\Delta}^B(t) \neq 0$  (a large  $\rho_{00}$ ) and  $\langle \beta_{p_1\Delta}^{\rho}(t) \rangle \approx \langle \beta_{p_1\Delta}^B(t) \rangle$  (since  $\langle \rho_{11} + \rho_{1-1} \rangle \approx \langle \rho_{11} - \rho_{1-1} \rangle$ ), <sup>26)</sup>

where the residues are averaged over t and the p,  $\Delta$  helicities. Let  $R_{p'\omega'\Delta'; p\omega\Delta}$  be the overall rotation-crossing matrix <sup>22)</sup> from t-CM to the s-channel  $\omega$  rest frame; then, the amplitudes we need, will be : ( see (F-9))

$$\begin{aligned} \Omega_{p'\omega'\Delta'} &= \sum_{p,\omega,\Delta} R_{p'\omega'\Delta'; p\omega\Delta} \widehat{\Sigma}_{p\omega\Delta} = \\ &= \gamma_{p'\omega'\Delta'}^{\rho}(t) \mathcal{F}^{\rho}(t) \left(\frac{s}{s_0}\right)^{\alpha_{\rho}(t)} + \gamma_{p'\omega'\Delta'}^B(t) \mathcal{F}^B(t) \left(\frac{s}{s_0}\right)^{\alpha_B(t)} \end{aligned} \quad (\text{II-6})$$

where

$$\gamma_{p'\omega'\Delta'}^{S,B}(t) = \sum_{p,\omega,\Delta} R_{p'\omega'\Delta'; p\omega\Delta} \beta_{p\omega\Delta}^{S,B}(t) \quad (\text{II-7})$$

will again be smooth functions of t (R depends on t only as  $s \rightarrow \infty$ )  
The elements of R are complicated functions of t; but remembering that at least five variables ( out of eight ) will eventually be integrated over (see II-2), we require only a "mean" description of the processes involved and put :

$$\Omega_{p'\omega'\Delta'} \Rightarrow \langle \Omega \rangle = \langle \gamma^P \rangle \beta_{(t)}^P \left( \frac{s}{s_0} \right)^{\alpha_P(t)} + \langle \gamma^B \rangle \beta_{(t)}^B \left( \frac{s}{s_0} \right)^{\alpha_B(t)} \quad (\text{II-8})$$

where we have assumed that all  $\omega$  helicity states are produced with equal probability in its rest frame (from the s-channel reaction  $\pi^+ p \rightarrow \omega \Delta^{++}$ ), and the average of the residues is taken over both  $t$ , and helicities. The crucial point, as far as interference terms are concerned is that, at high energies, the Regge phases are independent of the helicities of the particles involved. In view of these arguments, it would be superficial to start with a many-parameter good fit for  $\widehat{\Omega}_{p\omega\Delta}$  in (II-3); we only need to observe, that by taking  $s_0 \simeq 1 \text{ GeV}^2$  we can fit the slope of the dif. cross-section for  $\pi^+ p \rightarrow \omega \Delta^{++}$  at  $3.7 \text{ GeV}/c$  <sup>24)</sup>.

The  $\pi^+ p \rightarrow \pi^0 \Delta^{++}$  process.

In complete analogy with  $\pi^+ p \rightarrow \omega \Delta^{++}$ ; for the  $\pi^+ p \rightarrow \pi^0 \Delta^{++}$  amplitudes, we write :

$$\widehat{\Pi}_{p\Delta} = \beta_{p\Delta}^P(t) \beta_{(t)}^P \left( \frac{s}{s_0} \right)^{\alpha_P(t)} \quad (\text{t-channel CM}) \quad (\text{II-9})$$

$$\Pi_{p'\Delta'} = \beta_{p'\Delta'}^P(t) \beta_{(t)}^P \left( \frac{s}{s_0} \right)^{\alpha_P(t)} \quad (\text{s-channel, } \omega \text{ rest frame}) \quad (\text{II-10})$$

$$\Pi_{p'\Delta'} \Rightarrow \langle \Pi \rangle = \langle \beta^P \rangle \beta_{(t)}^P \left( \frac{s}{s_0} \right)^{\alpha_P(t)} \quad (\text{II-11})$$

(residues averaged in helicities and  $t$ )

Taking  $s_0 \approx 1 \text{ GeV}^2$  we can have a reasonable "mean" slope for the dif. cross-section<sup>25), 27)</sup>. For the channel  $\eta^0 p \rightarrow \eta^- \Delta^{++}$  required in  $B_1$ , note that it is the  $u$ -channel of  $\eta^+ p \rightarrow \eta^0 \Delta^{++}$ , and the crossed particles are spinless. So, in the approximation  $m_{\pi^\pm} = m_{\pi^0}$ , the  $s$ -channel CM and the  $u$ -channel CM coincide, hence the corresponding helicity amplitudes should be equal, one by one, in any frame (because crossing from  $u$ -CM to  $s$ -CM does not involve any change, and from then on they rotate together).

The  $\omega \rightarrow \pi^+ \pi^- \pi^0$  decay.

For the invariant amplitudes describing the  $\omega \rightarrow \pi^+ \pi^- \pi^0$  decay we have<sup>28)</sup>: (C-conservation)

$$T_M \propto w^{1/2} (\vec{p}_- \times \vec{p}_+) \cdot \vec{\epsilon}(M) \quad (\text{II-12})$$

where  $w^{1/2}$  is the  $3\pi$  invariant mass and  $\vec{p}_+$ ,  $\vec{p}_-$  are the 3-momenta of  $\pi^+$ ,  $\pi^-$  in the  $\omega$  rest frame. Putting our  $z$ -axis along

the direction :  $\lim_{\vec{p}_\omega \rightarrow 0} \frac{\vec{p}_\omega}{|\vec{p}_\omega|}$  ,

where  $\vec{p}_\omega$  is the  $\omega$  3-momentum,  $T_M$  become helicity amplitudes  $T_\omega$ , so for amplitude  $A$  in (II-1) we have :

$$A_{p\Delta} = \sum_{\omega} \frac{\Omega_{p\omega\Delta} T_\omega}{m_\omega - W^{1/2} + i \frac{\Gamma_\omega}{2}} \Rightarrow \frac{\langle \Omega \rangle \sum_{\omega} T_\omega}{m_\omega - W^{1/2} + i \frac{\Gamma_\omega}{2}} \equiv \langle A \rangle \quad (\text{II-13})$$

$\pi$ - $\pi$  amplitudes

We now estimate the  $\pi$ - $\pi$  scattering amplitudes required in our background diagrams  $B_{1(2)}$ . Since we are interested in  $3\pi$  invariant mass near the mass of the  $\omega$ , we need  $m_{\pi\pi} \lesssim m_\rho$  in order to have  $m_{3\pi} \simeq m_\omega$ <sup>29)</sup>, so we need an accurate description of our  $\pi$ - $\pi$  amplitude below the  $\rho$  mass, through the available<sup>30)</sup> phase shifts for  $S_0$ ,  $S_2$  and  $P_1$  waves. For the  $\pi$ - $\pi$  amplitudes of definite isospin I we have : (see Appendix F)

$$T^I = 8\pi s^{\frac{1}{2}} \sum_{\ell} (2\ell+1) a_{\ell}^I P_{\ell} \quad (\text{II-14})$$

with 
$$a_{\ell}^I = \frac{1}{q} \frac{1}{\cot \delta_{\ell}^I - i} \quad (\text{II-15})$$

where  $q$  is the  $2\pi$  centre of mass momentum. We put :

$$q^{2\ell+1} \cot \delta_{\ell}^I = f_{\ell}^I(q) \quad (\text{II-16})$$

and interpolate simple polynomials in  $q$ , through the  $f_{\ell}^I(q)$  values found from the  $\pi\pi$  phase shifts, taken from Morgan's review<sup>30)</sup> (see Figure II-5). We find : (all units in GeV.)

$$f_{0(q)}^0 = 0.6 - 5.17q^2 \quad (\text{II-17a})$$

$$f_{1(q)}^1 = 0.09 - 4.76q^4 - 5.25q^6 \quad (\text{II-17b})$$

$$f_{0(q)}^2 = -5.76 + 26.12q - 37.31q^2 \quad (\text{II-17c})$$

\* MOROAN'S REVIEW

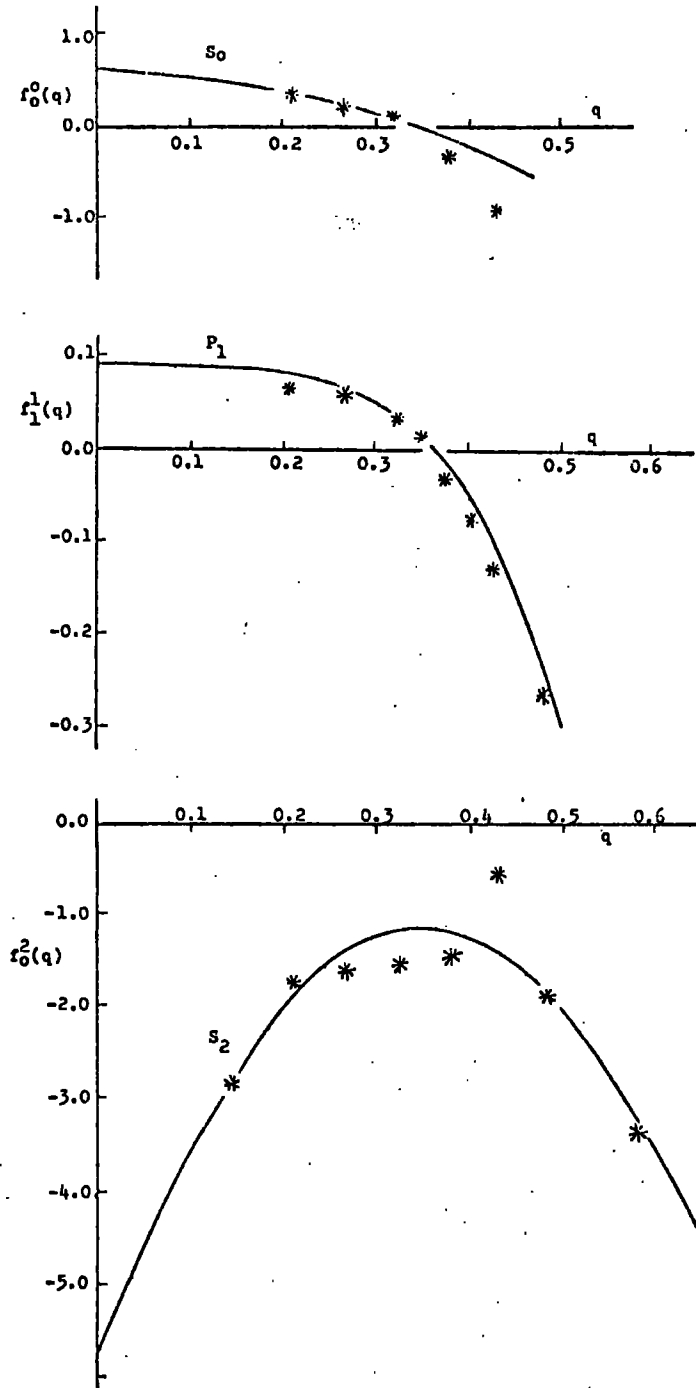


FIG. II-5 Polynomial interpolations for the quantities  $f_l^I = q^{2l+1} \cot \delta_l^I$ . Phase shifts from reference 30). All units in GeV .

Expressions (II-17) are consistent with the results of a recent compilation <sup>31)</sup> of  $\pi-\pi$  scattering lengths. For the  $\pi^+\pi^-\rightarrow\pi^+\pi^-$  and  $\pi^+\pi^0\rightarrow\pi^+\pi^0$  scattering amplitudes, we have :

$$T_{(+ -)} = \frac{1}{3}T^0 + \frac{1}{2}T^1 + \frac{1}{6}T^2 \quad (\text{II-18a})$$

$$T_{(+ 0)} = \frac{1}{2}T^1 + \frac{1}{2}T^2 \quad (\text{II-18b})$$

If combined with (II-11), these amplitudes give for our "average" background amplitudes :

$$\langle B_1 \rangle = \langle \pi \rangle \frac{1}{m_\eta^2 - p_1^2} T_{(+ 0)} \quad (\text{II-19a})$$

$$\langle B_2 \rangle = \langle \pi \rangle \frac{1}{m_\eta^2 - p_2^2} T_{(+ -)} \quad (\text{II-19b})$$

where  $p_{1(2)}$  is the four-momentum of the pion which is exchanged in  $B_{1(2)}$ .

### Results and Conclusions.

By Monte Carlo phase space integration (standard FOWL has been employed), we calculate the Dalitz-plot distribution (II-2), together with the  $3\pi$ -invariant mass distributions for positive

and negative  $x$ ,  $\left. \frac{d\sigma}{dw^{1/2}} \right\}_{x \gtrless 0}$ , using expressions (II-13,19)

for amplitudes A and B in (II-1). Although we may estimate the

absolute normalization of our diagrams, we vary the ratio  $A/B$  and search whether we can have a substantial asymmetry in the Dalitz plot, and at the same time, a reasonably low background. It turns out that although we get an asymmetry of the correct sign, we would need a very high background in order to make it as large as experimentally observed ; if we have an  $\omega$ -signal to background ratio 15-5, we get no more than 1-3 % net overall asymmetry, both in the Dalitz plot and in the  $\omega$  signal, in the  $3\pi$ -invariant mass distribution. In figures II-6  $\rightarrow$  11 we give a sample of results for  $\alpha_P(t) = \frac{1}{2} + t$ ,  $\alpha_B(t) = t$ ,  $s_0 = 1 \text{ GeV}^2$ , and  $\langle \gamma^P \rangle / \langle \gamma^B \rangle = 1$ . In figures II-6,7 we show the quantities  $\left. \frac{d\sigma}{dW^{1/2}} \right]_{x \geq 0}$  and the Dalitz plot distribution, together with its x,y projections, calculated from diagram A only, which is completely symmetric with respect to  $\pi^+$ ,  $\pi^-$ . We get an asymmetry  $\alpha = 4.3 \%$ , which should be interpreted as a random fluctuation of the Monte Carlo events generator ; we subtract it from latter results. In figures II-8  $\rightarrow$  11 we show the same quantities, but for  $\sigma_\omega / \sigma_B \approx 3,7$ .

TABLE II-1

	$\sigma_\omega / \sigma_B$	$\sigma_\omega]_{x>0} / \sigma_\omega]_{x<0}$	$\alpha$
Experiment	20.44	1.54	$18 \pm 5 \%$
Model	A only	1.03	4.30%
	7.04	1.10	5.25%
	3.05	1.14	8.20%







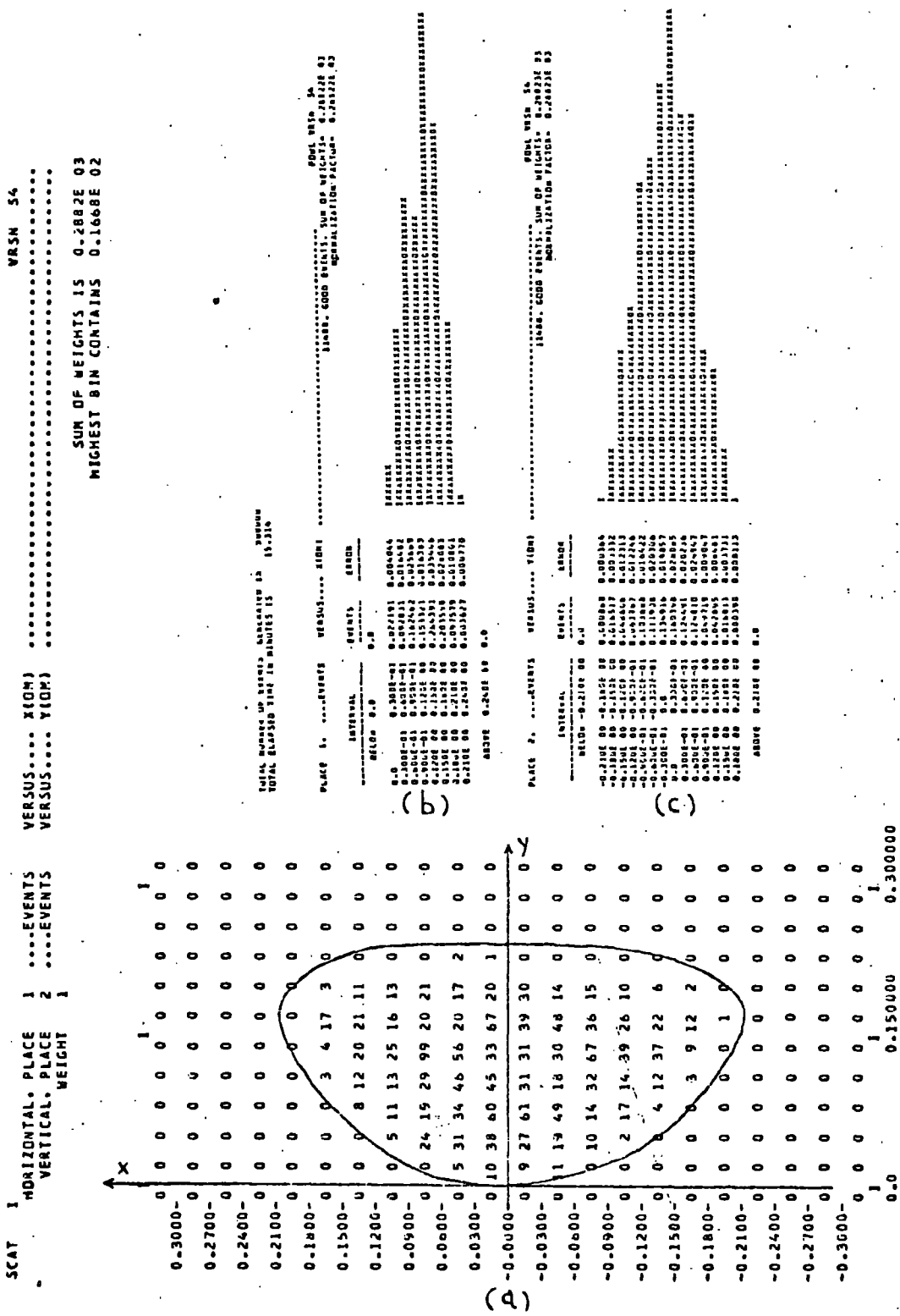


FIG. II-7 Calculated decay Dalitz-plot distributions for  $\omega \rightarrow \pi^+ \pi^- \pi^0$  without the background term:  
 (a) Two dimensional distribution.  
 (b) x-distribution ;  $x = T_+ - T_-$   
 (c) y-distribution ;  $y = T_0$  , units in GeV .



DOI 0850 16  
 190010. 5000 FREQS. SUM OF RESIDUALS 0.137618 95  
 AVERAGE RESIDUAL 0.137618 95

INTERVAL	EVENTS	ERROR
0.4100 00 0.4200 00	0.000000	0.000000
0.4200 00 0.4300 00	0.000000	0.000000
0.4300 00 0.4400 00	0.000000	0.000000
0.4400 00 0.4500 00	0.000000	0.000000
0.4500 00 0.4600 00	0.000000	0.000000
0.4600 00 0.4700 00	0.000000	0.000000
0.4700 00 0.4800 00	0.000000	0.000000
0.4800 00 0.4900 00	0.000000	0.000000
0.4900 00 0.5000 00	0.000000	0.000000
0.5000 00 0.5100 00	0.000000	0.000000
0.5100 00 0.5200 00	0.000000	0.000000
0.5200 00 0.5300 00	0.000000	0.000000
0.5300 00 0.5400 00	0.000000	0.000000
0.5400 00 0.5500 00	0.000000	0.000000
0.5500 00 0.5600 00	0.000000	0.000000
0.5600 00 0.5700 00	0.000000	0.000000
0.5700 00 0.5800 00	0.000000	0.000000
0.5800 00 0.5900 00	0.000000	0.000000
0.5900 00 0.6000 00	0.000000	0.000000
0.6000 00 0.6100 00	0.000000	0.000000
0.6100 00 0.6200 00	0.000000	0.000000
0.6200 00 0.6300 00	0.000000	0.000000
0.6300 00 0.6400 00	0.000000	0.000000
0.6400 00 0.6500 00	0.000000	0.000000
0.6500 00 0.6600 00	0.000000	0.000000
0.6600 00 0.6700 00	0.000000	0.000000
0.6700 00 0.6800 00	0.000000	0.000000
0.6800 00 0.6900 00	0.000000	0.000000
0.6900 00 0.7000 00	0.000000	0.000000
0.7000 00 0.7100 00	0.000000	0.000000
0.7100 00 0.7200 00	0.000000	0.000000
0.7200 00 0.7300 00	0.000000	0.000000
0.7300 00 0.7400 00	0.000000	0.000000
0.7400 00 0.7500 00	0.000000	0.000000
0.7500 00 0.7600 00	0.000000	0.000000
0.7600 00 0.7700 00	0.000000	0.000000
0.7700 00 0.7800 00	0.000000	0.000000
0.7800 00 0.7900 00	0.000000	0.000000
0.7900 00 0.8000 00	0.000000	0.000000
0.8000 00 0.8100 00	0.000000	0.000000
0.8100 00 0.8200 00	0.000000	0.000000
0.8200 00 0.8300 00	0.000000	0.000000
0.8300 00 0.8400 00	0.000000	0.000000
0.8400 00 0.8500 00	0.000000	0.000000
0.8500 00 0.8600 00	0.000000	0.000000
0.8600 00 0.8700 00	0.000000	0.000000
0.8700 00 0.8800 00	0.000000	0.000000
0.8800 00 0.8900 00	0.000000	0.000000
0.8900 00 0.9000 00	0.000000	0.000000
0.9000 00 0.9100 00	0.000000	0.000000
0.9100 00 0.9200 00	0.000000	0.000000
0.9200 00 0.9300 00	0.000000	0.000000
0.9300 00 0.9400 00	0.000000	0.000000
0.9400 00 0.9500 00	0.000000	0.000000
0.9500 00 0.9600 00	0.000000	0.000000
0.9600 00 0.9700 00	0.000000	0.000000
0.9700 00 0.9800 00	0.000000	0.000000
0.9800 00 0.9900 00	0.000000	0.000000
0.9900 00 1.0000 00	0.000000	0.000000

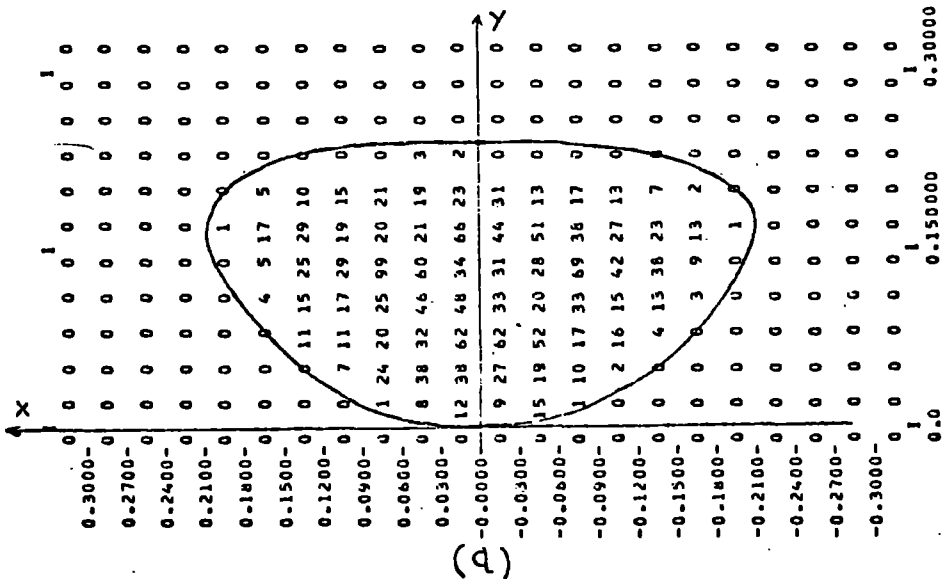
00300 0.1376 01 0.0

FIG. II-8b As in Figure II-6b , but with  $\sigma_{\omega} / \sigma_B \approx 7 \quad (x < 0)$ .

SCAT 3 HORIZONTAL PLACE 9 .....EVENTS  
 VERTICAL PLACE 10 .....EVENTS  
 WEIGHT 9

VERSUS.... X(2)  
 VERSUS.... Y(2)

VRSN S4  
 SUM OF WEIGHTS IS 0.7307E 08  
 HIGHEST BIN CONTAINS 0.4031E 07



PLACE 9: .....EVENTS VERSUS..... SIZE

INITIAL..... 0.0  
 WLDG 0.0

EVENTS	SIZE
0.0000-01	0.0000
0.0000-02	0.0000
0.0000-03	0.0000
0.0000-04	0.0000
0.0000-05	0.0000
0.0000-06	0.0000
0.0000-07	0.0000
0.0000-08	0.0000
0.0000-09	0.0000
0.0000-10	0.0000
0.0000-11	0.0000
0.0000-12	0.0000
0.0000-13	0.0000
0.0000-14	0.0000
0.0000-15	0.0000
0.0000-16	0.0000
0.0000-17	0.0000
0.0000-18	0.0000
0.0000-19	0.0000
0.0000-20	0.0000
0.0000-21	0.0000
0.0000-22	0.0000
0.0000-23	0.0000
0.0000-24	0.0000
0.0000-25	0.0000
0.0000-26	0.0000
0.0000-27	0.0000
0.0000-28	0.0000
0.0000-29	0.0000
0.0000-30	0.0000
0.0000-31	0.0000
0.0000-32	0.0000
0.0000-33	0.0000
0.0000-34	0.0000
0.0000-35	0.0000
0.0000-36	0.0000
0.0000-37	0.0000
0.0000-38	0.0000
0.0000-39	0.0000
0.0000-40	0.0000
0.0000-41	0.0000
0.0000-42	0.0000
0.0000-43	0.0000
0.0000-44	0.0000
0.0000-45	0.0000
0.0000-46	0.0000
0.0000-47	0.0000
0.0000-48	0.0000
0.0000-49	0.0000
0.0000-50	0.0000
0.0000-51	0.0000
0.0000-52	0.0000
0.0000-53	0.0000
0.0000-54	0.0000
0.0000-55	0.0000
0.0000-56	0.0000
0.0000-57	0.0000
0.0000-58	0.0000
0.0000-59	0.0000
0.0000-60	0.0000
0.0000-61	0.0000
0.0000-62	0.0000
0.0000-63	0.0000
0.0000-64	0.0000
0.0000-65	0.0000
0.0000-66	0.0000
0.0000-67	0.0000
0.0000-68	0.0000
0.0000-69	0.0000
0.0000-70	0.0000
0.0000-71	0.0000
0.0000-72	0.0000
0.0000-73	0.0000
0.0000-74	0.0000
0.0000-75	0.0000
0.0000-76	0.0000
0.0000-77	0.0000
0.0000-78	0.0000
0.0000-79	0.0000
0.0000-80	0.0000
0.0000-81	0.0000
0.0000-82	0.0000
0.0000-83	0.0000
0.0000-84	0.0000
0.0000-85	0.0000
0.0000-86	0.0000
0.0000-87	0.0000
0.0000-88	0.0000
0.0000-89	0.0000
0.0000-90	0.0000
0.0000-91	0.0000
0.0000-92	0.0000
0.0000-93	0.0000
0.0000-94	0.0000
0.0000-95	0.0000
0.0000-96	0.0000
0.0000-97	0.0000
0.0000-98	0.0000
0.0000-99	0.0000
0.0000-100	0.0000

PLAC 9: GOOD EVENTS..... 0.0000  
 SUM OF WEIGHTS..... 0.7307E 08  
 HIGHEST BIN CONTAINS..... 0.4031E 07

PLACE 10: .....EVENTS VERSUS..... SIZE

INITIAL..... 0.0  
 WLDG 0.0

EVENTS	SIZE
0.0000-01	0.0000
0.0000-02	0.0000
0.0000-03	0.0000
0.0000-04	0.0000
0.0000-05	0.0000
0.0000-06	0.0000
0.0000-07	0.0000
0.0000-08	0.0000
0.0000-09	0.0000
0.0000-10	0.0000
0.0000-11	0.0000
0.0000-12	0.0000
0.0000-13	0.0000
0.0000-14	0.0000
0.0000-15	0.0000
0.0000-16	0.0000
0.0000-17	0.0000
0.0000-18	0.0000
0.0000-19	0.0000
0.0000-20	0.0000
0.0000-21	0.0000
0.0000-22	0.0000
0.0000-23	0.0000
0.0000-24	0.0000
0.0000-25	0.0000
0.0000-26	0.0000
0.0000-27	0.0000
0.0000-28	0.0000
0.0000-29	0.0000
0.0000-30	0.0000
0.0000-31	0.0000
0.0000-32	0.0000
0.0000-33	0.0000
0.0000-34	0.0000
0.0000-35	0.0000
0.0000-36	0.0000
0.0000-37	0.0000
0.0000-38	0.0000
0.0000-39	0.0000
0.0000-40	0.0000
0.0000-41	0.0000
0.0000-42	0.0000
0.0000-43	0.0000
0.0000-44	0.0000
0.0000-45	0.0000
0.0000-46	0.0000
0.0000-47	0.0000
0.0000-48	0.0000
0.0000-49	0.0000
0.0000-50	0.0000
0.0000-51	0.0000
0.0000-52	0.0000
0.0000-53	0.0000
0.0000-54	0.0000
0.0000-55	0.0000
0.0000-56	0.0000
0.0000-57	0.0000
0.0000-58	0.0000
0.0000-59	0.0000
0.0000-60	0.0000
0.0000-61	0.0000
0.0000-62	0.0000
0.0000-63	0.0000
0.0000-64	0.0000
0.0000-65	0.0000
0.0000-66	0.0000
0.0000-67	0.0000
0.0000-68	0.0000
0.0000-69	0.0000
0.0000-70	0.0000
0.0000-71	0.0000
0.0000-72	0.0000
0.0000-73	0.0000
0.0000-74	0.0000
0.0000-75	0.0000
0.0000-76	0.0000
0.0000-77	0.0000
0.0000-78	0.0000
0.0000-79	0.0000
0.0000-80	0.0000
0.0000-81	0.0000
0.0000-82	0.0000
0.0000-83	0.0000
0.0000-84	0.0000
0.0000-85	0.0000
0.0000-86	0.0000
0.0000-87	0.0000
0.0000-88	0.0000
0.0000-89	0.0000
0.0000-90	0.0000
0.0000-91	0.0000
0.0000-92	0.0000
0.0000-93	0.0000
0.0000-94	0.0000
0.0000-95	0.0000
0.0000-96	0.0000
0.0000-97	0.0000
0.0000-98	0.0000
0.0000-99	0.0000
0.0000-100	0.0000

PLAC 10: GOOD EVENTS..... 0.0000  
 SUM OF WEIGHTS..... 0.7307E 08  
 HIGHEST BIN CONTAINS..... 0.4031E 07

FIG. II-9 Same distributions as in Figure II-7, but with  $\sigma_{\omega} / \sigma_B \approx 7$ .





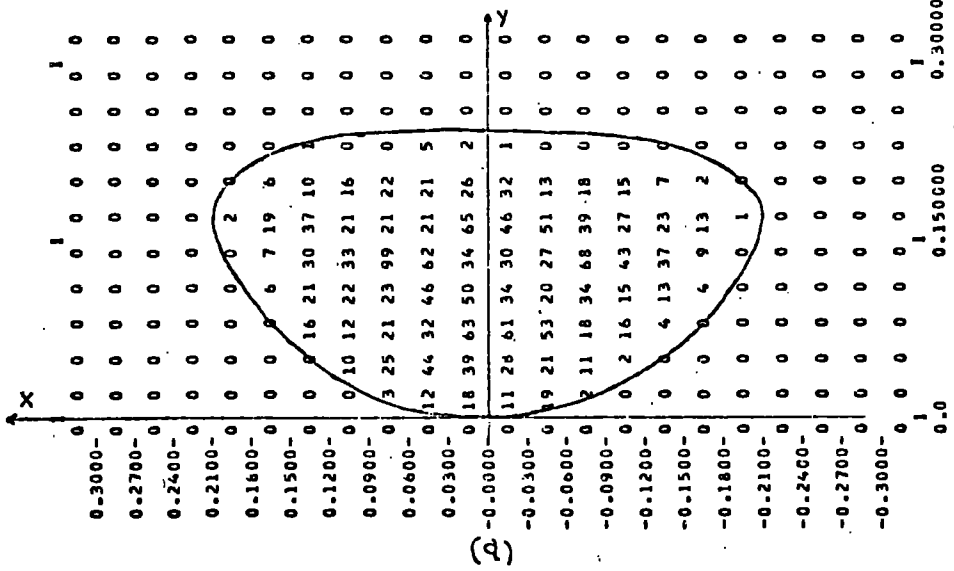


SCAT 2 HORIZONTAL PLACE 5 .....EVENTS  
 VERTICAL PLACE 6 .....EVENTS  
 WEIGHT 5

VERSUS..... X(1)  
 VERSUS..... Y(1)

VRSN \$4

SUM OF WEIGHTS IS 0.2836E 08  
 HIGHEST BIN CONTAINS 0.1464E 07



PLACE 9. ....EVENTS VERSUS..... BIN

15000. GOOD EVENTS. SUM OF WEIGHTS IS  
 NORMALIZATION FACTOR = 0.2836E 08

INTERVAL	EVENTS	WEIGHTS	BIN
BELOW 0.0	0.0	0.0	0.0
0.0-0.05	0.0	0.0	0.0
0.05-0.1	0.0	0.0	0.0
0.1-0.15	0.0	0.0	0.0
0.15-0.2	0.0	0.0	0.0
0.2-0.25	0.0	0.0	0.0
0.25-0.3	0.0	0.0	0.0
0.3-0.35	0.0	0.0	0.0
0.35-0.4	0.0	0.0	0.0
0.4-0.45	0.0	0.0	0.0
0.45-0.5	0.0	0.0	0.0
0.5-0.55	0.0	0.0	0.0
0.55-0.6	0.0	0.0	0.0
0.6-0.65	0.0	0.0	0.0
0.65-0.7	0.0	0.0	0.0
0.7-0.75	0.0	0.0	0.0
0.75-0.8	0.0	0.0	0.0
0.8-0.85	0.0	0.0	0.0
0.85-0.9	0.0	0.0	0.0
0.9-0.95	0.0	0.0	0.0
0.95-1.0	0.0	0.0	0.0
ABOVE 0.240E 00 0.0	0.0	0.0	0.0

(b)

PLACE 9. ....EVENTS VERSUS..... BIN

15000. GOOD EVENTS. SUM OF WEIGHTS IS  
 NORMALIZATION FACTOR = 0.2836E 08

INTERVAL	EVENTS	WEIGHTS	BIN
BELOW 0.0	0.0	0.0	0.0
0.0-0.05	0.0	0.0	0.0
0.05-0.1	0.0	0.0	0.0
0.1-0.15	0.0	0.0	0.0
0.15-0.2	0.0	0.0	0.0
0.2-0.25	0.0	0.0	0.0
0.25-0.3	0.0	0.0	0.0
0.3-0.35	0.0	0.0	0.0
0.35-0.4	0.0	0.0	0.0
0.4-0.45	0.0	0.0	0.0
0.45-0.5	0.0	0.0	0.0
0.5-0.55	0.0	0.0	0.0
0.55-0.6	0.0	0.0	0.0
0.6-0.65	0.0	0.0	0.0
0.65-0.7	0.0	0.0	0.0
0.7-0.75	0.0	0.0	0.0
0.75-0.8	0.0	0.0	0.0
0.8-0.85	0.0	0.0	0.0
0.85-0.9	0.0	0.0	0.0
0.9-0.95	0.0	0.0	0.0
0.95-1.0	0.0	0.0	0.0
ABOVE 0.210E 00 0.0	0.0	0.0	0.0

(c)

FIG. II-11 As in Figure II-7, but with  $\sigma_w / \sigma_B \approx 3$ .

Our results, are summarized in Table II-1 ; we define :

$$\sigma_{\omega}]_{x \geq 0} \equiv \left\langle \frac{d\sigma}{dw'^2} \right\rangle_{x \geq 0} \quad (\text{average in the interval } 0.77 \leq w'^2 \leq 0.80 \text{ GeV})$$

$$\sigma_B}]_{x \geq 0} \equiv \left\langle \frac{d\sigma}{dw'^2} \right\rangle_{x \geq 0} \quad (\text{average in } 0.85 \leq w'^2 \leq 0.95 \text{ GeV})$$

$$\frac{\sigma_{\omega}}{\sigma_B} = \frac{\sigma_{\omega}]_{x > 0} + \sigma_{\omega}]_{x < 0}}{\sigma_B}]_{x > 0} + \sigma_B}]_{x < 0}} \quad (\text{II-20})$$

(The  $\omega$  band is defined by  $0.762 \leq w'^2 \leq 0.803$  GeV ; FOWL calculates

$$\left. \frac{1}{\sigma_T} \frac{d\sigma}{dw'^2} \right]_{x \geq 0} \quad , \text{ where } \sigma_T \text{ is the total cross-section, or the}$$

"normalization factor" of our histograms in figures II-6  $\rightarrow$  11 )

We have checked the stability of our results against changes of the Regge trajectories  $\alpha_p$ ,  $\alpha_B$ , the constant  $s_0$ , and the ratio

$$\langle \gamma^p \rangle / \langle \gamma^B \rangle \quad ; \text{ but the only parameter on which the asymmetry}$$

depends crucially is the ratio A/B .

What about the  $t'$ -dependence of this asymmetry ? It is

difficult to calculate accurately  $\left. \frac{d\sigma}{dt'} \right]_{x \geq 0}$  , since double selection

of events is required (both in the  $\omega$ -band, and for  $x \geq 0$ ), and we need to generate a very large total number of events (this is also the reason we use a sharp  $\Delta$  ). Although generally we have

$\left. \frac{d\sigma}{dt'} \right|_{x>0} > \left. \frac{d\sigma}{dt'} \right|_{x<0}$ , a clear dip in  $\left. \frac{d\sigma}{dt'} \right|_{x<0}$  for

$0.08 \leq t' \leq 0.20 \text{ GeV}^2$  does not appear to be present. We may have a qualitative understanding of the  $t$  dependence of our asymmetry remembering that the interference terms in this model fall exponentially with  $t$ , hence large  $t$ 's do not contribute significantly to our asymmetry. On the other hand, we have checked that when replacing the constant  $\langle \chi^{\rho} \rangle$  by  $t \langle \chi^{\rho} \rangle$  (a flipping  $\rho$ ) the results presented above do not change substantially.\* So, we arrive at the qualitative conclusion that neither the very small, nor the large  $t$ 's contribute significantly to the small asymmetry generated by our mechanism.

We conclude that the  $\omega$ -signal - background interference mechanism, can explain only a small fraction of the charge asymmetry observed in the  $\omega \rightarrow \eta^+ \eta^- \eta^0$  decay. This result may be qualitatively understood, if we remember that :

- (i) The experimentally observed background is very low.
- (ii) The  $\omega$  occupies a very small region in the phase space, so the background cannot vary significantly inside it, to produce much asymmetry.
- (iii) The  $3\eta$   $1^-$  state involves high angular momenta so it starts contributing significantly at energies higher than the  $\omega$  mass, as discussed in detail in the previous section, and as proved by the fact that most of the  $x > 0 - x < 0$  asymmetry in our  $\frac{d\sigma}{dw^{1/2}}$  distributions, in figures II-8,10, is introduced at energies higher than the  $\omega$  mass.

---

\* This is because the small  $t$  values are suppressed by phase space factors.

In view of the situation in  $\eta \rightarrow \pi^+ \pi^- \pi^0$  decay, discussed in section II-2 , before considering more exotic explanations ( discussed in section II-3 ) of a possible charge asymmetry in  $\omega \rightarrow \pi^+ \pi^- \pi^0$  decay, we should await for more accurate data.

# CHAPTER III

## THE $KN \rightarrow KN, K\Delta, K^*N$ PROCESSES .

### III-1 Introduction.

In this chapter we turn to  $KN$  scattering; our ultimate aim will be to understand possible exotic bumps in  $K^*N$  total cross-sections (chapter IV). Here, we examine in some detail the inelastic  $KN$  channels dominating at low energies, namely  $KN \rightarrow K\Delta$ ,  $KN \rightarrow K^*N$ , and we try to understand the nature of their  $t$ -channel exchanges on a concise basis.<sup>32)</sup> In view of the work to come next, it is desirable to have a very clear picture of the exchanges which are important in each helicity amplitude. The philosophy we adopt in treating our dynamics greatly helps in achieving this aim ; to construct our  $KN \rightarrow K\Delta, K^*N$  amplitudes , we proceed in the following two steps :

(i) Guided by the measured values of the density matrix elements for the production of the high spin particle , we find the particular way of coupling the pseudoscalar and vector meson exchanges-treated as "elementary" objects - to the external particles , which is consistent with the data , and then :

(ii) We reggeize our amplitudes , retaining any relations imposed on them by (i) , assuming exchange degeneracy between vector and tensor mesons . Thus , we always have our amplitudes parametrized in terms of Regge poles.

Finally , for completeness we give a very simple Regge model for elastic KN scattering. Since this process is dominated by pomeron-exchange even at very low energies , it cannot be treated in the way described above , but a purely phenomenological point of view has to be adopted.

The fits we are going to present should not be thought as the best results of careful chisquare minimizations ; this has been done during the past decade (see e.g. references 33) and 34) ; exhaustive lists of references for Regge fits for the  $KN \rightarrow KN$  ,  $K\Delta$  ,  $K^*N$  reactions may be found in reference 35) ) , and it is not our purpose. Here , we want to succeed in a concise and unambiguous determination of the exchanges which are important in each amplitude. This is very important , e.g. for  $K^*N \rightarrow K^*N$  , in deciding unambiguously whether any exotic  $K^*N$  resonances do exist- see chapter IV. On the other hand , we demonstrate that much simpler models can fit the data equally well as some sophisticated ones. We always manage to have no more than one or two free parameters , which can be easily determined. We believe these models to be quite realistic, at least in a global sense , although they do not succeed in describing every detailed aspect of the data, as discussed below.

III-2 The  $KN \rightarrow K\Delta$  channel.

We start by considering  $KN \rightarrow K\Delta$  scattering, where we can only have  $\rho$ ,  $A_2$  exchanges, in four independent helicity amplitudes. Since this reaction has a  $I_S = 1$  component only, all  $K^+p \rightarrow K^0 \Delta^{++}$ ,  $K^+n \rightarrow K^0 \Delta^+$ ,  $K^+ \Delta^0$  channels are simply related by isospin, so we explicitly discuss the  $K^+p \rightarrow K^0 \Delta^{++}$  channel only, for which we have the best data.

Lorentz-invariant couplings

The success of the Stodolsky-Sakurai <sup>36)</sup> model in predicting the  $\frac{3}{2}^+$  particle density matrix, enables us to use the M1 (magnetic dipole) transition Lagrangian <sup>37)</sup> for the  $\rho\Delta N$  vertex :

$$\mathcal{L} = g \bar{\Psi} \gamma^\mu \Psi \epsilon_{\mu\nu\lambda\tau} P_\Delta^\nu (P_p + P_\Delta)^\lambda A^\tau \quad (\text{III-1})$$

while the only parity conserving coupling of a vector meson to two pseudoscalar mesons may be written :

$$\mathcal{L} = g' \left[ \phi_1 \partial_\mu \phi_2 - (\partial_\mu \phi_1) \phi_2 \right] A_\mu \quad (\text{III-2})$$

Our notation is clarified by diagram III-1.

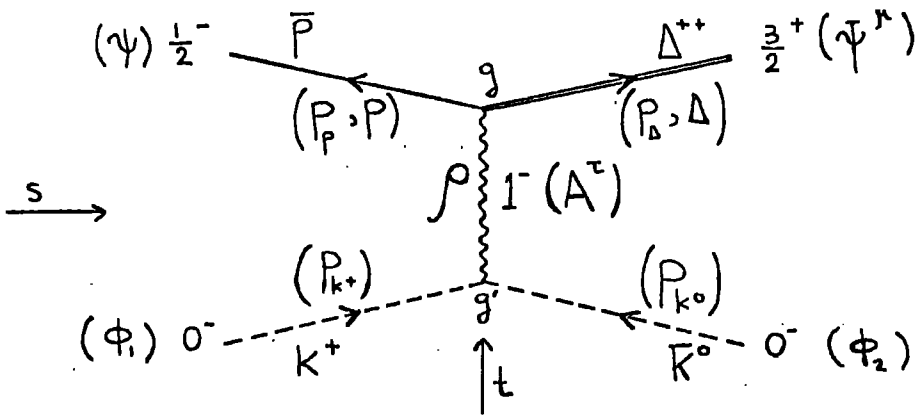


DIAGRAM III-1

Using these (phenomenological) Lagrangians, the t-channel (Born) helicity amplitudes, which do not vanish, may be calculated (see Appendix C-1) :

$$T_{p\Delta}^{(t)} = \frac{-igg'}{m_\rho^2 - t} \bar{u}_{(P, \Delta)}^\mu v_{(P, P)} \epsilon_{\mu\nu\gamma\tau} p_\Delta^\nu p_P^\gamma (p_{k^+} - p_{k^0})^\tau \quad (\text{III-3})$$

Or, finally :\*

$$T_{\frac{1}{2} \frac{3}{2}}^{(t)} = \frac{gg'}{2\sqrt{2}} \frac{\phi(s, t)^{1/2}}{m_\rho^2 - t} \left[ (m + m_\Delta)^2 - t \right]^{1/2} \quad (\text{III-4})$$

$$T_{\frac{1}{2} \frac{3}{2}}^{(t)} = \sqrt{3} T_{-\frac{1}{2} \frac{1}{2}}^{(t)} \quad (\text{III-5})$$

---

\* Throughout this thesis, we use the notation  $m = m_N$ ,  $\mu = m_K$ ,  $M = m_{K^*}$ , while  $\phi(s, t)$  is the Kibble function (the equation of the physical region boundary) of the process under discussion. We label our helicities by the name of the corresponding particle.



Relation (III-5) leads to the famous Stodolsky-Sakurai predictions for  $\Delta$  production :

$$\rho_{33} = \frac{1}{8}, \quad \rho_{31} = 0, \quad \rho_{3-1} = \frac{\sqrt{3}}{8} \quad (\text{III-6})$$

and it is by now well checked that these are satisfied, at least in a mean sense, over a wide range of energies (see e.g. figures III-2,3b,4 from references 40), 41),42) ).

One may also calculate the s-channel helicity amplitudes directly from Lagrangians (III-1,2) (see Appendix C-1) :

$$T_{\frac{1}{2}\frac{3}{2}}^{(s)} = \sqrt{3} T_{-\frac{1}{2}\frac{1}{2}}^{(s)} = F \frac{\sin\theta}{m_p^2 - t} (1 + D - 2D \cos\theta) \cos \frac{\theta}{2} \quad (\text{III-7a})$$

$$-T_{-\frac{1}{2}\frac{3}{2}}^{(s)} = \sqrt{3} T_{\frac{1}{2}\frac{1}{2}}^{(s)} = F \frac{\sin\theta}{m_p^2 - t} (1 - D - 2D \cos\theta) \sin \frac{\theta}{2} \quad (\text{III-7b})$$

F and D are functions of s, the form of which is given in Appendix C-1 (C-18,21) ;  $\theta$  is the s-channel scattering angle. It may now be checked (see Appendix C-1) that the relation  $\sum |T^{(s)}|^2 = \sum |T^{(t)}|^2$  is satisfied, a fact stemming from the locality of our Lagrangians (III-1,2). It would be an academically interesting exercise to calculate the angular distribution and total cross-section for  $K^+ p \rightarrow K^0 \Delta^{++}$  using amplitudes (III-7) as they stand. Figure III-1 shows the results of this calculation (which should be compared with the data on figures III-5,8) , and two major diseases of strong interactions calculations using first order perturbation theory are manifested :

- (1) not enough peripherality

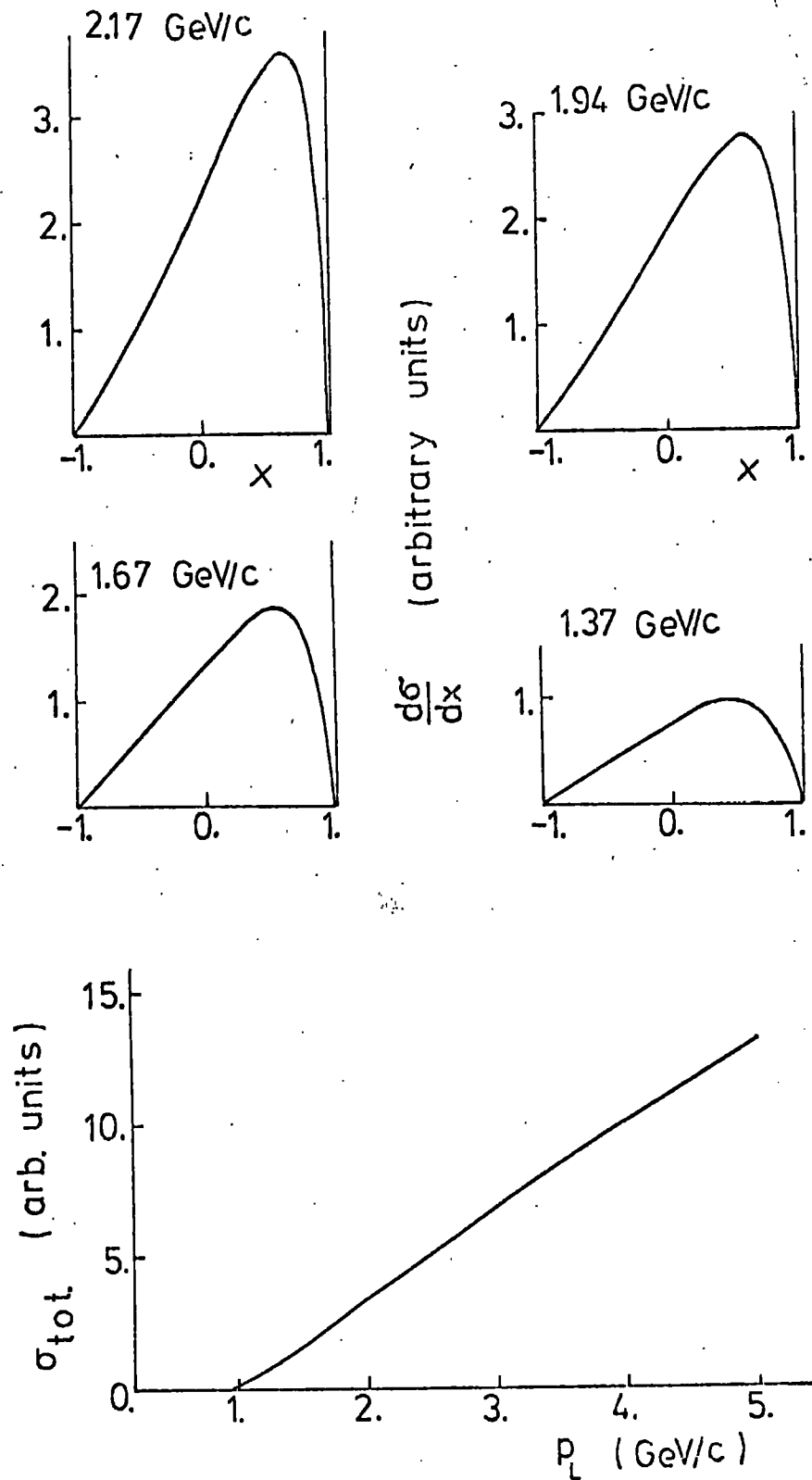


FIG. III-1 First order perturbation theory predictions for the differential and total cross-sections for  $K^+p \rightarrow K^0\Delta^{++}$  ( $\rho$ -exchange, M1 transition at the  $p\rho\Delta$  vertex);  $x = \cos\theta_s$ .

(ii) infinitely rising total cross-section.

Kinematic singularities.

It is interesting to note, that the t-channel amplitudes (III-4) have the correct kinematic singularities <sup>22)</sup> required e.g. by crossing matrix considerations. Let us explicitly construct the kinematic-singularity-free amplitudes, for this process, corresponding to amplitudes (III-4) ( $F^{(\pm)}$  denote the asymptotically parity conserving amplitudes;  $F^{(-)} \equiv 0$  <sup>22)</sup> ) :

$$\begin{Bmatrix} F_{\frac{1}{2}\frac{3}{2}}^{(+)} \\ F_{-\frac{1}{2}\frac{1}{2}}^{(+)} \end{Bmatrix} = \frac{t^{1/2} \sqrt{b_{\pm}}}{\sqrt{a_{+} a_{-}}} \frac{1}{\sin \theta_t} \begin{Bmatrix} T_{\frac{1}{2}\frac{3}{2}}^{(t)} \\ T_{-\frac{1}{2}\frac{1}{2}}^{(t)} \end{Bmatrix} = \frac{g g'}{4\sqrt{2}} \frac{b_{+} b_{-}}{m_{\rho}^2 - t} \begin{Bmatrix} 1 \\ \frac{1}{\sqrt{3}} \end{Bmatrix} \quad (\text{III-8})$$

Here,  $\theta_t$  is the t-channel scattering angle and

$$a_{\pm} = t - (m_{K^+} \pm m_{K^0})^2, \quad b_{\pm} = t - (m_p \pm m_{\Delta})^2 \quad (\text{C-7})$$

(see also equation (C-11) of Appendix C). So, besides the basic dynamics of this problem ( $\rho$ -exchange,  $\frac{1}{m_{\rho}^2 - t}$ ) the kinematic-singularity-free amplitudes contain factors which vanish at t-channel thresholds and pseudothresholds, something to be expected since angular momentum conservation is nicely built into Lagrangians (III-1,2) (the crossing matrix is diagonal at high energies).

Reggeization

Now, retaining relation (III-5), and the residue structure predicted by couplings (III-1,2), we want to alter the underlying dynamics, replacing the Feynman propagator in (III-4) by the proper "Regge propagator" (e.g. as in reference 38) ). Since  $\rho$  and  $A_2$  are the only allowed Regge exchanges, for the helicity amplitudes which are free of physical-region-boundary singularities (free from kin. singularities in  $s$ ) we have :

$$\begin{aligned} \widehat{T}_{\rho\Delta} &= -\beta_{\rho\Delta}^{\rho}(t) \frac{-1 + e^{-i\pi\alpha_{\rho}(t)}}{2\sin\pi\alpha_{\rho}(t)} \left(\frac{s-u}{2s_0}\right)^{\alpha_{\rho}(t)-M} + \beta_{\rho\Delta}^{A_2}(t) \frac{1 + e^{-i\pi\alpha_{A_2}(t)}}{2\sin\pi\alpha_{A_2}(t)} \left(\frac{s-u}{2s_0}\right)^{\alpha_{A_2}(t)-M} \\ &= \frac{1}{\eta} \gamma_{\rho\Delta}(t) \Gamma(1-\alpha) \left(\frac{s-u}{2s_0}\right)^{\alpha-M} \quad (M=|\rho-\Delta|) \quad \text{(III-9)} \end{aligned}$$

where we got the second equality by assuming

$$\alpha_{\rho}(t) = \alpha_{A_2}(t) = \alpha(t) \quad , \quad \beta_{\rho\Delta}^{\rho}(t) = \beta_{\rho\Delta}^{A_2}(t) = \frac{\gamma_{\rho\Delta}(t)}{\Gamma(\alpha)} \quad \text{(III-10)}$$

that is, strong exchange degeneracy between  $\rho$  and  $A_2$  (see section I-2), and a usual ghost-killing mechanism <sup>35)</sup>, since we need our amplitudes for  $-1 \leq \cos\theta \leq 1$ , and at low energies. We now reggeize amplitudes (III-4) by the substitution :

$$\frac{1}{m_{\rho}^2 - t} \longrightarrow \Gamma(1-\alpha) \left(\frac{s-u}{2s_0}\right)^{\alpha-1} \quad \text{(III-11)}$$

so, we end up with :

$$T_{\frac{1}{2}\frac{3}{2}}^{(t)} = \sqrt{3} T_{-\frac{1}{2}\frac{1}{2}}^{(t)} = \frac{gg'}{2\sqrt{2}} \left[ (m_{\Delta} + m)^2 - t \right]^{\frac{1}{2}} \Phi_{(s,t)}^{\frac{1}{2}} \Gamma_{(1-\alpha)} \left( \frac{s-u}{2s_0} \right)^{\alpha-1} \quad (\text{III-12})$$

For our  $\rho$ - $A_2$  trajectory we have

$$\alpha(t) = 1 + \alpha'(t - m_{\rho}^2) \quad (\text{III-13})$$

with  $\alpha' = 1 \text{ GeV}^{-2}$ , while the natural unit <sup>39)</sup> in our problem is

$s_0 = \mu \sqrt{mm_{\Delta}} \simeq 0.5$ , so the only "free" parameter we have is the over-all normalization.

#### Comparison with experiment

Before proceeding to a comparison of the cross-sections to which amplitudes (III-12) lead, with experiment, let us check once again how good the Stodolsky-Sakurai predictions (III-6) are. In figure III-2 (from reference 41) ) we show the  $\Delta^{++}$  production density matrix elements at low energies ( $p_L = 1.21-1.69 \text{ GeV}/c$ ), and the agreement with the Stodolsky-Sakurai predictions (dashed lines) is, in a mean sense, satisfactory. In figure III-3b (from reference 42) ) we show that they remain good, except for small  $t$ , at  $p_L = 4.6 \text{ GeV}/c$ . In figure III-4 (from reference 40) ) the averaged over  $t$  density matrix elements are shown, from threshold up to  $5 \text{ GeV}/c$ , and the agreement with the Stodolsky-Sakurai predictions is remarkable.

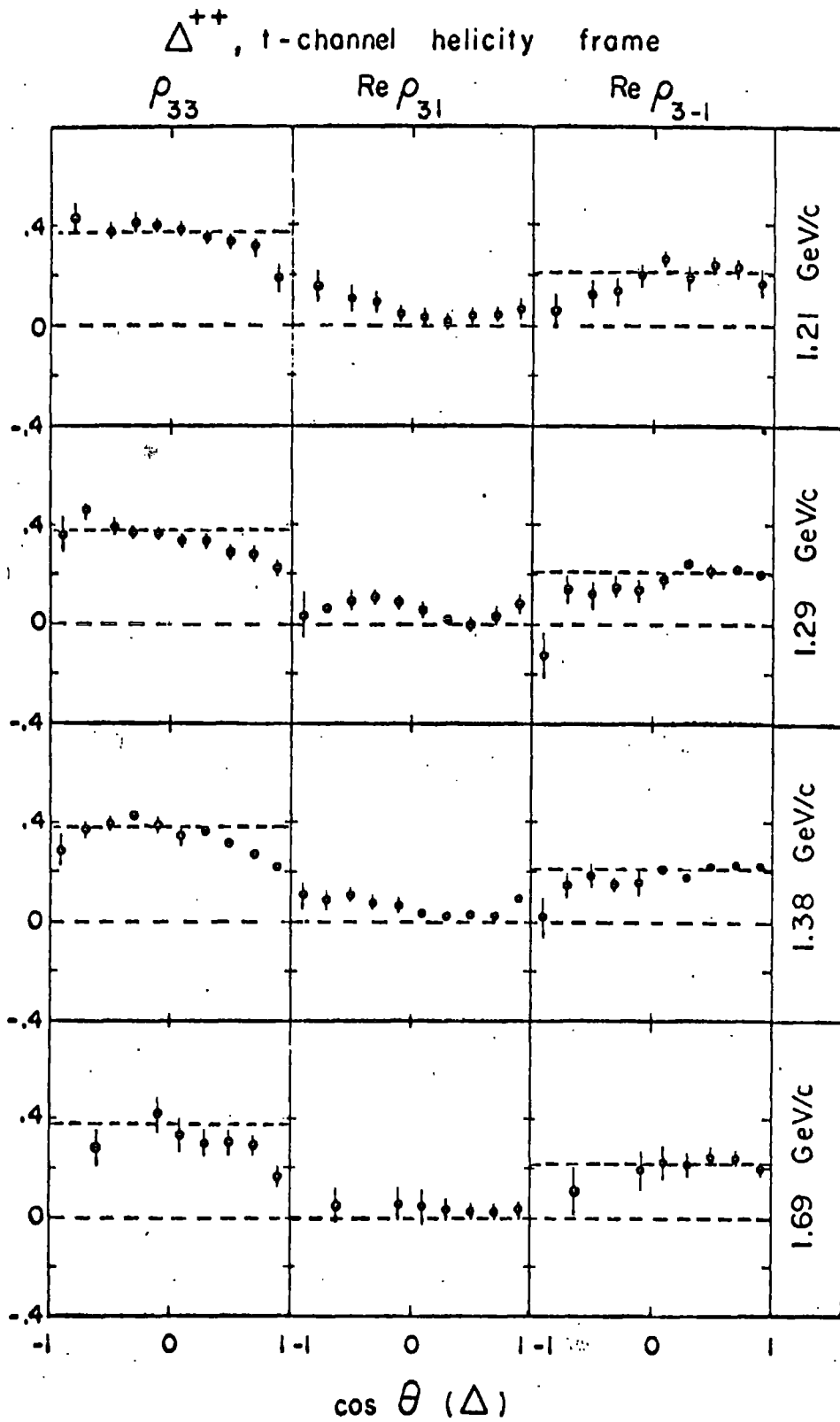


FIG. III-2 From reference 41).  
 $\Delta^{++}$  production density matrix elements, compared with  
the Stodolsky - Sakurai predictions (dashed lines).

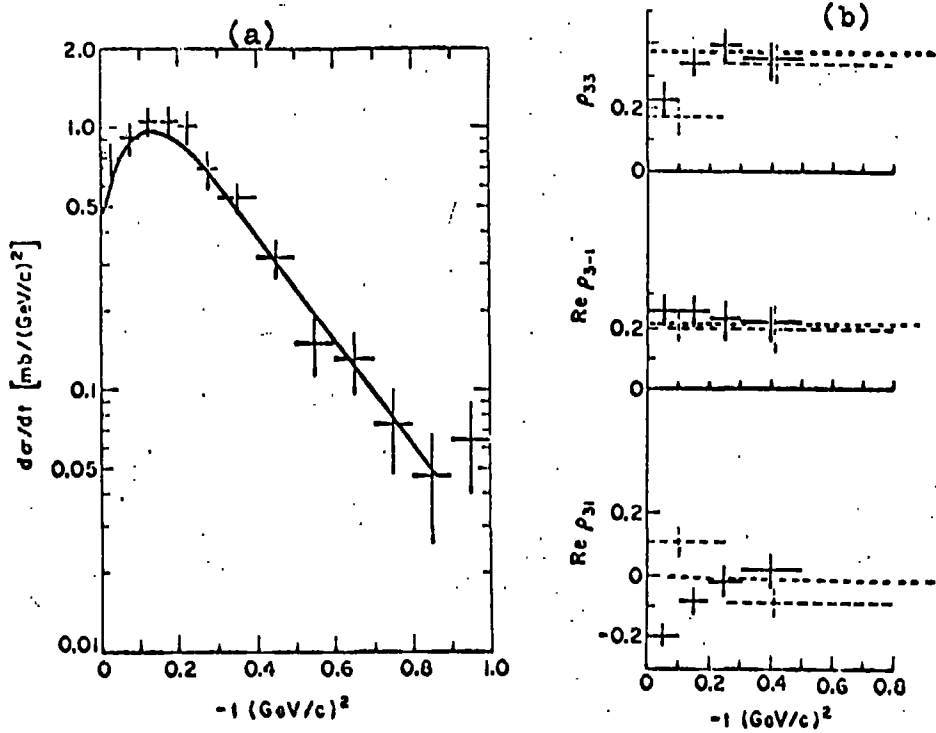


FIG. III-3 From reference 42) .

- (a) Dif. cross-section for  $K^+p \rightarrow K^0\Delta^{++}$  at  $p_L = 4.6 \text{ GeV}/c$  , compared with the fit of reference 33) .
- (b) The corresponding density matrix elements ; the dotted lines are the Stodolsky - Sakurai predictions. Dashed crosses are from the reaction  $K^-n \rightarrow \bar{K}^0\Delta^-$  , at essentially the same momentum, from reference 48) .

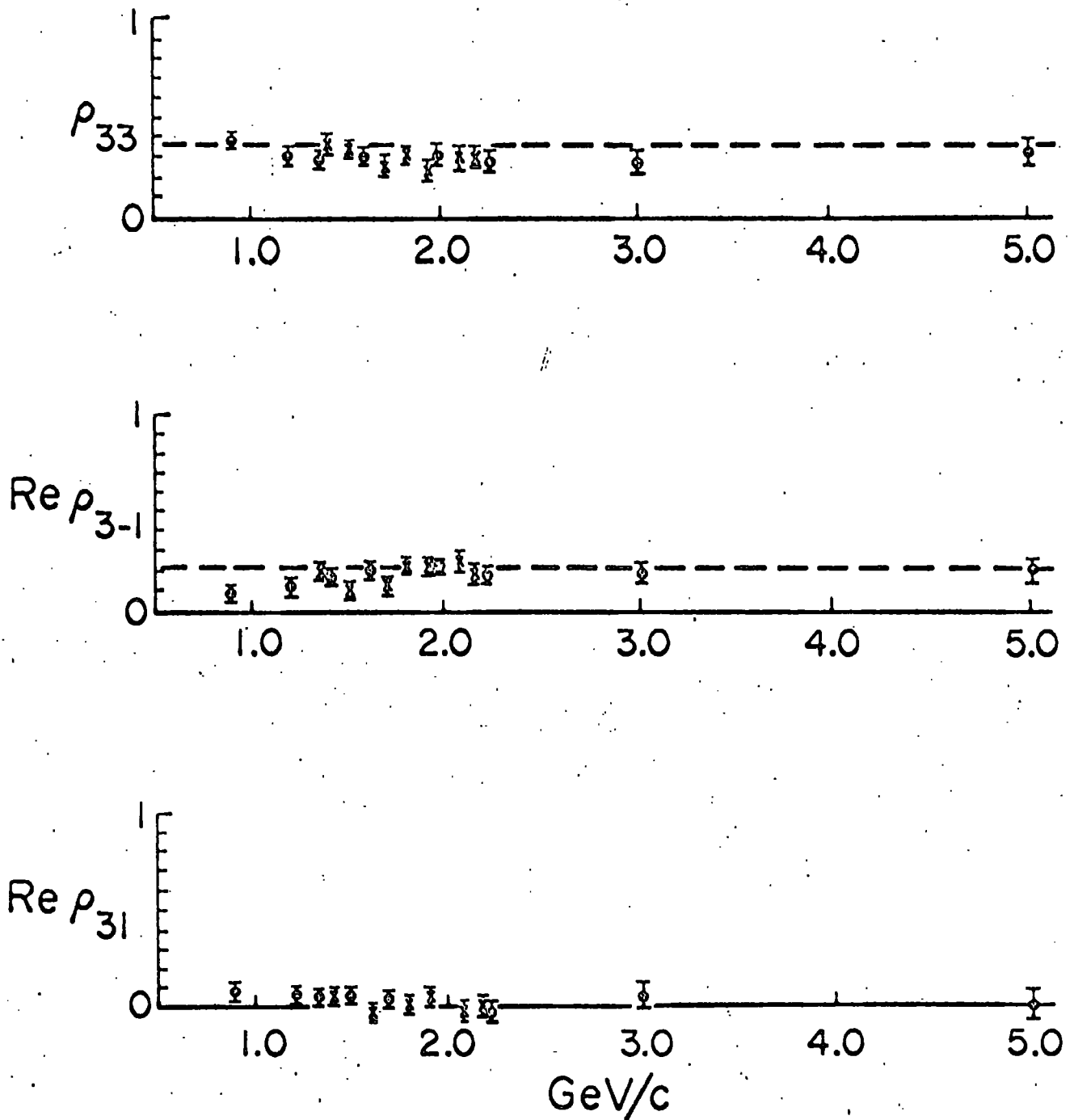


FIG. III-4 From reference 40).  
 Averaged over  $t$ ,  $\Delta^{++}$ -production density matrix elements  
 for  $1 \lesssim p_L \lesssim 5$  GeV/c compared with the Stodolsky -  
 Sakurai predictions (dashed lines).



In figures III-5,6 we show low energy,  $1.21 \leq p_L \leq 2.17$  GeV/c, dif. cross-sections for  $K^+p \rightarrow K^0 \Delta^{++}$  (data from references 40), 41), compared with the present model, and the agreement is generally satisfactory, except for the lowest energies,  $p_L \leq 1.29$  GeV/c where Regge seems to have ceased being good. It is interesting to note that had we used amplitudes (III-4) as they stand, we could have fitted the lowest energies data (compare with curves on fig. III-1). This remark may not be uncorrelated with the observation that exchanges tend to behave as "composite" when the ratio  $\frac{S}{1/\alpha'}$  is large : at presently available "high" energies, this ratio is large for strong, but small for weak or electromagnetic interactions (the Regge slope  $\alpha'$  may be thought as characterizing the square of the fundamental length associated with the interaction under consideration) ; on the basis of this observation alone, one argues that, at truly asymptotic energies, leptons will reggeize as well (see reference 43), and references therein). In figure III-7 (data from reference 42) ), we show that the model extrapolates satisfactorily to higher energies,  $p_L = 4.6$  GeV/c ; for comparison, in figure III-3a (from reference 42) ) we show the same data, compared with the sophisticated Krammer and Maor fit <sup>33)</sup>. Finally, in figure III-8 we have total  $K^+p \rightarrow K^0 \Delta^{++}$  cross-section data (compiled in reference 41) ) compared with the prediction of this model, normalized to the data at 4.6 GeV/c shown in figure III-7. Again, we see that Regge fails below  $p_L \sim 1.4$  GeV/c (since our  $\Delta$  is sharp, we have a  $K\Delta$  threshold at higher momentum).

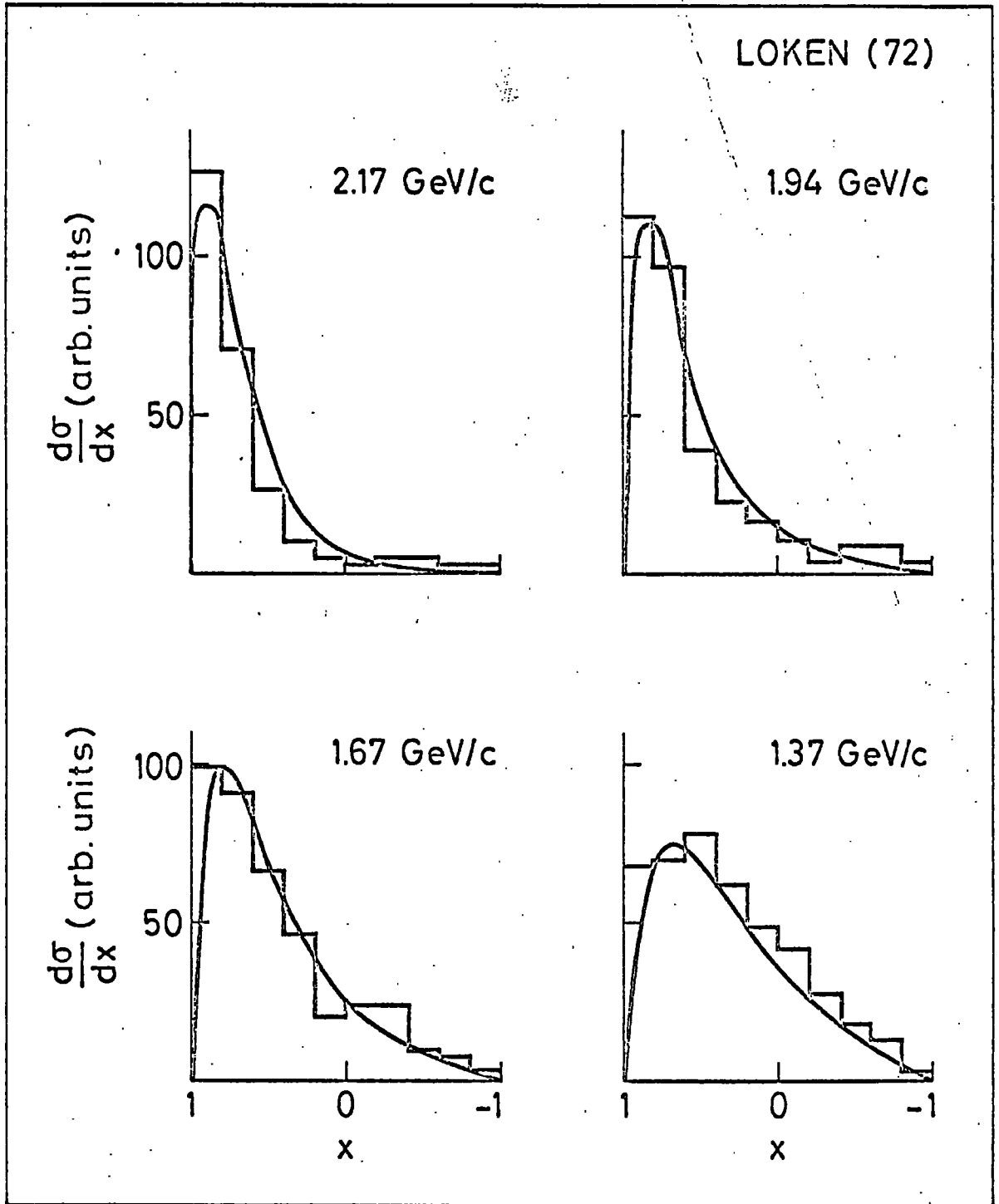


FIG. III-5 Dif. cross-sections for  $K^+ p \rightarrow K^0 \Delta^{++}$  at various low energies, compared with the model of section III-2.

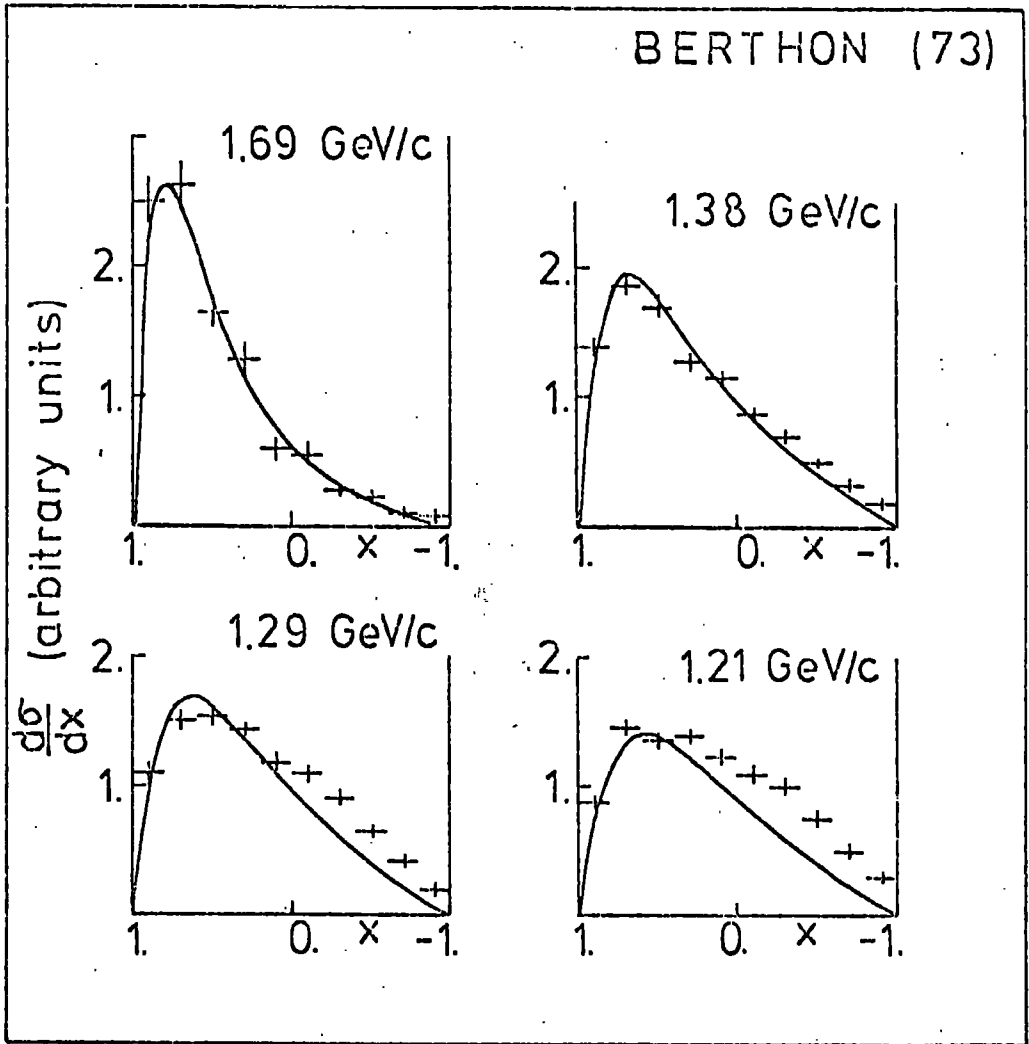


FIG. III-6 Same as in Figure III-5 , at different energies .

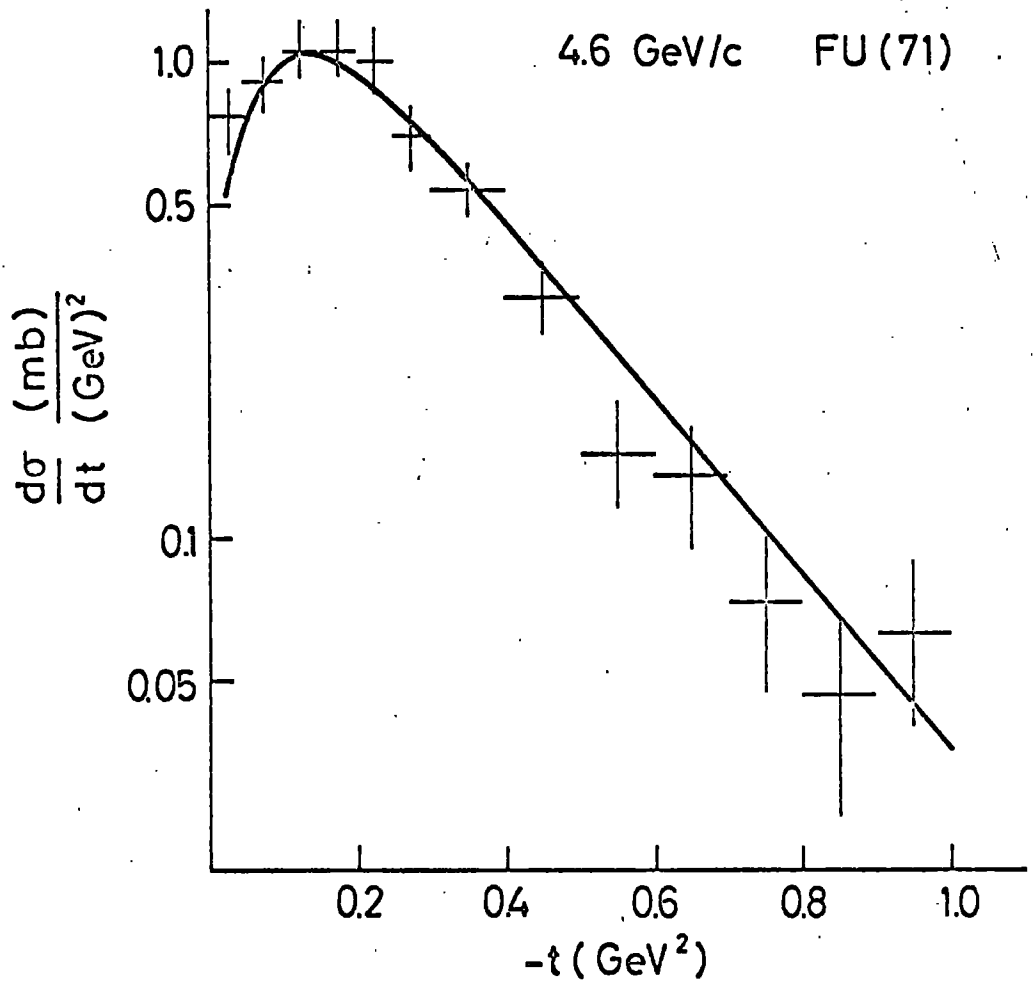


FIG. III-7 Same as in Figure III-5 , but at higher energy,  $p_L = 4.6$  GeV/c .

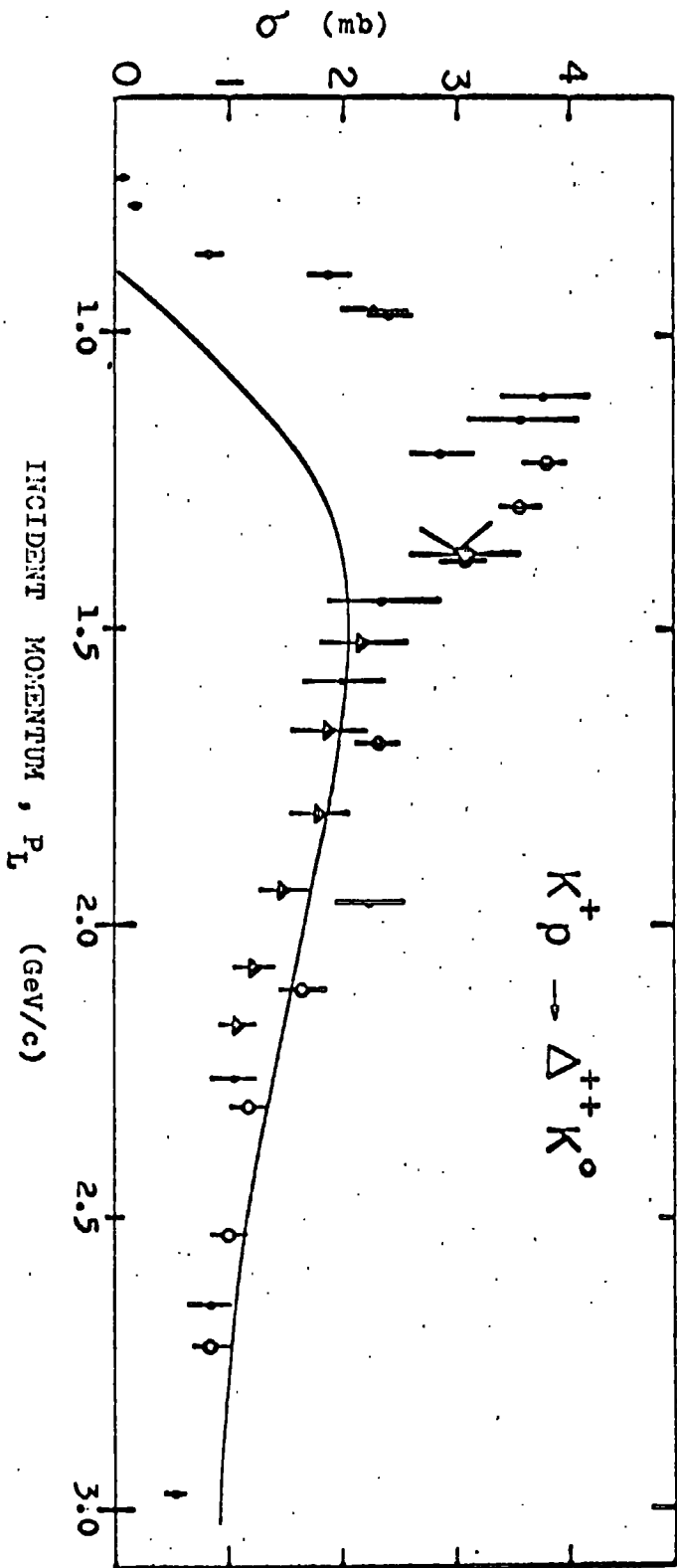


FIG. III-8 Total cross-section for  $K^+ p \rightarrow K^0 \Delta^{++}$  (from reference 41), compared with the prediction of the model described in section III-2 .

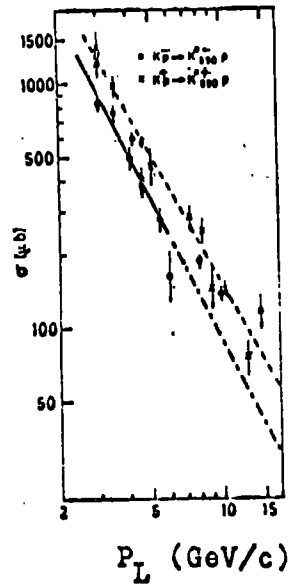


FIG. III-9

From reference 44).  
Total cross-sections for  $K^\pm p \rightarrow K^{*\pm} p$  .

III-3 Model for the  $KN \rightarrow K^*N$  process.

The success and simplicity of the model for  $KN \rightarrow K\Delta$ , developed in the previous section, makes it serve as a guide in constructing an equally good model for the more complicated  $KN \rightarrow K^*N$  channel, to which we now turn. Here, we can have  $\mathbb{P}$ ,  $\mathbb{T}$ ,  $\omega$ -f,  $\rho$ - $A_2$  exchanges. But if the pomeron is an  $SU(3)$  singlet, then, in the limit of exact  $SU(3)$ , it decouples from this reaction, and we do not expect it to become important until all the meson exchanges have become negligible, as is well established experimentally (see figure III-9 - from reference 44) ; but see also reference 52) for a discussion of a possible  $SU(3)$  non-singlet  $\mathbb{P}$ -exchange). As in the previous section, we start by considering the possible Lorentz-invariant, parity conserving couplings of the pseudoscalar and vector meson exchanges to the external particles.

pseudoscalar meson exchange

We first look at pion exchange ; Lagrangian (III-2), together with the usual

$$\mathcal{L} = g_{NN\pi} \bar{\Psi} \gamma_5 \Psi \phi \quad (\text{III-14})$$

coupling of the pion to  $N\bar{N}$  (and these are essentially the only parity conserving couplings available), lead to the following t-channel helicity amplitudes for  $KN \rightarrow K^*N$  (see Appendix C-2) :

$$\begin{aligned}
 T_{K;N\bar{N}}^{(\eta)} &= \bar{v}_{(N)} \gamma_5 \mathcal{U}_{(N)} \frac{g_{KK^*\eta} g_{NN\eta}}{m_\eta^2 - t} P_K^\mu \epsilon_\mu^*(K) = \\
 &= \sigma g_{KK^*\eta} g_{NN\eta} \frac{M t^{1/2}}{m_\eta^2 - t} \frac{\sqrt{a_+ a_-}}{4M^2} (-1)^{N-1/2} S_{N\bar{N}} S_{K0} \quad (\text{III-15})
 \end{aligned}$$

where  $\sigma=1(2)$  for the 'elastic'(cex) reaction - see Appendix D-3 - and  $a_\pm = (M \pm \mu)^2 - t$ . We multiply and divide by the  $K^*$  mass in order to make all factors in this amplitude explicitly dimensionless (to facilitate comparison with  $\eta$ -exchange amplitude for  $K^*N \rightarrow K^*N$  in chapter IV); of course, we could had scaled with any constant  $\sim 1$  GeV.

Amplitudes (III-15) lead to the well-known predictions :

$$\rho_{00} = 1, \quad \rho_{1-1} = \rho_{10} = 0 \quad (\text{III-16})$$

for the decay density matrix elements of the vector meson, when produced via  $\eta$ -exchange only. Although we cannot isolate the  $\eta$ -exchange contribution in  $KN \rightarrow K^*N$ , looking at the data in figures III-14  $\rightarrow$  17 we can make the following simple observations in support of these predictions :

(a) For small  $t$ , where  $\eta$ -exchange is largest, we have a large

$\rho_{00}$  and a small  $\rho_{1-1}$ .

(b) For the cex reaction, where the  $\eta$ -exchange contribution is

doubled, we have a larger  $\rho_{00}$  and a smaller  $\rho_{1-1}$  than in the "elastic" reaction.

(c) As the energy becomes larger,  $\rho_{00}(\rho_{1-1})$  is getting smaller

(larger) (the pion dies down with energy more quickly than the vector and tensor mesons ).

(d) The prediction  $\text{Re } \rho_{10} = 0$  is more or less well satisfied.

We now reggeize amplitudes (III-15) by the substitution :

$$\frac{M t^{1/2}}{m_{\pi}^2 - t} \longrightarrow \frac{1 + e^{-i\pi\alpha_{\eta}}}{2} \left(\frac{s}{s_0}\right)^{\alpha_{\eta}} \quad (\text{III-17})$$

having in mind that the evasive pion ( $\propto t^{1/2}$  35) is ruled out by the data ; by substitution (III-17) we accept the presence of conspiratorial or absorptive effects. Finally, anticipating the work in chapter IV, where we will want to partial wave analyse this amplitude analytically (this was also the reason for choosing an

$\left(\frac{s}{s_0}\right)^{\alpha}$  Regge behaviour, instead of  $\left(\frac{s-u}{2s_0}\right)^{\alpha}$ , as in the

previous section), we make the residue constant, by taking its value at  $t = 0$ . So we end up with :

$$T_{0\frac{1}{2}\frac{1}{2}}^{(\eta)} = \sigma_{\beta} \frac{1 + e^{-i\pi\alpha_{\eta}}}{2} \left(\frac{s}{s_0}\right)^{\alpha} \equiv \pi_0 \quad (\text{III-18})$$

where :

$$\beta = \epsilon_{KK^*\eta} \epsilon_{NN\eta} \frac{M^2 - \mu^2}{4M^2} \quad (\text{III-19})$$

vector meson exchange

We now turn to vector meson exchange ; the only parity



conserving coupling of a pseudoscalar meson to two vector mesons may be written as :

$$\mathcal{L} = g \phi \epsilon_{\mu\nu\rho\sigma} P_k^\mu P_{k^*}^\nu A_{k^*}^\rho A_f^\sigma \quad (\text{III-20})$$

but for the coupling of the vector meson to  $N\bar{N}$  we have several choices, e.g. :

$$g' \bar{\psi} \gamma_\mu \psi A_f^\mu \quad (\text{III-21})$$

$$g' \bar{\psi} \gamma_\mu \psi A_f^\mu, \quad g' \bar{\psi} P_f^\mu \sigma_{\mu\nu} \psi A_f^\nu, \quad \text{etc} \quad (\text{III-21a})$$

(diagram III-2 clarifies our notation )

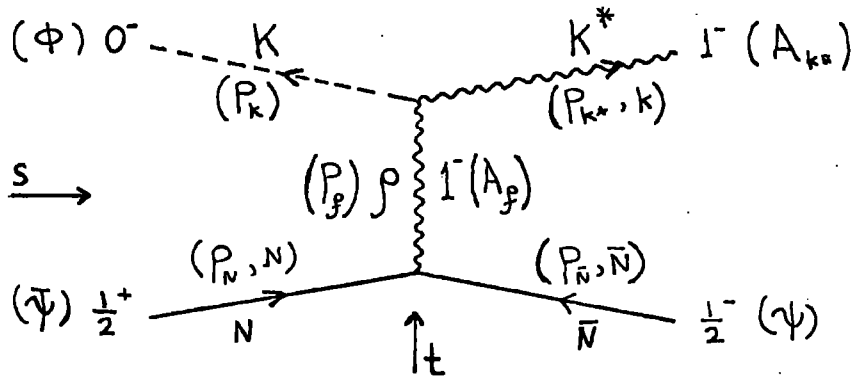


DIAGRAM III-2

Already, success in the previous section, would favour a  $B\bar{B}$  coupling of the type (III-21), which if combined with (III-20) leads to :

$$T_{K;N\bar{N}}^{(M)} = \frac{-ig g'}{m_f^2 - t} \bar{v}_{(N)} u_{(N)} \epsilon_{\nu\rho\mu\sigma} P_k^\nu P_{k^*}^\rho P_N^\mu \epsilon_{(k)}^{\sigma*} \quad (\text{III-22})$$

Notice the similarity between (III-22) and (III-3) : here, we have the  $\mathcal{U}$  and  $\mathcal{E}$  fields uncorrelated ; in order to go from (III-22) to (III-3) we have to couple them into a Schwinger-Rarita spinor  $\mathcal{U} \otimes \mathcal{E}$  . From (III-22) we find (see Appendix C-3) :

$$T_{K;N\bar{N}}^{(M)} = gg' \frac{\sin \theta_t}{m_\rho^2 - t} \frac{(4m^2 - t)(q_+ q_-)^{1/2}}{8\sqrt{2}} \delta_{N\bar{N}} \delta_{|K|1} \quad (\text{III-23})$$

leading to the immediate predictions :

$$\rho_{00} = \rho_{10} = 0, \quad \rho_{1-1} = \frac{1}{2} \quad (\text{III-24})$$

Again, from the data on figures III-14  $\rightarrow$  17, we see that at higher energies, where the pion is small,  $\rho_{1-1}$  approaches 0.5, except at small  $t$  where the pion is largest. The prediction  $\text{Re} \rho_{10} = 0$  persists, and it is always satisfactory.

Consider now Lagrangian (III-20) coupled with a  $B\bar{B}$  current of the form  $\bar{\psi} \gamma_\mu \psi$  . In Appendix C-3 we find :

$$T_{K;N\bar{N}} = \frac{-igg'}{m_\rho^2 - t} \epsilon_{\nu\rho\mu\sigma} P_\nu^\rho P_\mu^\sigma \bar{u}_{(N)} \gamma^\mu u_{(N)} \mathcal{E}_{(K)}^{\sigma*} \quad (\text{III-25})$$

So :

$$T_{0;N\bar{N}} = 0 \quad (\text{III-26a})$$

$$T_{1; \pm \frac{1}{2} \pm \frac{1}{2}} = - \frac{m g g'}{m_\rho^2 - t} \frac{\sin \theta_t}{2\sqrt{2}} (q_+ q_-)^{1/2} \quad (\text{III-26b})$$

$$T_{1; \mp \frac{1}{2} \pm \frac{1}{2}} = \frac{g g'}{m_\rho^2 - t} \frac{1 \pm \cos \theta_t}{2\sqrt{2}} t^{1/2} (q_+ q_-)^{1/2} \quad (\text{III-26c})$$

hence, for the  $K^*$  density matrix elements we get :

$$\rho_{00} = \rho_{10} = 0 \quad (\text{III-27})$$

$$\rho_{1-1} = \frac{1}{2} \frac{\sin^2 \theta_t + \frac{|t|}{m^2} (\cos^2 \theta_t - 1)}{\sin^2 \theta_t + \frac{|t|}{m^2} (\cos^2 \theta_t + 1)} \quad (\text{III-28})$$

That is :

$$\rho_{1-1} \sim \frac{1}{2} \quad \text{for } |t| \sim 0 \quad (\text{III-29a})$$

$$\rho_{1-1} \sim 0 \quad \text{for } |t| \sim m^2 \quad (\text{III-29b})$$

From the data in figures III-14  $\rightarrow$  17 we cannot find evidence in favour of (III-29), on the contrary,  $\rho_{1-1}$ , in general, increases with  $t$ . In fact (III-29b) should persist at all energies, even if  $\pi$ -exchange is appreciable, provided that it mainly contributes to  $T_{0;p\bar{p}}$ , but at no available energy we see evidence for (III-29b). Of course, (III-29a) cannot be checked confidently since at small  $t$ , pion exchange cannot be neglected, even at higher energies.

The above example, shows that  $\Psi \rightarrow \rho \Psi$  is the favoured  $B\bar{B}$  current for this process. Reggeizing (III-23) by substitution (III-11) - but with  $s-u \cong 2s$  - and putting back the  $t$ -channel initial state threshold branch point, which should be present in (III-23) (it contains all other kinematic singularities required <sup>35</sup>), we end up with :

$$T_{1;\frac{1}{2}\frac{1}{2}}^{(M)} = T_{1;\frac{1}{2}-\frac{1}{2}}^{(M)} = \gamma \phi_{(s,t)}^{1/2} \Gamma(1-\alpha) \left(\frac{s}{s_0}\right)^{\alpha-1} \quad (\text{III-30})$$

where strong exchange degeneracy in the form  $f+A_2 = \omega + \rho = 2M$  has been taken into account (see section I-2) and  $\alpha$  is the common  $\rho, A_2, \omega, f$  trajectory.

### Natural-Unnatural parity exchanges

From the above considerations, we have learned two important lessons :

(i)  $\pi$  -exchange contributes mainly to the production of  $K^{*}$ 's with helicity zero, and it is mainly non-flipping the  $N\bar{N}$  vertex.

(ii) Vector (and by exchange degeneracy also tensor) meson exchange produces mainly helicity-one  $K^{*}$ 's, and it is mainly non-flipping.

We now come to consider, what experiment tells us about the relative contributions of natural/unnatural parity exchanges to the various helicity amplitudes for  $K^+p \rightarrow K^{*+}p$ . In figure III-10, we plot the quantities  $\sigma_K^+$  ( $\sigma_K^-$ ), which - in the  $s \rightarrow \infty$  limit - measure <sup>26)</sup> the averaged over  $t$  percentage of natural (unnatural) parity exchange contribution to the production of  $K^{*}$ 's with helicity  $K$  (data from references 42), 45), 46), 47), 49), 50), ). This figure, makes clear that unnatural parity exchange contribution to  $T_{1;N\bar{N}}$  is very small, in fact consistent with zero for  $p_L \geq 4.6$  GeV/c ; on the contrary,  $T_{1;N\bar{N}}$  are mainly fed by natural parity exchanges, as the large  $\sigma_1^+$  indicates, in agreement with the previous conclusion that only  $\omega, f, \rho, A_2$  contribute to  $T_{1;N\bar{N}}$ . Unnatural parity exchanges contribute mainly to  $T_{0;N\bar{N}}$ , and become more important at lower energies, again in support of the previous statement,

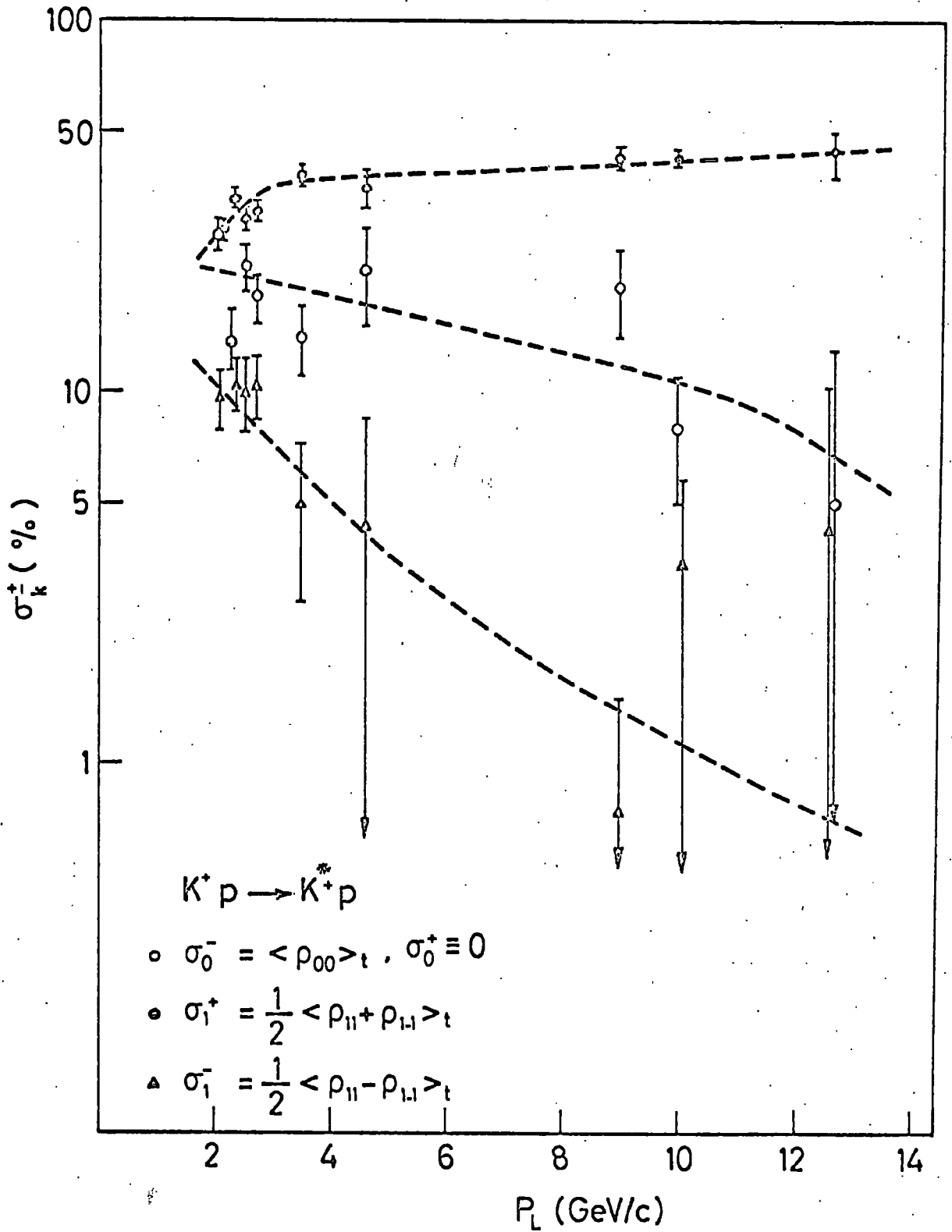


FIG. III-10 Averaged over  $t$  natural/unnatural parity exchange contributions to the production of  $K^{*+}$ 's with helicity  $k=0,1$  as functions of  $p_L$  (curves to guide the eye).

that the pion mainly feeds the  $T_{0;N\bar{N}}$  amplitudes.

Comparison with experiment.

We next come to a quantitative comparison of this model with experiment (selected data from references 42), 45)  $\rightarrow$  51) ; for an exhaustive list of references to data, see reference 62) ). We have our Regge trajectories fixed :

$$\alpha_{\pi} = \alpha'_{\pi} (t - m_{\pi}^2) , \quad \alpha_{\omega} = 1 + \alpha'_{\omega} (t - m_{\omega}^2) \quad (\text{III-31})$$

with slopes also fixed :

$$\alpha'_{\pi} = \alpha'_{\omega} = 1 \text{ GeV}^{-2} \quad (\text{III-32})$$

We then find  $s_0$  from the slope of the dif. cross-sections  $\frac{d\sigma}{dt}$  , and the ratio  $\beta/\gamma$  from  $\beta_{00}/\beta_{1-1}$  .

In figures III-11  $\rightarrow$  13 we plot the dif. cross-sections for  $K^+p \rightarrow K^{*+}p$  at various energies covering the range  $2.11 \leq p_L \leq 12.7 \text{ GeV}/c$  , and the agreement with this model is satisfactory, except for small  $t$  at the lowest energies (The small  $t$  peaks-fig. III-13- are typical evidence <sup>35)</sup> for absorbed  $\pi$  - exchange, while here we have a pure pole model - see section IV-2). There are some over-all normalization problems - the absolute normalization between the curve at 4.6 GeV/c and the group of curves between 2.11 and 2.72 GeV/c differ by a factor of 1.4 which may not be too bad if we remember the inconsistencies between different experiments as far as over-all normalization is concerned. For  $s_0$

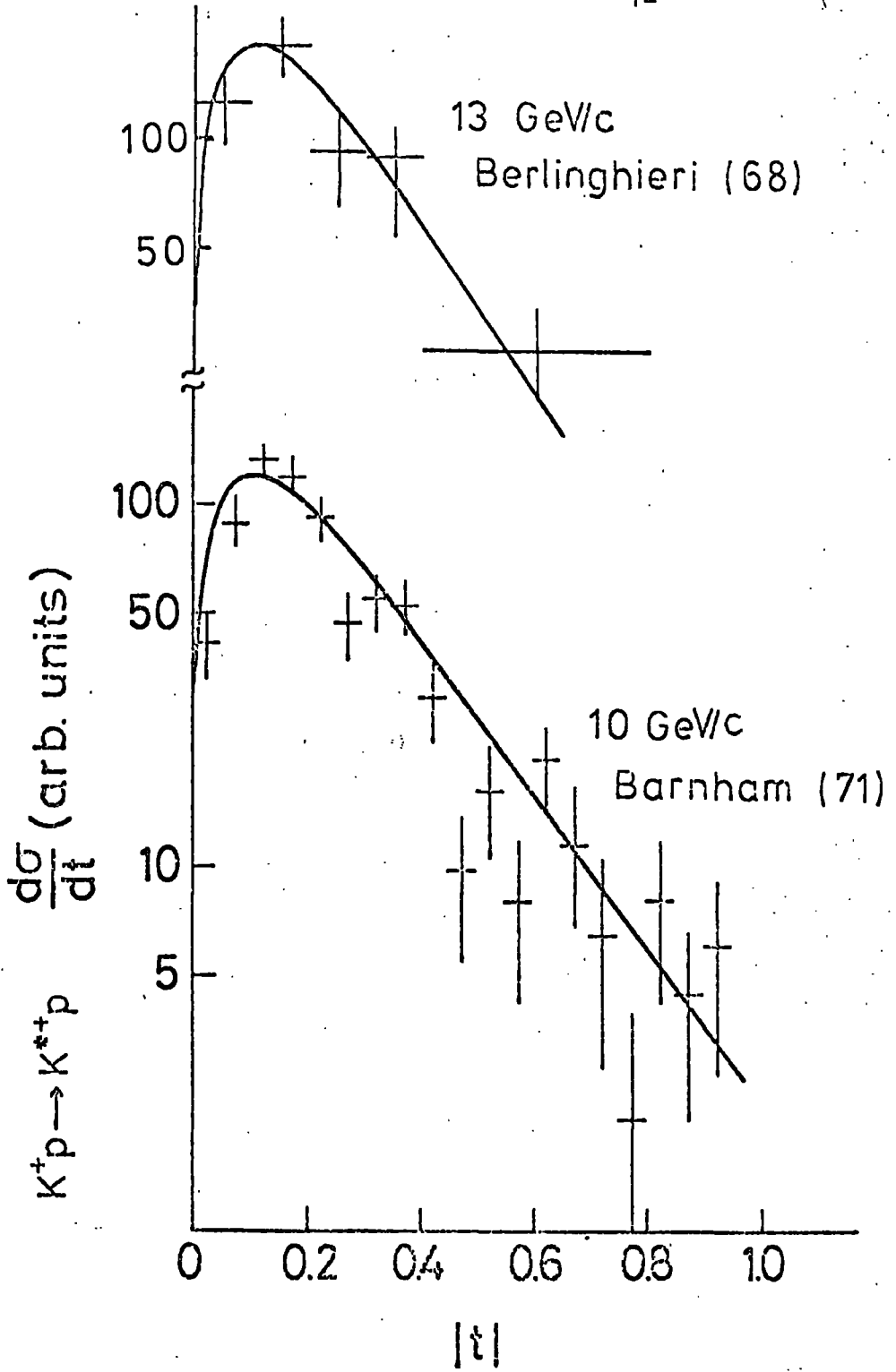


FIG. III-11 Dif. cross-sections for  $K^+ p \rightarrow K^{*+} p$ , compared with the model of section III-3.

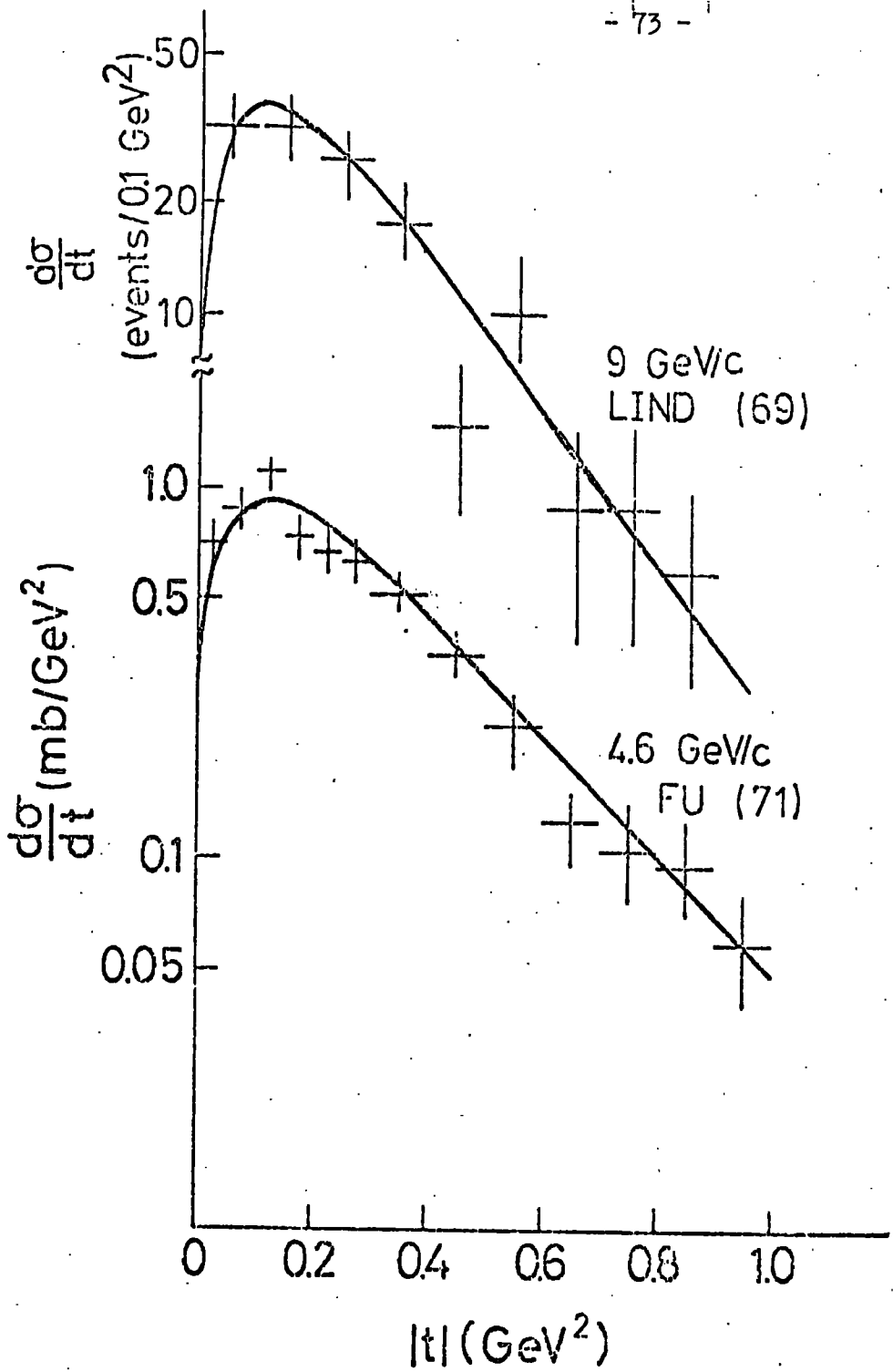


FIG. III-12 Same as in Figure III-11 , at different energies.



Brunet (72)  $\frac{d\sigma}{dt} [K^+p \rightarrow K^{*+}p]$  (mb/GeV<sup>2</sup>)

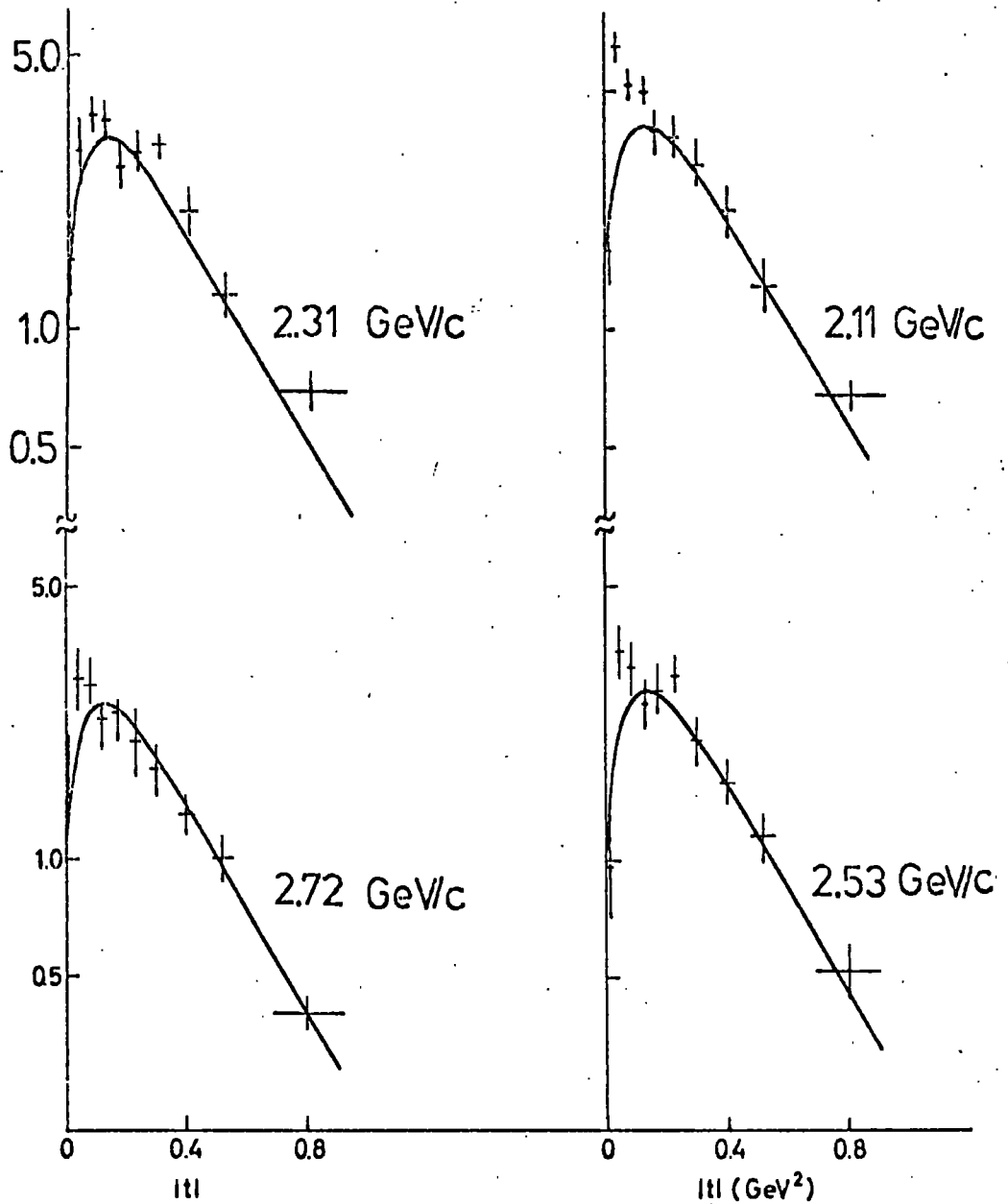


FIG. III-13 Same as in Figure III-11, but at low energies .

we find the natural and satisfactory value :

$$s_0 = 1 \text{ GeV}^2 = \frac{1}{\alpha'_\pi} = \frac{1}{\alpha'} \quad (\text{III-33})$$

in accordance with the Veneziano model.

In figures III-14→16 we plot the corresponding density matrix elements. Again, we have consistency although both  $\rho_{00}$  and  $\rho_{1-1}$  may seem to be somehow large, presumably because we have some contribution from the amplitudes we have completely neglected. In figure III-17 we plot the density matrix elements for  $K^\pm p \rightarrow K^{*\pm} p$  and  $K^\mp p \rightarrow K^{*0} n$  at 4.6 GeV/c (in this model all the corresponding observable quantities  $\frac{d\sigma}{dt}$ ,  $\rho_{00}$ ,  $\rho_{1-1}$ ,  $\rho_{10}$  for  $K^\pm p \rightarrow K^{*\pm} p$ ,  $K^+ n \rightarrow K^{*0} p$  and  $K^- p \rightarrow K^{*0} n$  should be the same). The agreement is satisfactory, and this provides good evidence that we have correctly distributed our exchanges between our amplitudes, and that exchange degeneracy between vector and tensor mesons works (in the  $\pi$  reaction, the pion contribution is doubled; so with  $\rho$  mesons in  $T_{\pm 1; \frac{1}{2} \frac{1}{2}}$ , we correctly predict both the relative magnitudes and the  $t$ -dependence of  $\rho_{00}$ ,  $\rho_{1-1}$ ). We find:

$$\beta / \gamma = 1.34 \quad (\text{III-34})$$

and for the normalized residue constants:

$$\beta = 60, \quad \gamma = 45 \text{ GeV}^{-3} \quad \text{if normalize to ref. 42) } \quad (\text{III-35a})$$

$$\beta = 71, \quad \gamma = 53 \text{ GeV}^{-3} \quad \text{if normalize to ref. 50) } \quad (\text{III-35b})$$

For reasons explained above, in this model the Regge behaviour was given by  $(s/s_0)^\alpha$  with  $s_0 = 1 \text{ GeV}^2$ . The agreement

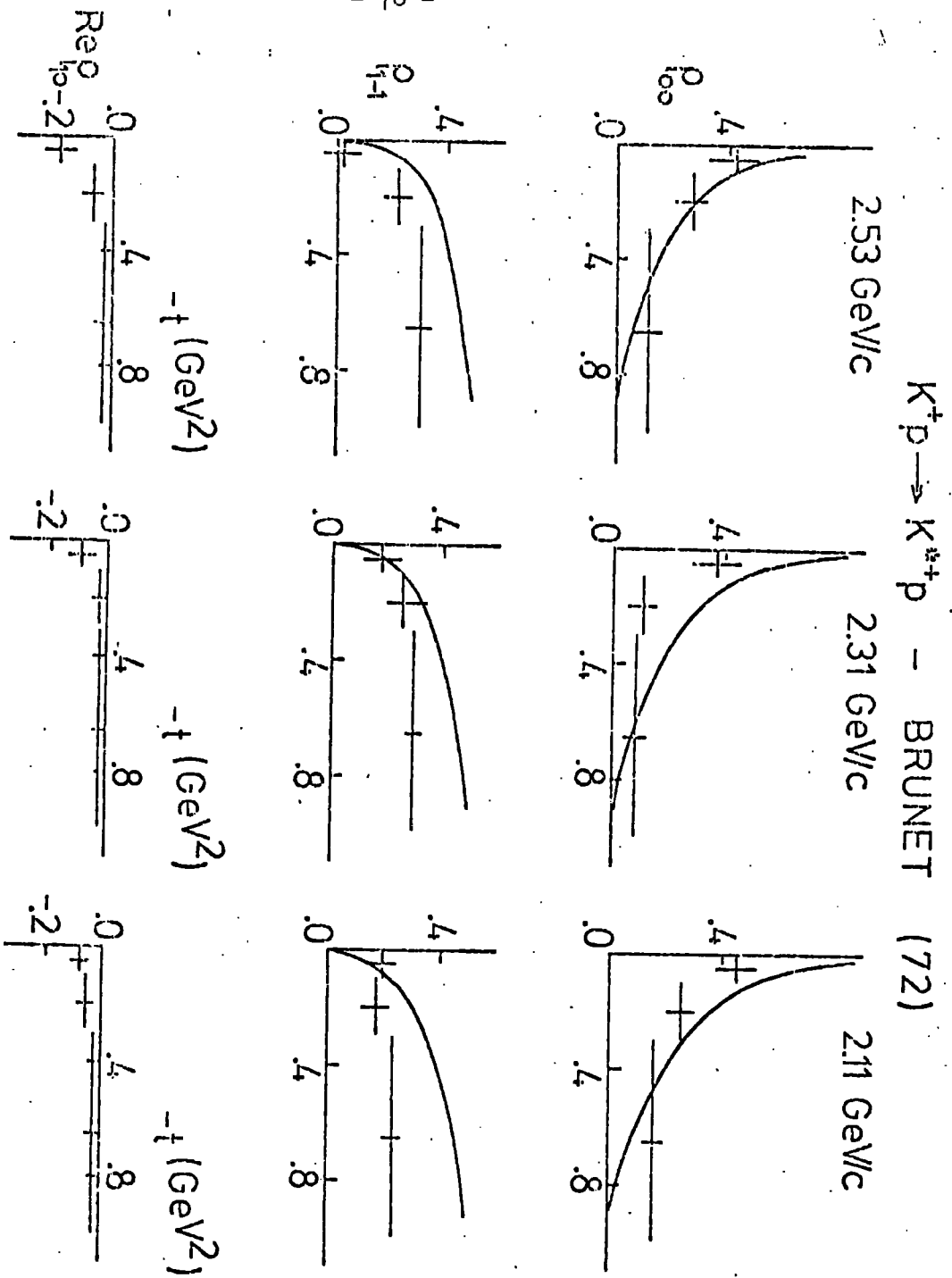


FIG. III-14  $K^{*+}$  production density matrix elements at low energies, compared with the model of section III-3 .

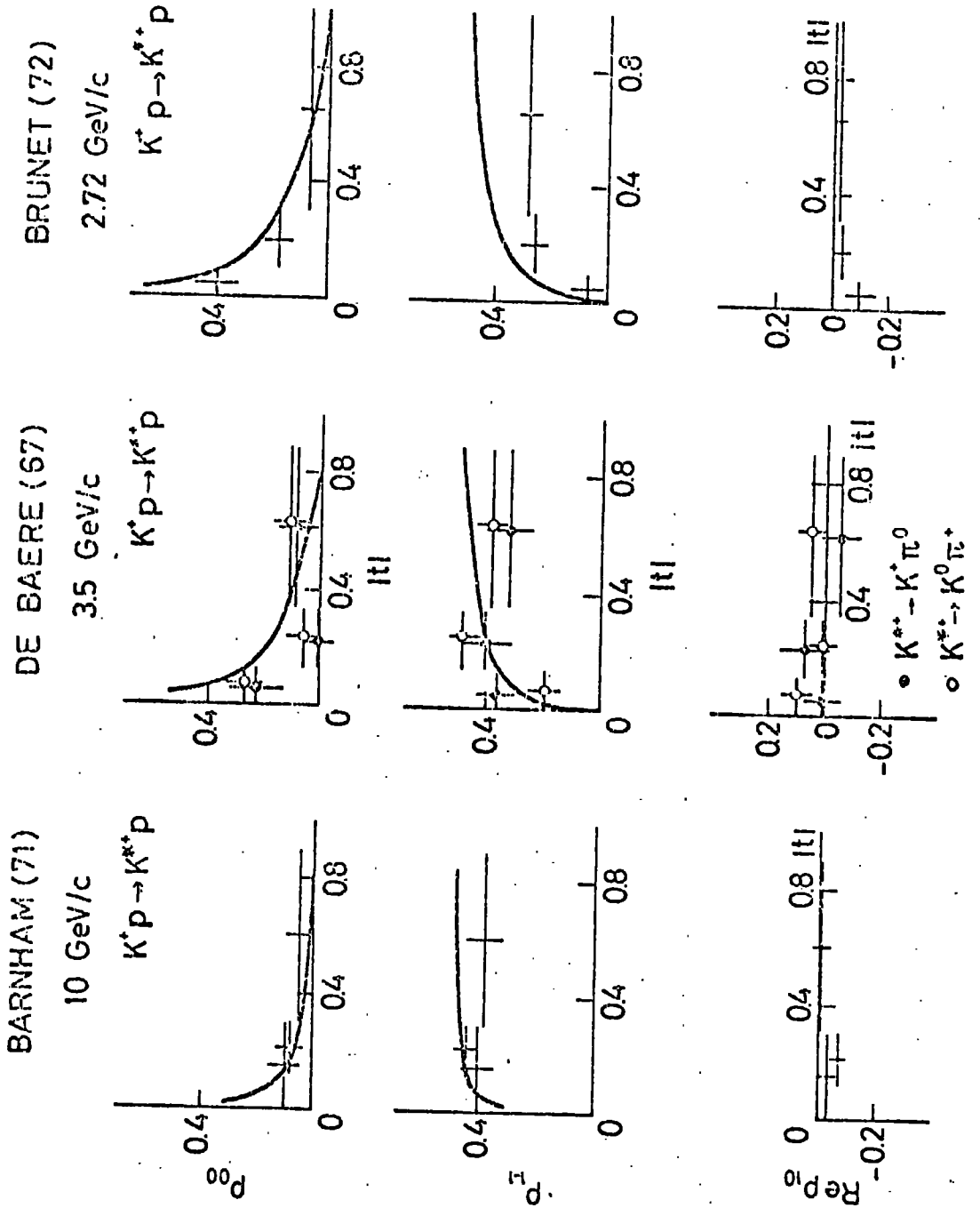


FIG. III-15 Same as in Figure III-14 , at low and higher energies.

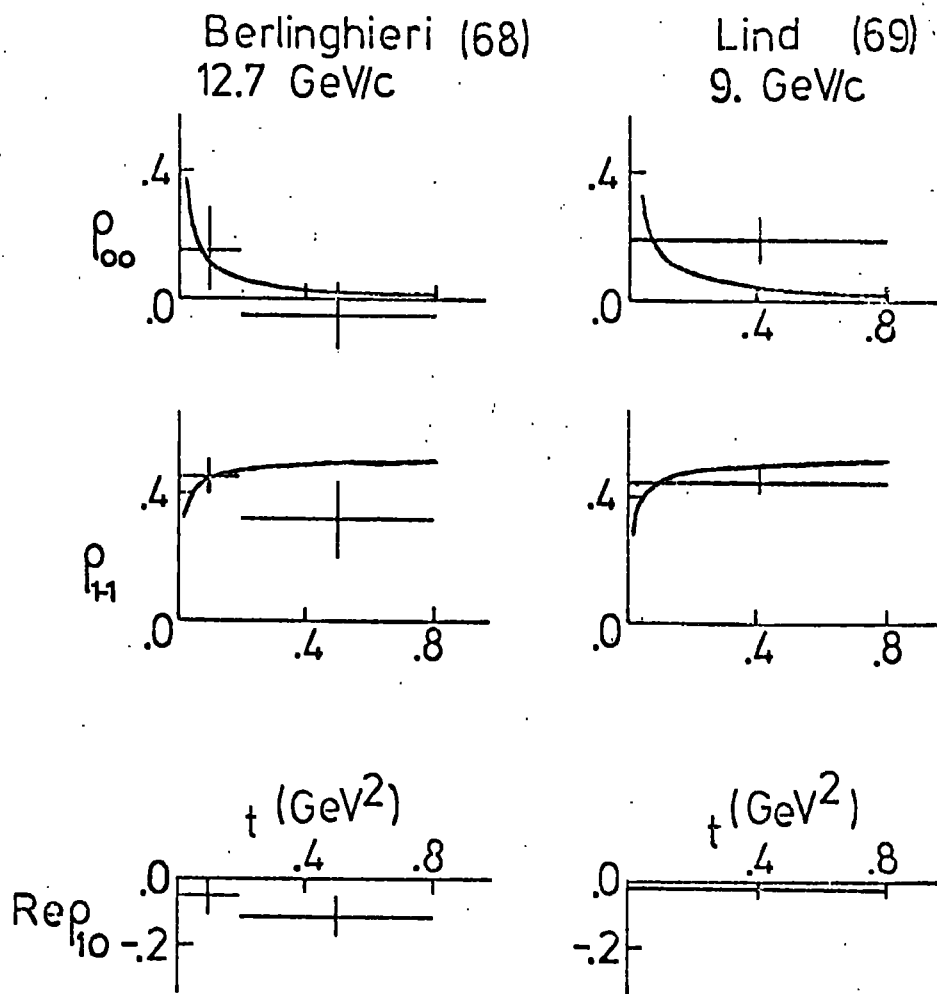


FIG. III-16 Same as in Figure III-14 , at higher energies .

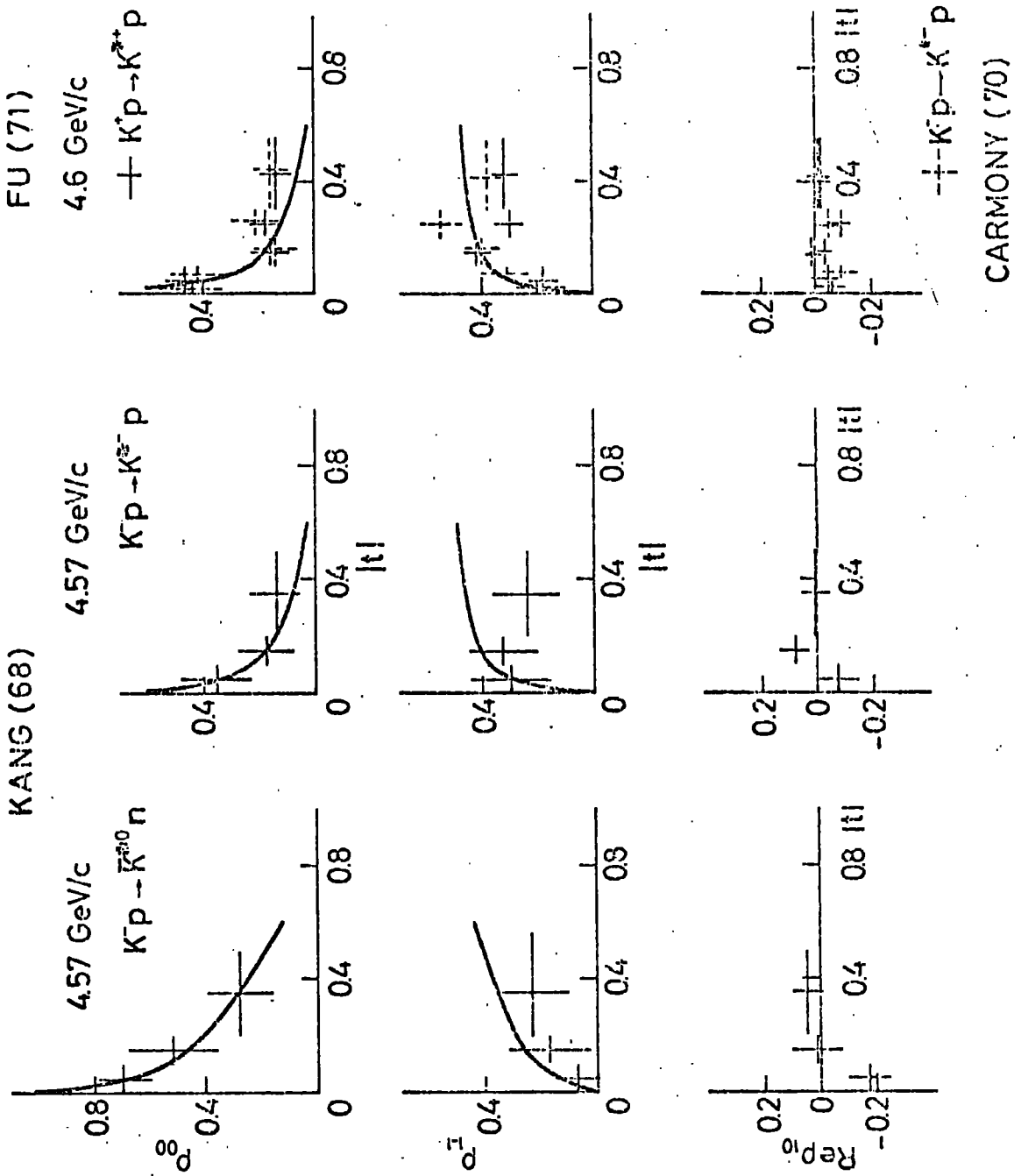


FIG. III-17  $K^{*\pm}$ ,  $K^{*0}$  production density matrix elements, compared with the predictions of section III-3 at various energies.

is generally slightly better if we use  $\left(\frac{s-u}{2s_0}\right)^\alpha$ , with  $s_0 = \sqrt{\mu M m^2}$ , as in the previous section, in which case the model can extrapolate to even lower energies. Note, that the analysis of the t-channel exchange contributions to  $KN \rightarrow K^*N$ , recently done by Michael <sup>52)</sup>, is consistent with the gross features of this model, except from his conclusion  $\omega-f > \rho-A_2$  while here, we have  $\omega-f = \rho-A_2$  ( and a non-flipping  $\rho$  ) which is rather unconventional.

There are two important features of the data ( see e.g. the recent review by Eisner <sup>53)</sup> ) which are not accounted for by this model, namely the striking difference in  $\rho_{1-1}$  between  $K^-p \rightarrow K^{*0}n$  and  $K^+n \rightarrow K^{*0}p$  (  $\rho_{1-1} < 0!$  ), and the difference in slope between the  $K^+p \rightarrow K^{*+}p$  and  $K^-p \rightarrow K^{*-}p$  dif. cross-sections. Now, a pure pole model, cannot accommodate the difference in polarization between  $K^-p \rightarrow K^{*0}n$  and  $K^+n \rightarrow K^{*0}p$ , but a  $\pi$ -cut, interfering with the  $\rho$ -pole, is needed <sup>53)</sup> in order to explain it. On the other hand, one could fit the difference in slope between the  $K^+p \rightarrow K^{*+}p$  and  $K^-p \rightarrow K^{*-}p$  dif. cross-sections by assuming exchange breaking, in which case a different constant  $s_0$  would correspond to each meson. But here, we insisted on a pure pole, exchange degenerate model, in anticipation of the work to follow (see chapter IV) .

III-4 Simple model for elastic  $K^+N \rightarrow KN$  scattering.

We now consider, for completeness, the elastic  $K^+N \rightarrow KN$  channel, which obviously cannot be treated in the same way as  $K^*$  and  $\Delta$  production, since it is known to be dominated by pomeron-exchange. Since only some gross qualitative features of this model are going to be used in chapter IV, we write down the following simple phenomenological amplitudes for pomeron (P) and meson (M) exchanges (as in the past two sections, we assume strong exchange degeneracy between  $\rho, A_2, \omega, f$ ):

$$P_{++} = i s_{op} \sigma_T^{\infty} \left( \frac{s}{s_{op}} \right)^{\alpha_p(t)} \quad ; \quad P_{+-} = 0 \quad (\text{III-36})$$

$$M_{++} = \beta_{++} \left( \frac{s}{s_{oM}} \right)^{\alpha_M(t)} \quad ; \quad M_{+-} = \beta_{+-} |t|^{\frac{1}{2}} \left( \frac{s}{s_{oM}} \right)^{\alpha_M(t)} \quad (\text{III-37})$$

where :

$$\alpha_p(t) = 1 + \alpha'_p t \quad ; \quad \alpha_M(t) = \frac{1}{2} + \alpha'_M t \quad (\text{III-38})$$

and we fix :

$$\alpha'_p = 0.6 \text{ GeV}^{-2} \quad ; \quad \alpha'_M = 1.0 \text{ GeV}^{-2} \quad (\text{III-39})$$

$\sigma_T^{\infty}$  is the total asymptotic  $K^+N$  cross-section, and we take  $\sigma_T^{\infty} = 18 \text{ mb}$ . These amplitudes lead to the following simple expressions for the dif. cross-sections (see also Appendix D-3) :

$$\left. \frac{d\sigma}{dt} \right|_{\text{cex}} = \frac{1}{64\pi p^2} \frac{\beta_{++}^2 + |t| \beta_{+-}^2}{s_{oM}} \left( \frac{s}{s_{oM}} \right)^{2\alpha'_M t} \quad (\text{III-40})$$



$$\left. \frac{d\sigma}{dt} \right]_{el} = \frac{1}{64\pi p^2} \left[ \frac{\beta_{++}^2 + |t| \beta_{+-}^2}{s_{0M}} \left( \frac{s}{s_{0M}} \right)^{2\alpha'_M t} + (\sigma_T^\infty)^2 s \left( \frac{s}{s_{0P}} \right)^{2\alpha'_P t} \right] \quad (\text{III-41})$$

By fitting the cex dif. cross-sections at  $\sim 12 \text{ GeV}/c$  <sup>54), 55)</sup> we can determine  $s_{0M}$  (in order to fit the slope of  $\left. \frac{d\sigma}{dt} \right]$ ) and  $\beta_{++}$ ,  $\beta_{+-}$  (in order to fit the small curvature for small  $t$  of  $\left. \frac{d\sigma}{dt} \right]$ ); we find :

$$s_{0M} = 0.75 \text{ GeV}^2 ; \beta_{++} = 20 , \beta_{+-} = 40 \text{ GeV}^{-1} \quad (\text{III-42})$$

Then, we go to the elastic  $K^+p$  dif. cross-sections <sup>56)</sup> and find  $s_{0P}$ , in order to fit its slope ; we find :

$$s_{0P} = 0.2 \text{ GeV}^2 \quad (\text{III-43})$$

The absolute magnitude of  $\left. \frac{d\sigma}{dt} \right]_{el}$  is correctly predicted by using the values of  $\beta_{++}$ ,  $\beta_{+-}$  found from the cex reactions and  $\sigma_T^\infty = 18 \text{ mb}$ . Figure III-18 shows that this fit is in good agreement with the data.

We next look at the elastic  $K^+p$  polarization ; since

$|P_{++}| \gg M_{++}, M_{+-}$ , we have :

$$P_{K^+p} = \frac{\text{Im}(T_{++}T_{+-}^*)}{|T_{++}|^2 + |T_{+-}|^2} \approx \frac{M_{+-}}{P_{++}} = \frac{\beta_{+-}}{\sigma_T^\infty (s_{0M})^{1/2}} s^{-1/2} |t|^{1/2} \exp \left[ \alpha'_M \lg \frac{s}{s_{0M}} - \alpha'_P \lg \frac{s}{s_{0P}} \right] \quad (\text{III-44})$$

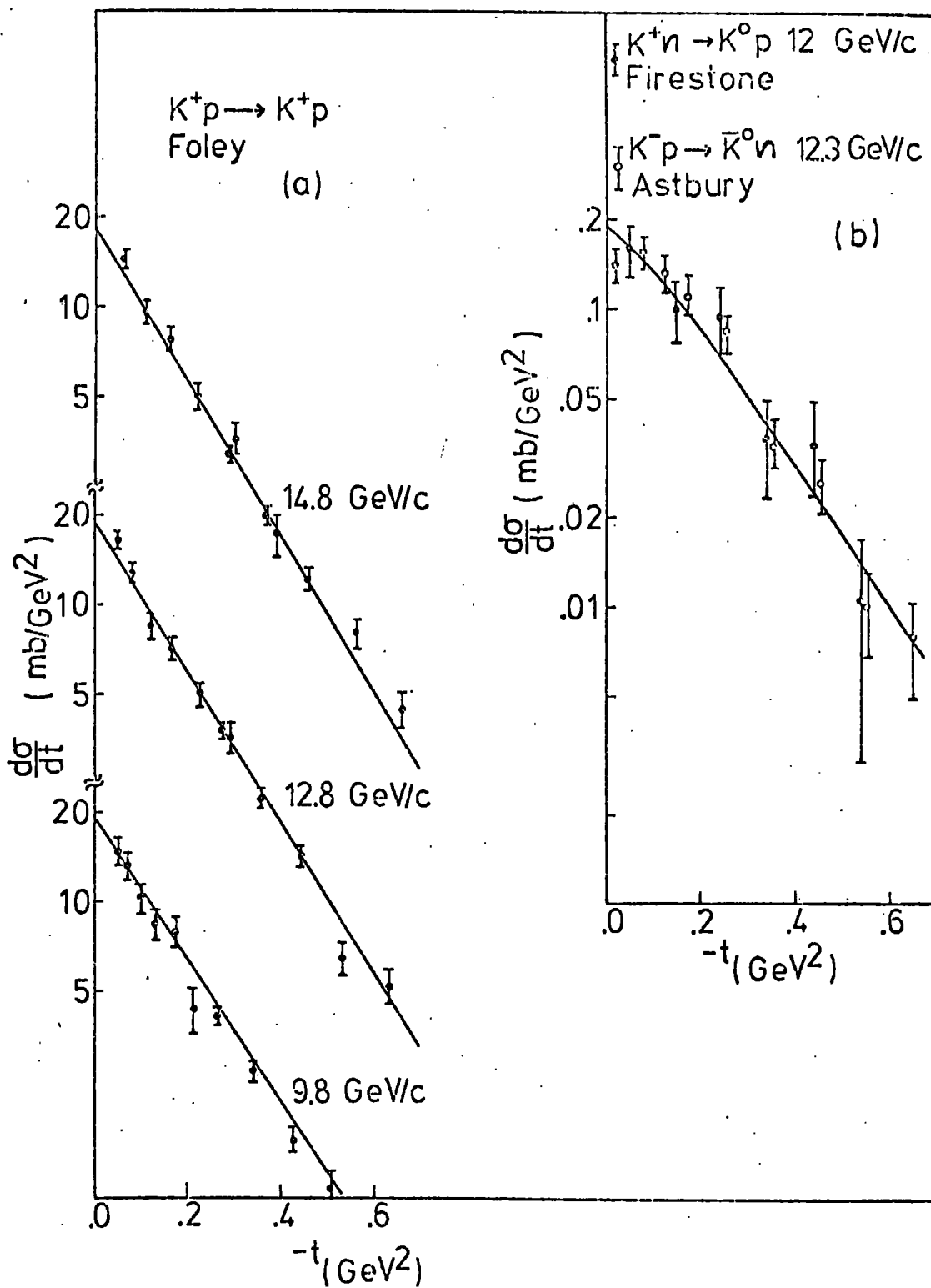


FIG. III-18 Dif. cross-sections for (a)  $K^+p \rightarrow K^+p$  elastic scattering (b)  $K^+n \rightarrow K^0p$ ,  $K^-p \rightarrow \bar{K}^0n$  charge exchange, at high energies, compared with the simple model of section III-4.

In figure III-19 we compare this expression with the data <sup>57)</sup>, and the agreement is not impressive ; the only thing we can say is that we correctly predict the magnitude of the  $K^+p$  polarization.

In this model we have :

$$\left[ M_{p\bar{p}} \right]_{k^-p \rightarrow k^-p} = e^{-i\pi\alpha_M(t)} \left[ M_{p\bar{p}} \right]_{k^+p \rightarrow k^+p} \quad (\text{III-45})$$

so, for the  $K^-p$  polarization, we get :

$$P_{K^-p} = \cos \pi \alpha_M(t) P_{K^+p} \quad (\text{III-46})$$

Hence, by varying  $\alpha_M(t)$ , the model may be able to account for  $K^-p$  polarization as well. So, despite its crudeness, this model is able to account for several features of  $KN \rightarrow KN$  elastic scattering.

Borghini

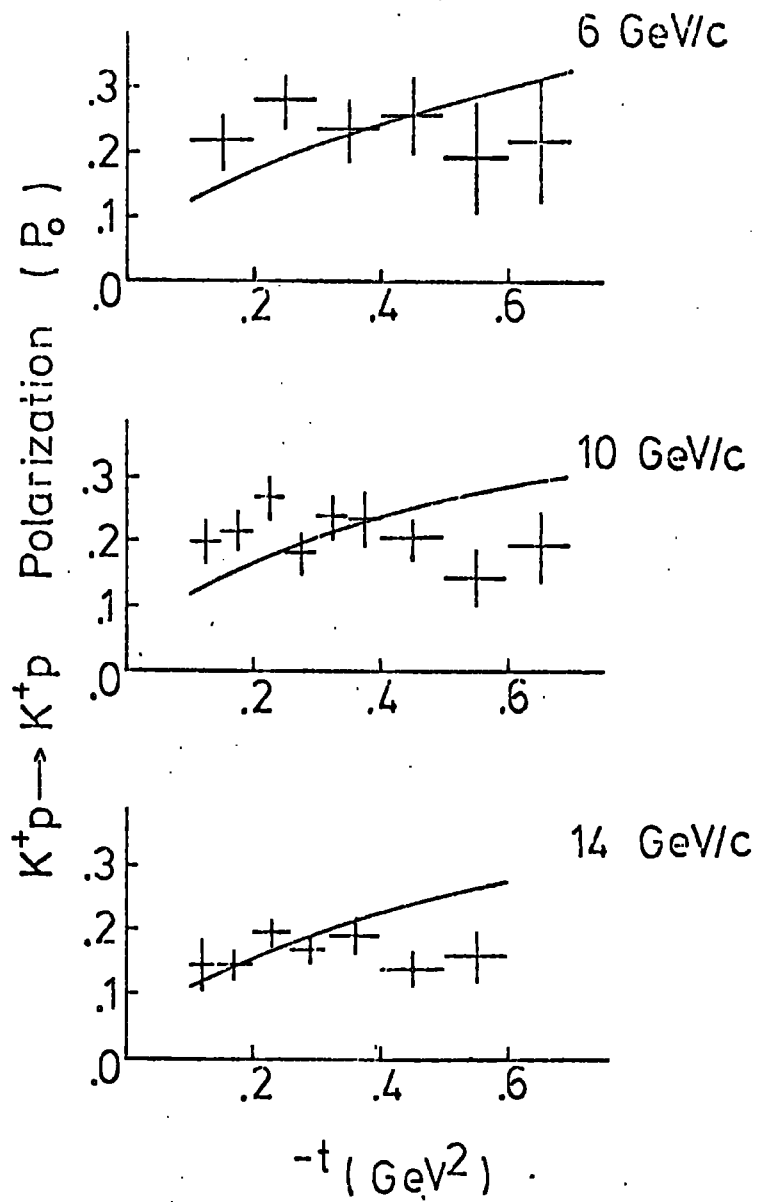


FIG. III-19  $K^+p \rightarrow K^+p$  polarization parameter, compared with the simple model of section III-4 .

III-5 Conclusions.

First of all, we should mention that factorization would immediately lead to predictions (III-6) and (III-24) - for vector and tensor meson exchange only - in  $KN \rightarrow K^* \Delta$ . Now, looking at high energy data for this process (e.g. from reference 45), at  $\sim 13$  GeV/c), where the pion exchange is expected to be smallest, we see that these predictions are no good at all. This observation would lead to the sad conclusion that the couplings which predictions (III-6,24) followed from, are not of universal validity. But, of course, the pion exchange pole is so close to the physical region, that it cannot be assumed <sup>61)</sup> to be negligible even at energies as high as 13 GeV/c.

To conclude, we have shown, that quite simple models for  $KN \rightarrow K\Delta$ ,  $KN \rightarrow K^*N$ ,  $KN \rightarrow KN$ , assuming :

- (i) Strong exchange degeneracy between all  $\rho, A_2, \omega, f$  ;
- (ii) magnetic dipole type transition at the  $N\Delta\rho$  vertex for  $KN \rightarrow K\Delta$ , while having the behaviour of the amplitudes at t-channel thresholds and pseudothresholds determined by the chosen Lorentz-invariant couplings (and this behaviour turns out to be the same as suggested by crossing matrix or t-channel angular momentum considerations) ;

(iii) coupling of the vector mesons to the  $N\bar{N}$  pair of the form

$\bar{\Psi} \gamma_\mu \Psi A_\mu$  for  $KN \rightarrow K^*N$ , while not caring much about the residue structure of the pion exchange amplitudes (we are using these amplitudes far from the t-channel thresholds and pseudothresholds) ;

(iv) large  $P$ -exchange contribution in elastic  $KN \rightarrow KN$  scattering, are able to give a satisfactory over-all description of the dif. cross-sections and production density matrix elements over a rather wide range of energies, although there are aspects of the data in disagreement with these models, the most serious of which seems to be a negative  $\rho_{1-1}$  for  $K^+n \rightarrow K^{*0}p$ .

# CHAPTER IV

## LOW ENERGY ISOSCALAR KN SCATTERING.

### IV-1 Introduction.

Although much work, both theoretical and experimental has been done <sup>63),64)</sup> towards the understanding of the actual cause of the bumps seen in the total  $K^+N$  cross-sections, (see Figures IV-1,2 from references <sup>65)</sup> and <sup>70)</sup> ) it is not clear yet whether they are to be associated with "exotic" resonances or not. For an excellent review of the experimental situation, and a description of several phase shift analyses and related work, we refer to Dowell's review <sup>63)</sup> ; here, we are going to review very briefly those works of most immediate connection to ours.

In particular, Aaron Amado and Silbar <sup>66)</sup> , get two highly inelastic  $Z_0^*$ 's with  $J^P = \frac{1}{2}^- , \frac{3}{2}^-$  just above the  $K^+N$  threshold, driven by the rapid opening of this channel and a subsequent modified phase shift analysis <sup>67)</sup> , with some theoretical input (inelasticity parameters  $\eta$  ) from that calculation, confirms these results, and shows that such resonances would not conflict with the established  $\rho^-A_2$  exchange degeneracy. It is interesting

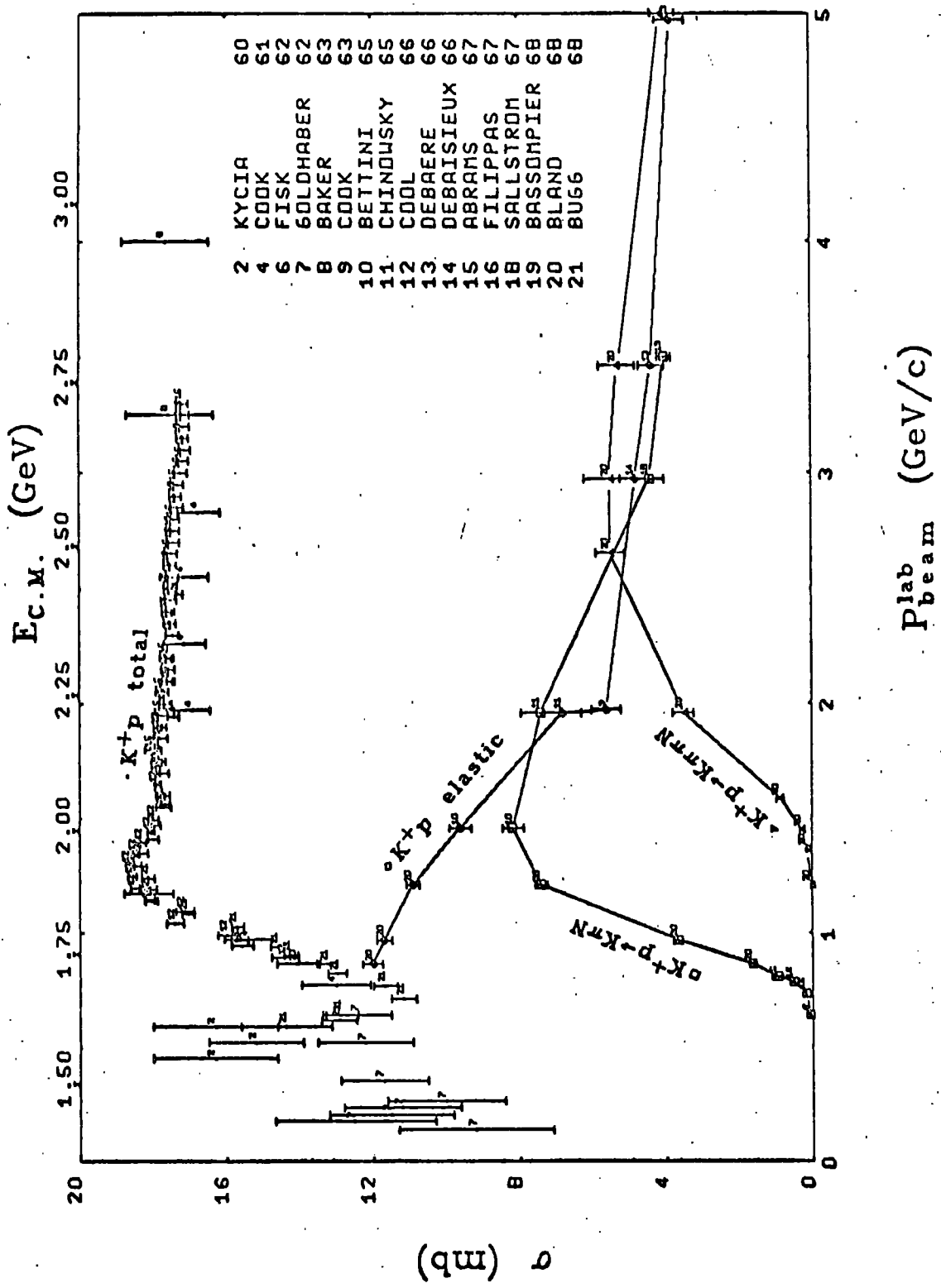


FIG. IV-1 From reference 65).  
 $K^+p$  ( $I=1$ ) total, total elastic, one, and two pion production cross-sections.



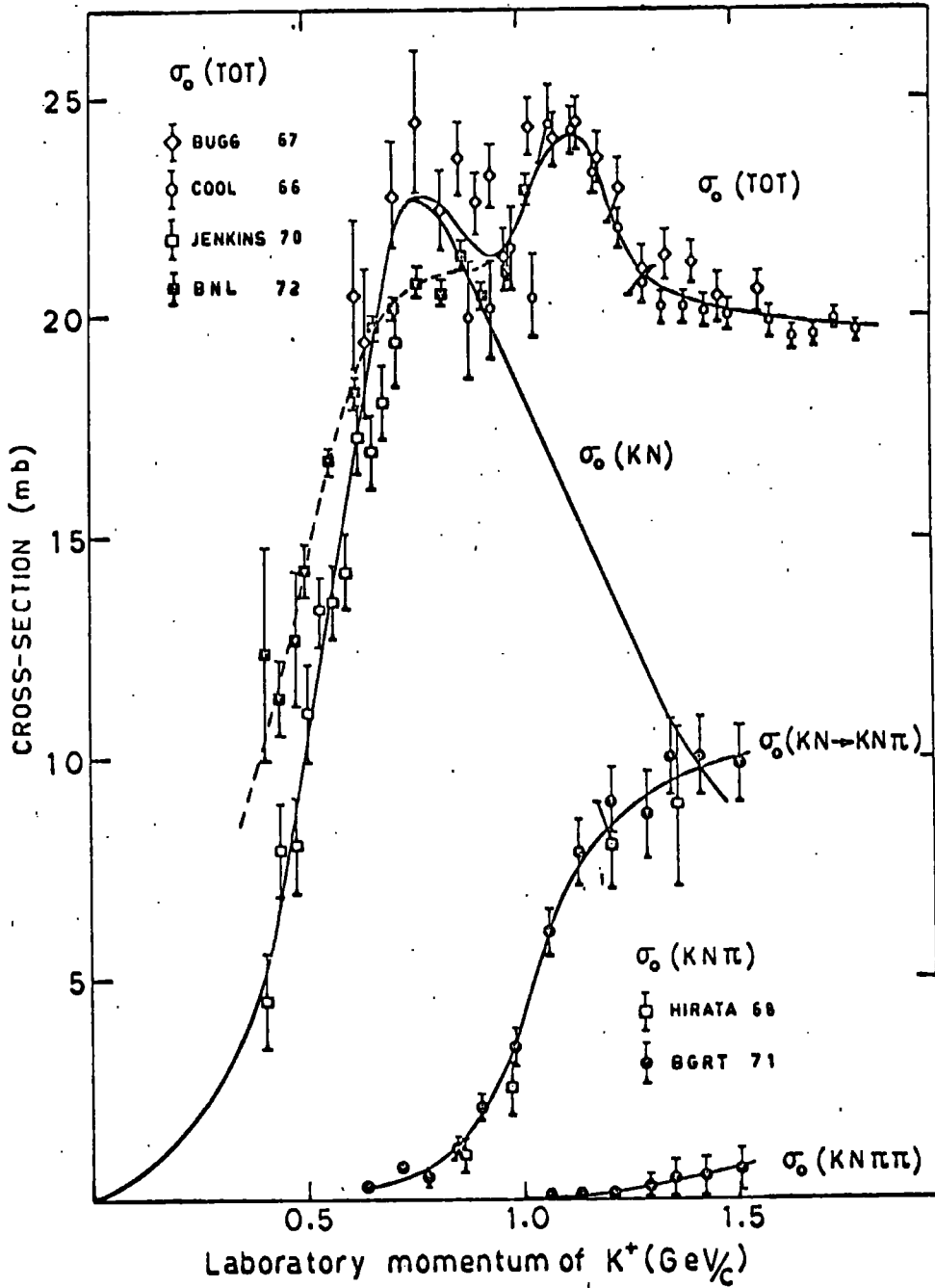


FIG. IV-2 From reference 70).  
Same as in Figure IV-1, but corresponding to the  $I=0$  channel.

to note that calculations on the same lines <sup>68)</sup>, show that some known  $\pi$ -N resonances are driven in the same way, by the rapid opening of the  $\rho$  and  $\Delta$  production channels in  $\pi$ N scattering.

More recently, strong evidence for an elastic  $Z_0^*$  in the  $P_{01}$  wave, below the  $K^*N$  threshold ( $\sim 1.70$  GeV) is found <sup>69)</sup> in Hedegaard-Jensen, Nielsen and Oades's KN scattering calculations using partial wave dispersion relations, in the same fashion as in  $\pi$ -N scattering.

BGRT Collaboration's most recent  $I = 0$  phase shift analysis <sup>70)</sup>, has two solutions (C and D, consistent with cex polarization) with a large, highly elastic, looping counterclockwise  $P_{12}$  wave below the  $K^*N$  threshold. If the favoured solution D is assumed to be resonant, and fitted with a Breit-Wigner form plus a quadratic background, the fit yields a resonance mass of 1.74 GeV ( $\sim 1.80$  GeV in the previous BGRT  $I=0$  KN phase shift analysis <sup>71)</sup>, 1.78 GeV in the Particle Data Group tables <sup>64)</sup>), with a width of about 0.3 GeV and an elasticity of  $x = 0.85$ .

The results of many existing phase shift analyses of the  $I = 1$  channel <sup>63),64)</sup>, are rather inconclusive <sup>63)</sup>; but the clear bump in the  $I = 0$  elastic cross-section at  $p_L \simeq 0.7$  GeV/c (see Figure IV-1b), and the suspicion that the  $\pi$ -exchange in  $KN \rightarrow K^*N$  (which is a 9 times larger effect in the  $I = 0$ , than in the  $I = 1$  cross-section) would be responsible <sup>66),67)</sup>, via unitarity, for any duality breaking effects (see also section IV-6), hint that the best place to look for any  $Z^*$ 's is the  $I = 0$  channel. In the following, we are going to concentrate on isoscalar KN scattering,

not only because of the above mentioned reasons, but also because of the relative simplicity of this channel : The dominant  $K\pi N$  inelastic channel ( $K\eta\pi N$  may be neglected below:  $s^{\frac{1}{2}} \approx 2.0$  GeV ) is almost exclusively ( $\sim 90$  %) taken up by  $K^*N$ . So, in the suspected mass region of a possible  $Z_0^*$  ( $1.7 \lesssim s^{\frac{1}{2}} \lesssim 2.0$  GeV ), we have, to a good approximation, to deal with a two-channel problem, since the narrow  $K^*$  may be treated as stable without essentially affecting reality. In the  $I = 1$  channel, not only is there the additional  $K\Delta$  threshold, but also the wider  $\Delta$  could less realistically be treated as stable.

IV-2 Philosophy:

To proceed, we adopt the following philosophy, which has been developed by several authors (73)→(76), (78) as discussed below, and is described in the following three steps :

(i) We start, by constructing a non-unitary Born approximation for the two channel ( $K^+N$ ,  $K^{*+}N$ ) problem, in the form of non-diffractive, high energy, Regge pole amplitudes. Exact duality (72), hence strong exchange degeneracy will be assumed in this input stage. Already, the work in chapter III provides us with the necessary  $KN \rightarrow KN$  and  $KN \rightarrow K^*N$  amplitudes, in the required form; in the following section we are going to estimate the  $K^*N \rightarrow K^*N$  amplitudes, through  $SU(6)$ .

(ii) We extrapolate our input Regge models down to the  $K^*N$  threshold region. Duality is the guiding principle, but some care is required since our amplitudes are predominantly real, and it is not easy to understand how can only two channels contributing, in our simple model, to the unitarity sum :

$$\frac{1}{s} \text{Im} T_0(s,0) \propto \frac{1}{s^2} \int dt \sum_{\eta=0}^1 \left[ \text{Im} T_{\eta}(s,t) \right]^2 + \frac{1}{s^2} \int dt \sum_{\eta=0}^1 \left[ \text{Re} T_{\eta}(s,t) \right]^2 \quad (\text{IV-1})$$

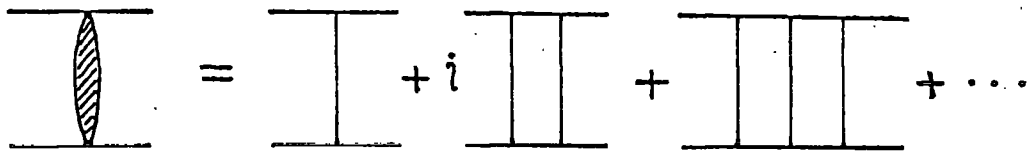
$$( 0 = [K^+N \rightarrow KN] , 1 = [K^+N \rightarrow K^*N] )$$

add up to make the second term on the right hand side of (IV-1) constant (The  $P$  is the main contributor to  $\text{Im} T_n$ , while  $\text{Re} T_n \propto s^{\alpha_n}$ ). However, the success of our models in chapter III in fitting the data from  $p_L \approx 13 \text{ GeV}/c$  down to  $p_L \approx 2 \text{ GeV}/c$ , justifies this extrapolation (the  $K^*N$  threshold is at  $p_L \approx 1.4 \text{ GeV}/c$ ).

(iii) We interpret these "input" Regge pole amplitudes as K-matrix elements, and find the unitary, corrected for cuts <sup>35)</sup> T-matrix :

$$T = K(I - i\rho K)^{-1} = K + i\rho K \cdot K - \rho^2 K \cdot K \cdot K - \dots \quad (\text{IV-2})$$

or, in a pictorial notation :



Thus, we build the low energy pomeron, from purely non-diffractive high energy scattering <sup>73)</sup> - any t-channel structure found as output will be dual to this pomeron. This K-matrix unitarization is what will effectively introduce the necessary absorption of  $\pi$ -exchange in  $KN \rightarrow K^*N$ , which, as pointed out at the last subsection of section III-3, was the reason for the small t peaks of  $K^+p \rightarrow K^{*+}p$  dif. cross-section (Fig. III-13), not described by our input pure pole model of section III-3. One could also hope that the effective cut corrections introduced in this way might also explain the difference in polarization between  $K^-p \rightarrow K^{*0}n$  and  $K^+n \rightarrow K^{*0}p$  (see section III-3), but we do not want to pursue this point further.

Explicit calculations along the above lines have been proved successful in the past. In particular, Lovelace first identified <sup>74)</sup> partial wave projections of the  $B_4$  amplitudes (which have poles on the real axis) for the coupled  $\pi\pi, \bar{K}K$  system, with K-matrix elements, and successfully calculated  $\pi\pi$  phase shifts. For the  $I = 2$  smooth "exotic" channel, the full  $B_4$  structure is irrelevant, and simpler estimates of the Regge exchanges are equally successful. Also, unitarizing Regge amplitudes by the same method, he was able to make good few parameter fits for  $\pi N, KN, \bar{K}N$

scattering <sup>75)</sup>. On similar ideas, the Schrempp's Finite Energy Sum Rules (FESR) <sup>76)</sup> are based : FESR, for pole terms only, are written for processes in which both poles and cuts are important, where the bare poles are identified with K-matrix elements ; then, e.g. the K-FESR for the  $\rho$ -pole exchanged in  $\pi^- p \rightarrow \eta^0 n$  is satisfied more accurately and more locally than the usual <sup>77)</sup> FESR. The idea of building the Pomeron ( $\mathbb{P}$ ) via equation (IV-2), from pure Reggeon exchange is employed in Drechsler's calculation <sup>78)</sup>, from which he gets a reasonable output  $\mathbb{P}$ . Similar ideas are also applied in calculating the  $\mathbb{P}$  contribution for the  $K^+ p$  channel specifically <sup>79)</sup>.

The important new feature which we have present in this problem, is large  $\eta$ -exchange amplitudes in the  $KN \rightarrow K^* N$  and  $K^* N \rightarrow K^* N$  channels. We shall presently show that, in the  $I = 0$  channel, all vector and tensor meson amplitudes in  $KN \rightarrow KN$  and  $KN \rightarrow K^* N$  may be neglected, to a good approximation, as compared with  $\eta$ -exchange in  $KN \rightarrow K^* N$ . Guided by this result, we shall assume later that only  $\eta$ -exchange is important for  $K^* N \rightarrow K^* N$  as well (we consistently neglect the  $\mathbb{P}$  as input). This is the decisive simplification which allows an analytic solution. For the  $I = 0$   $KN \rightarrow K^* N$  (see Appendix D-3) and at  $s^{\frac{1}{2}} = 1.83$  GeV where the amplitudes are to be unitarized, the model developed in section III-3 predicts the ratio of  $\eta$ -exchange (III-18) to M-exchange amplitude (III-30) to be  $|\eta/M| \simeq 7$  at  $t = -0.05$  GeV<sup>2</sup> falling to  $|\eta/M| \simeq 2$  at  $t = -0.5$  GeV<sup>2</sup>. So, it is an excellent approximation, especially after partial wave projection, to retain only the  $\eta$ -exchange amplitude as far as the low energy,  $I = 0$   $K^*$  production

is concerned. To see that M-exchange amplitudes in KN elastic scattering are very small as compared with the  $\pi$ -exchange ones in  $K^*$  production, it suffices to observe that the ratio of  $K^\pm$  cex cross-sections (54), (55), (80), to non-cex  $K^*$  production cross-sections (41), (42), (45)  $\rightarrow$  (50) ( $\pi$ -dominated), is about 1/5 for small  $t$ . More quantitatively, the model amplitudes (III-37) for  $KN \rightarrow KN$  constructed in section III-4, together with the  $\pi$ -exchange amplitude (III-18) for  $K^*$  production, predict the ratio of the real part of  $\pi$ -exchange to non-flip (flip) meson exchange amplitudes

to be about  $\frac{\text{Re}\pi}{M_{++}} \approx 5$   $\left( \frac{\text{Re}\pi}{M_{+-}} \approx 10 \right)$  at  $t = -0.05 \text{ GeV}^2$ , falling to about  $\frac{\text{Re}\pi}{M_{++}} \approx 2.5$   $\left( \frac{\text{Re}\pi}{M_{+-}} \approx 2 \right)$  at  $t = -0.5 \text{ GeV}^2$ , for the  $I = 0$

channel and at  $s^{\frac{1}{2}} = 1.83 \text{ GeV}$ . Figure IV-3 demonstrates these results. On the same figure, we also plot the ratio of the real part of the  $\pi$ -exchange amplitude to its imaginary part,

$\frac{\text{Re}\pi}{\text{Im}\pi}$ , to demonstrate that especially after partial wave projection, it may be considered as real, to a good approximation. We will identify with  $K^{J^\pm}$  matrix elements the real parts of the  $\pi$ -exchange partial wave amplitudes,  $\text{Re } \pi^{J^\pm}$ , but numerically  $|\pi^{J^\pm}|$  are checked to be little different, so little or no ambiguity in this identification is present.

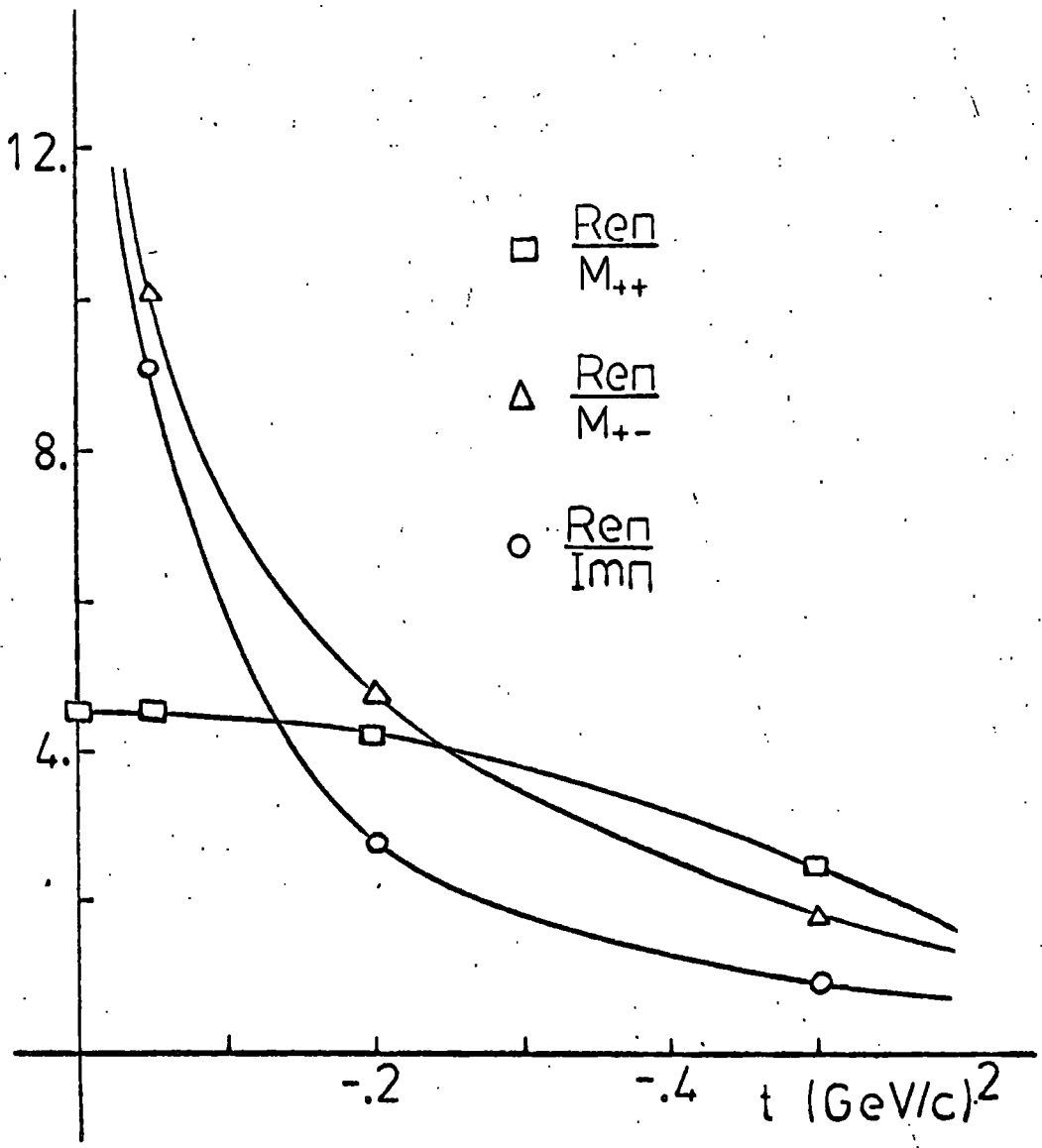


FIG. IV-3 The ratios  $\frac{\text{Re}\pi}{\text{Im}\pi}$ ,  $\frac{\text{Re}\pi}{M_{++}}$ ,  $\frac{\text{Re}\pi}{M_{+-}}$ , as explained in section IV-2, for  $I=0$  and at  $\sqrt{s}=1.83$  GeV.



IV-3 Model for the  $K^*N \rightarrow K^*N$  channel.

Unitarity couples in the channel  $K^*N \rightarrow K^*N$ , and it turns out that it is important in determining the properties of the elastic  $KN$  scattering output in our model. We can again have  $\pi$ ,  $M$ ,  $\mathbb{P}$  exchanges in the t-channel, but we need only be concerned with  $\pi$ -exchange, since we neglect all diffractive amplitudes in the input, and guided by the  $KN \rightarrow K^*N$  results, we assume that all vector and tensor meson exchanges may be neglected as compared to the  $\pi$ -exchange. We proceed as in chapter III, and using Lagrangians (III-14, 20) (which are essentially unique), we calculate in Appendix C-2 the following t-channel Born helicity amplitudes for pseudoscalar meson exchange in  $K^*N \rightarrow K^*N$  :

$$\Pi_{K^*N; N\bar{N}}^* = \sigma g_{K^*K^*\eta} g_{NN\eta} \frac{t}{m_\eta^2 - t} \frac{(4M^2 - t)^{1/2}}{4} (-1)^{N - \frac{k}{2}} \delta_{N\bar{N}} \delta_{K^*K^*} \delta_{|K|1} \quad (IV-3)$$

where  $\sigma = 1(2)$  for elastic (cex) scattering (see Appendix D-3).

We can confirm which amplitudes are non-vanishing by simple t-channel angular momentum-parity considerations. Analogously to (III-17), we reggeize (IV-3) by the substitution :

$$\frac{M^2}{m_\eta^2 - t} \longrightarrow \frac{1 + e^{-i\pi\alpha_\eta}}{2} \left( \frac{s}{s_0} \right)^{\alpha_\eta} \quad (IV-4)$$

As with (III-17), there may be some ambiguity as far as the scaling constant is concerned ; we again choose here the  $K^*$  mass,  $M$ .

Note, that here the evasive pion ( $\alpha t^1$  35) is required by unitarity and analyticity - otherwise we would get s-channel p-waves

not vanishing at threshold\*. Taking again the value of the residue at  $t = 0$  we end up with the following non vanishing  $t$ -channel helicity amplitude (no nucleon flip allowed) :

$$\Pi_{11}^* = \lambda \frac{|t|}{M^2} \frac{1 + e^{-i\pi\alpha_\eta}}{2} \left(\frac{s}{s_0}\right)^{\alpha_\eta} \quad (\text{IV-5})$$

where : -see (III-19)-

$$\lambda = \frac{M}{2} g_{K^*K^*\eta} g_{NN\eta} = \frac{2M^3}{M^2 - \mu^2} \frac{g_{K^*K^*\eta}}{g_{KK^*\eta}} \beta \quad (\text{IV-6})$$

Thus, our procedure starting with elementary particle exchange, was able to determine the awkward  $K^*N \rightarrow K^*N$  channel from the measurable  $KN \rightarrow K^*N$  scattering in terms of one parameter, namely the ratio of coupling constants  $g_{K^*K^*\eta} / g_{KK^*\eta}$ . This parameter may be determined by SU(6) to be <sup>81)</sup> :

$$\frac{g_{K^*K^*\eta}}{g_{KK^*\eta}} = \frac{2}{3} \frac{1}{m_\rho} \left(\frac{m_\rho}{M}\right)^2 \left[ 2 + \left(\frac{m_\rho}{M}\right)^2 \right] \quad (\text{IV-7})$$

and in the approximation  $M = m_\rho$ , we get

$$\frac{\lambda}{M^2} = \frac{4}{M^2 - \mu^2} \beta \quad (\text{IV-8})$$

---

\* In this case,  $\left\{ \text{reggeize by : } \frac{t}{m_\pi^2 - t} \implies g_\eta \left(\frac{s}{s_0}\right)^{\alpha_\eta} \right\}$  one would have to introduce the proper threshold behaviour, when required, by hand. We have checked that - providing the constant  $\beta$  remains the same - this would not alter qualitatively our results in section IV-4 (but would lead to a somehow lighter  $Z_0^*$ ).

In the following table IV-1, we summarize the non-diffractive, pure pole, high energy t-channel pion exchange amplitudes, which, if extrapolated to low energy, dominate the  $KN \rightarrow K^*N$  and  $K^*N \rightarrow K^*N$  processes near the  $K^*N$  threshold for  $I_S = 0$ .

TABLE IV-1

$KN \rightarrow K^*N : \quad \Pi_0 = \beta \frac{1+e^{-i\pi\alpha_\eta}}{2} \left(\frac{s}{s_0}\right)^{\alpha_\eta}$	$\alpha_\eta = \alpha'_\eta(t - m_\eta^2)$ $\alpha'_\eta = 1 \text{ GeV}^{-2}$
$K^*N \rightarrow K^*N : \quad \Pi_{11}^* = \frac{4 t }{M^2 - \mu^2} \beta \frac{1+e^{-i\pi\alpha_\eta}}{2} \left(\frac{s}{s_0}\right)^{\alpha_\eta}$	$s_0 = 1 \text{ GeV}^2$ $\beta = 65$

IV-4 Phase shifts.

As explained in section IV-2, we now imagine the input amplitudes, in table IV-1, being extrapolated near the  $K^*N$  threshold. Since we shall presently need the s-channel partial waves, we now have to cross these low energy, t-channel amplitudes into the s-channel. Luckily enough, the limits of the crossing angles (F-11) for our processes, as  $q \rightarrow 0$  ( $s^{\frac{1}{2}} \rightarrow 1.83$ ,  $K^*N$  threshold) are very simple - see equations (E-3,4) - and the crossing matrices (F-10) corresponding to  $KN \rightarrow K^*N$  and  $K^*N \rightarrow K^*N$  take very simple forms. In Appendix E we summarize the simple algebraic calculation leading to the s-channel amplitudes (E-5,6), at the  $K^*N$  threshold. Note that all of the flip s-channel amplitudes (E-5,6) vanish identically in the forward direction ( $x = \cos \theta_s = 1$ ) as they should do (conservation of angular momentum), because of the properties of the crossing matrix. We shall then extrapolate these amplitudes slightly ( $\approx 150$  MeV) above and below the  $K^*N$  threshold -  $1.7 \lesssim s^{\frac{1}{2}} \lesssim 2.0$  GeV is the region of interest to us, as discussed in the introduction of this chapter - where we have  $q^3 \lesssim \frac{m^2}{10} q$ . Since the parity conserving (s-channel) partial wave amplitudes (pcpwa) come out to contain only alternate powers of  $q$ , we can achieve further great simplification at no loss, by working to lowest order in  $q$  consistent with the proper threshold behaviour - (F-24) - that our parity conserving partial wave amplitudes should enjoy. To lowest order in  $q$  - see (E-8,9,10) - the  $K^*N \rightarrow K^*N$  are real, so there is no ambiguity as far as their interpretation as K-matrix elements is concerned, while, as explained at the end of section IV-2 we shall associate with K-matrix elements the real parts of  $KN \rightarrow K^*N$  input amplitudes.

The next step is to find the partial wave projections



(F-18) of the low energy s-channel amplitudes (E-5,6) and construct the corresponding pcpwa (F-23). This is also done in Appendix E; the square root factors of the d-functions nicely cancel the square root factors multiplying our amplitudes (E-5,6), so we are left with integrals over polynomials in x. We then construct our pcpwa, which come out to have the correct threshold behaviour (F-24), and this provides a good check of this calculation, and a check for the self-consistency of this model as a whole, since it was a completely non-trivial thing to happen! We then interpret these amplitudes as K-matrix elements, after removing their explicit threshold factors - see (E-12→15) - since the K-matrix elements (F-22) should not have any threshold branchpoints on the real axis.

We can now immediately obtain the expressions for the KN isoscalar phase shifts, inserting (E-12→15) into (F-22), and using (F-21). For  $J^P = \frac{1^\pm}{2}$  ( $S_{\frac{1}{2}}$  and  $P_{\frac{1}{2}}$  waves) we get for  $q > 0$  (above the  $K^*N$  threshold) :

$$\cot \delta_0^\circ = \frac{1}{3ipq(K_0^{\frac{1}{2}-})^2} \quad (\text{IV-9})$$

$$\cot \delta_1^\circ = \frac{1 + q^2(K_{01}^{\frac{1}{2}+})^2 - 2\sqrt{2}iqK_{01}^{\frac{1}{2}+}}{ipq(K_{01}^{\frac{1}{2}+})^2(1 - 2\sqrt{2}iqK_{01}^{\frac{1}{2}+})} \quad (\text{IV-10})$$

Continuation below the  $K^*N$  threshold is by  $q \rightarrow i|q|$ . For  $J^P = \frac{3^\pm}{2}$  ( $P_{\frac{3}{2}}$  and  $D_{\frac{3}{2}}$  waves) the inversion of the 4x4 matrix leads to much more involved formulas, which we do not write down, but directly input into a small program to compute the corresponding Argand plots of figure IV-4.

From (IV-9,10) we see that we can never have an  $S_{01}$  resonance in this model, but the  $P_{01}$  wave may contain an elastic resonance below the  $K^*N$  threshold, if  $K_{01}^{\frac{1}{2}+}$  is such that the quadratic equation:

$$1 - |q|^2 \left( K_{01}^{\frac{1}{2}+} \right)^2 + 2\sqrt{2} |q| K_{01}^{\frac{1}{2}+} = 0 \quad (\text{IV-11})$$

has a solution for  $|q| > 0$ . With our parameters listed in table IV-1 we get a  $Z_0^*$  with  $J^P = \frac{1}{2}^+$  at  $s_R^{\frac{1}{2}} = m_R = 1.778$  GeV (as it has already become clear, we define the resonance mass as the energy at which  $\cot \delta$  for the corresponding wave becomes zero); the

corresponding width (defined as  $\Gamma_R/2 = -1 / (\cot \delta_0^1)'_{s^{\frac{1}{2}}} = \frac{1}{s_R^{\frac{1}{2}}}$ )

is  $\Gamma_R = 0.405$  GeV. From (E-13c) and (E-10) we see that the mass of this resonance does not depend on the constant  $s_0$ , in the determination of which we had some ambiguity (difference in slope between  $K^+p \rightarrow K^{*+}p$  and  $K^-p \rightarrow K^{*-}p$  - see last subsection of section IV-3), but it crucially depends - through  $\beta$  - on the strength of  $\eta$ -exchange in  $KN \rightarrow K^*N$  which we believe to have determined unambiguously), and of course, on the SU(6) prediction (IV-7) for the ratio  $\epsilon_{K^*K^*\eta} / \epsilon_{KK^*\eta}$ , which may be considered as a quasi-free parameter in our model.

In figure IV-4a we plot the partial wave amplitudes  $S_{01}$ ,  $P_{01}$ ,  $P_{03}$ ,  $D_{03}$ , and besides the large resonant  $P_{01}$  wave, two other characteristic features of this model are apparent, namely all phase shifts are small near the  $K^*N$  threshold, and all our waves

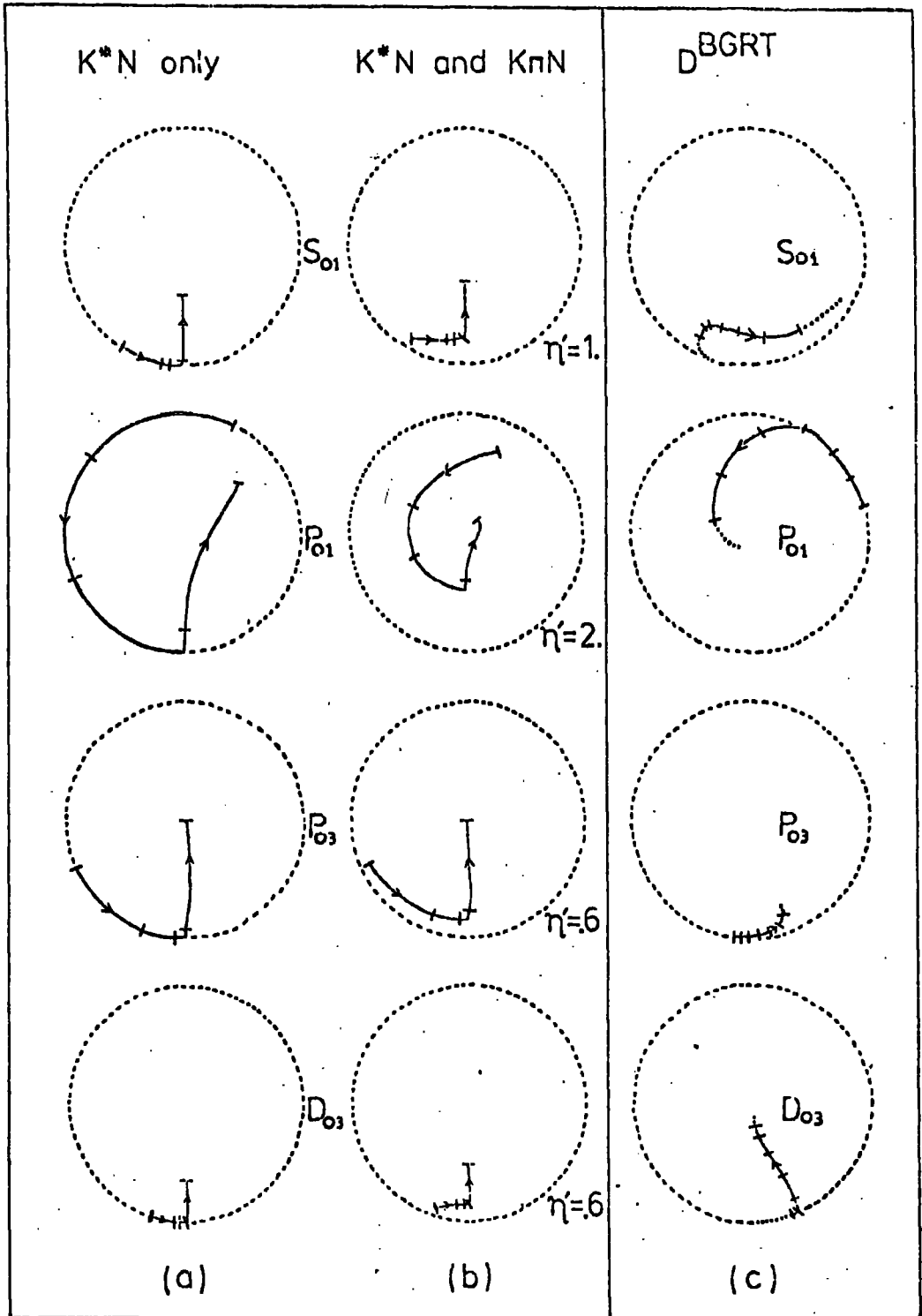


FIG. IV-4 Comparison between:

- (a)  $I=0$  KN phase shifts calculated as described in section IV-4, from a K-matrix model (reference points at  $\sqrt{s}=1700, 1820, 1827, 1830, 1950$  MeV).
- (b) Same as in (a), but arbitrary inelasticity parameters have been introduced, as explained in section IV-4.
- (c) Phase shifts of the BGRT-D (Sens  $\gamma$ ) solution, as described in section IV-1, from reference 70 (reference points at:  $\sqrt{s}=1700, 1747, 1794, 1840, 1887, 1932, 1977$  MeV).

are negative below this threshold. Considering the crudeness of this model, we can say that the agreement of its qualitative features with the preferred solution D of the recent BGRT phase shift analysis of the  $I = 0$   $KN$  elastic channel <sup>70)</sup> - shown for comparison in figure IV-4c, see also the introduction to this chapter - is rather good. Of course, it is not safe to extrapolate the present model much below the  $K^*N$  threshold (say, below  $s^{\frac{1}{2}} = 1.7$  GeV), but we may well suspect that our picture would lead to negative  $I = 0$  scattering lengths for  $S_{01}$  and  $P_{03}$ , as suggested in reference 70).

The fit in chapter III indicated that the pion, which is exchanged in  $KN \rightarrow K^*N$ , does not have an exchange degenerate partner (e.g. a B); if it had, we would not be able to fit  $\rho_{00}$ . What would the effect of such an object, exchanged in  $K^*N \rightarrow K^*N$ , be on our results, stated above? The answer is, none in this model - providing that the constant  $\beta$ , determining the over-all strength of  $\eta+B$  exchange, remains the same - because, as we can see from (E-7b) and (E-10), the pion signature factor does not contribute, in lowest order in  $q^2$ , to the real parts of the  $K^*N \rightarrow K^*N$  amplitudes:

$$\text{Re } g_{\eta} = \frac{1 + \cos \alpha_{\eta}^{\prime}}{2} = 1 + O(q^4) \quad (\text{IV-12})$$

If we assume that for some reason there is, after all, B exchange in  $KN \rightarrow K^*N$ , then its effect would only affect the  $Z_0^*$  width in this model, since because of the (inelastic) kinematics the pion signature factor contributes to the  $KN \rightarrow K^*N$  amplitudes to lowest order in  $q^2$  - see (E-7a,8,9) - .



What about any uncorrelated  $K\bar{\eta}$  production? We can qualitatively feel its effect by introducing fictitious inelasticity parameters : ( $w_0 \approx 1.57$  GeV )

$$\eta = 1 - 2\eta'(s^{1/2} - w_0) \quad (\text{IV-13})$$

and put :

$$\rho T \longrightarrow \frac{\eta e^{2i\delta_{el}} - 1}{2i} \quad (\text{IV-14})$$

In figure IV-4b we illustrate the results of this calculation (the parameters  $\eta'$  have been chosen arbitrarily), and it is apparent, that apart from the inelasticity introduced, the qualitative features of our model remain unchanged (but all our amplitudes become non-zero at  $q = 0$ ).

As explained in section IV-1, in this model we treated  $K^*$  as stable ; we may give it width via the easy prescription :

$$g^2(s, m^2, M^2) \equiv \int g^2(s, m^2, u) \delta(u - M^2) du \quad (\text{IV-15})$$

$$\delta(u - M^2) \longrightarrow \frac{M\Gamma_{K^*}/\pi}{(u - M^2)^2 + (M\Gamma_{K^*})^2} \quad (\text{IV-16})$$

but it is checked that no essential change is made, because of the smallness of its width, as argued in the introduction of this chapter. In particular, all our waves become non-zero but very small at  $q = 0$ , that is, the dip in our total  $I = 0$   $KN$  cross-section at  $K^*N$  threshold persists. We may suspect that the neglected meson exchanges in  $KN \rightarrow KN$  could have filled the dip, as well as any uncorrelated  $K\bar{\eta}$  production, as explained above.

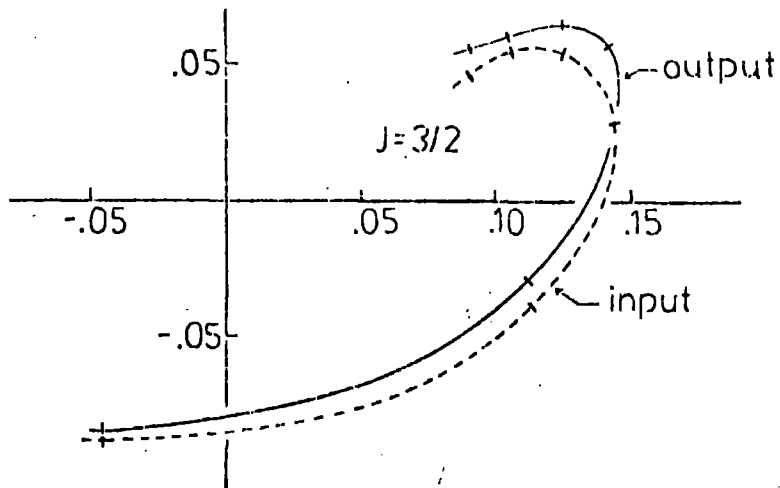
IV- An alternative unitarization technique.

An alternative method to unitarize our input partial wave amplitudes, but with not so clear a physical meaning, would be to iterate the partial wave unitarity equations (F-19). Using non-unitary input amplitudes very much similar to the ones employed in the previous section, we have found that iteration of the system of partial wave unitarity equations (F-19) for the coupled channels  $KN \rightarrow KN$ ,  $KN \rightarrow K^*N$ ,  $K^*N \rightarrow K^*N$ , may result in unitary output isoscalar elastic  $KN$  scattering amplitudes with resonance-like behaviour for certain partial waves. No particular model for the  $K^*N \rightarrow K^*N$  channel is required, but these amplitudes follow in terms of those for  $KN \rightarrow KN$  and  $KN \rightarrow K^*N$  by solving the unitarity equations and iterating the solutions. The  $J = 3/2$  waves prefer to show counterclockwise slow movement in their Argand plot in this model, and if they are interpreted as resonating, they would suggest resonance masses much above the  $K^*N$  threshold.

In figure IV-5, we present a sample result of this calculation. In (a) we show the  $J = 3/2$  wave for the isoscalar  $KN \rightarrow K^*N$  channel; the input is a reggeized pion in the t-channel with slope  $\alpha'_n = 1 \text{ GeV}^{-2}$ , and the output unitary wave is not much different. The output elastic  $J^P = \frac{3}{2}^+$  waves in (b) show a resonance-like behaviour, although the effect is very small.

We do not want to pursue this discussion further, since this calculation has met with several "technical" problems, especially with the convergence of our iteration procedure.

(a)



(b)

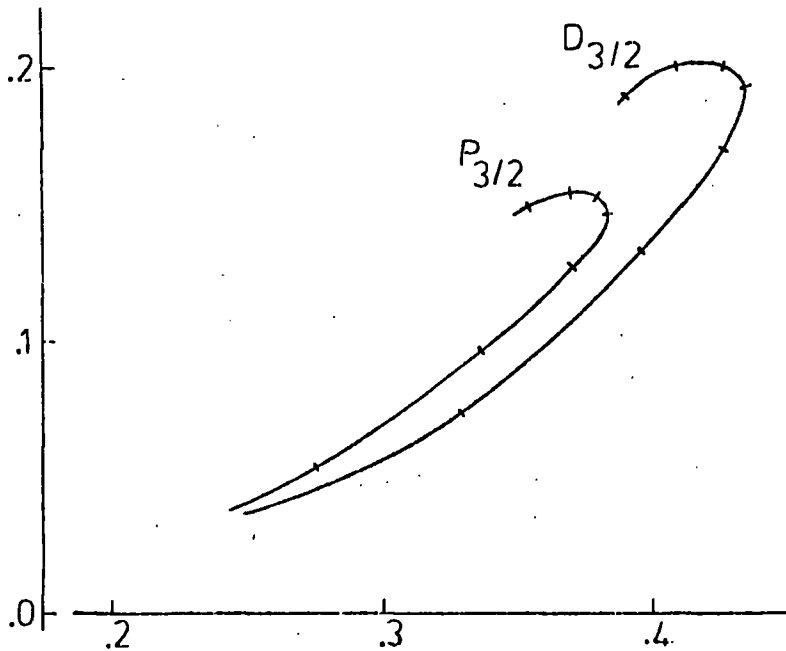


FIG. IV-5 Argand diagrams of the  $J = 3/2$  partial wave, calculated from the iterative model outlined in section IV-5 for:

- (a) Input pion exchange, and unitarized output for the  $I=0$   $KN \rightarrow K^*N$  channel (reference points at:  $\sqrt{s} = 1840, 1932, 2022, 2109, 2193, 2274$  MeV).
- (b) Unitary output for the  $I=0$   $KN$  elastic channel (reference points at:  $\sqrt{s} = 1932, 2022, 2109, 2193, 2274, 2353, 2430$  MeV).

IV-6 Conclusions.

We have shown that the current ideas of exchange degeneracy and approximate duality can accommodate a  $Z_0^*$  direct channel resonance in the  $I = 0$   $K^+N$  system, with the experimentally favoured quantum numbers ( $J^P = \frac{1}{2}^+$ ,  $m = 1.778$  GeV  $\Gamma = 0.405$  GeV), in contrast with Aaron's calculations (66), (67), which would rather favour S and D wave resonances, and in agreement with dispersion relation calculations (69). The magnitude of  $\eta$ -exchange in  $K^*N \rightarrow K^*N$ , adjusted by SU(6), was the crucial factor to produce a  $P_{01}$  resonance, and make  $S_{01}$  and  $P_{03}$  waves negative below the  $K^*N$  threshold.

This object  $Z_0^*$  will be "dual", via unitarity, to  $\eta$ -exchange in  $KN \rightarrow K^*N$  and  $K^*N \rightarrow K^*N$ , and will break the duality scheme to the same extent as the pion cannot be accommodated within it. Schematically, we would have the following "inconsistency":

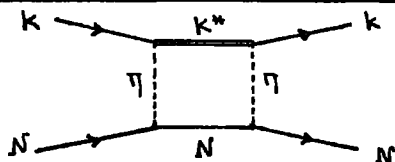
In  $K^+N \rightarrow KN$  assume :

$$0 = \sum \alpha_m \left[ \text{diagram} \right] \stackrel{(d)}{=} \sum \alpha_m \left[ \text{diagram} \right]$$

come to conclude that this sum was not zero

unitarity

"P"  $\propto$



then, get exd :  
 $f + A_2 = \omega + \rho = 2M$

come to  $K^*N \rightarrow K^*N$ , where we have  $4M + \eta$  exchanges

the most obvious remedy to which would be to assume that equality (d), duality, is only an approximate one, as everybody would have expected!

Needless to say that there is no reason either theoretical or experimental to assume that all possible physical particle states are  $q\bar{q}$  or  $qqq(\bar{q}\bar{q}\bar{q})$  combinations, other than the principle of maximal simplicity - again an approximate one !

## APPENDIX A

### CHARGE ASYMMETRY AND THE YUTA-OKUBO FORMULA <sup>11)</sup>

Consider the decay  $R \rightarrow \pi^+ \pi^- \pi^0$ ; the polar coordinates  $r, \theta$  in the usual Dalitz plot are defined by:

$$T_0 = \frac{Q}{3} (1 + r \cos \theta) \quad , \quad T_{\pm} = \frac{Q}{3} \left[ 1 + r \cos \left( \frac{2\pi}{3} \mp \theta \right) \right] \quad (\text{A-1})$$

where  $T_n$  is the kinetic energy of  $\pi^n$  and  $Q = m_R - 3m_\pi$  ( $m_R$  ( $m_\pi$ ) is the resonance (pion) mass) The "Cartesian" coordinates  $x, y$  are usually defined as:  $x = (T_+ - T_-) / Q\sqrt{3}$ ,  $y = T_0 / Q$  (A-2)

Let  $N_+$  ( $N_-$ ) be the number of events with  $x > 0$  ( $x < 0$ ). Then we define the charge asymmetry in the Dalitz plot by:

$$\alpha = \frac{N_+ - N_-}{N_+ + N_-} \quad (\text{A-3})$$

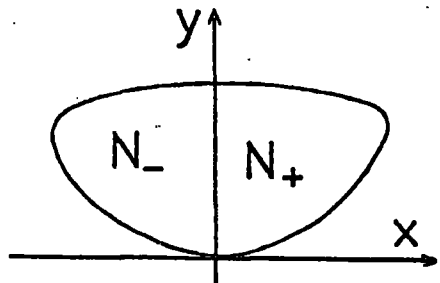


FIG. A-1

We now want to estimate the magnitude of the charge asymmetry, which might appear in the Dalitz plot for the decay  $R \rightarrow \pi^+ \pi^- \pi^0$ , when  $R$  is produced in  $\pi N \rightarrow RB$ , caused by interference between the

R-decay signal and some coherently added  $3\pi$  background.

We write :

$$T = \text{[Diagram 1]} + \text{[Diagram 2]} = \frac{M}{w^{1/2} - m_R + i\frac{\Gamma_R}{2}} + B \quad (\text{A-4})$$

where  $w = (p_+ + p_- + p_0)^2$  ( $p_n$  is the momentum of  $\pi^n$ ),  $m_R$  and  $\Gamma_R$  are the mass and width of the resonance R,  $M = M_S \cdot M_D$  where  $M_S$  represents the amplitude  $\eta N \rightarrow RB$  for R-production, while  $M_D$  is the amplitude for the R-decay,  $R \rightarrow \eta^+ \eta^- \eta^0$ , and the background B may be thought of as being separated into a charge symmetric ( $B_+$ ) and a charge asymmetric ( $B_-$ ) part, that is  $B = B_+ + B_-$ .

For the total cross-section in the region of R we have:

$$\sigma = \int_R |T|^2 dF = \int_R |T|^2 dF_{\{w^{1/2}\}} dw^{1/2} = \int_R dF_{\{w^{1/2}\}} dw^{1/2} \left[ \frac{|M|^2}{(w^{1/2} - m_R)^2 + (\frac{\Gamma_R}{2})^2} + \frac{2(w^{1/2} - m_R) \text{Re}(BM^*)}{(w^{1/2} - m_R)^2 + (\frac{\Gamma_R}{2})^2} + \frac{2(\frac{\Gamma_R}{2}) \text{Im}(BM^*)}{(w^{1/2} - m_R)^2 + (\frac{\Gamma_R}{2})^2} \right] \quad (\text{A-5})$$

( $F_{\{a,b,\dots\}}$  is that part of the phase space which remains if we leave out the  $da, db, \dots$  integrations). Supposing now that R is sufficiently narrow, we can: (a) approximate M and B by their mean values  $\bar{M}$  and  $\bar{B}$ , over  $F_{\{w^{1/2}\}}$ , and (b) approximate

$$\frac{1}{(w^{1/2} - m_R)^2 + (\frac{\Gamma_R}{2})^2} \quad \text{by} \quad \frac{2\pi}{\Gamma_R} \delta(w^{1/2} - m_R) \quad \text{to get:}$$

$$\sigma = \frac{2\pi}{\Gamma_R} |\bar{M}|^2 + \frac{2\pi}{\Gamma_R} \Gamma_R \text{Im}(\bar{B}\bar{M}^*) \quad (\text{A-6})$$

For the cross-sections associated with events with  $x \geq 0$  we have:

$$(\sigma_+ + \sigma_- = \sigma)$$

$$2\sigma_{\pm} = \frac{2\eta}{\Gamma_R} |\bar{M}|^2 + \frac{2\eta}{\Gamma_R} \Gamma_R \lambda_m(\overline{B_+ M^*}) \pm \frac{2\eta}{\Gamma_R} \Gamma_R \lambda_m(\overline{B_- M^*}) \quad (A-7)$$

so for the charge asymmetry we get:

$$\alpha = \frac{\sigma_+ - \sigma_-}{\sigma_+ + \sigma_-} = \frac{\sigma_+ - \sigma_-}{\sigma} \approx \Gamma_R \frac{\lambda_m(\overline{B_- M^*})}{|\bar{M}|^2} = \Gamma_R \frac{|\bar{B}_-|}{|\bar{M}|} \sin\phi \quad (A-8)$$

To get the maximum asymmetry which may be produced by this mechanism, we put: (i)  $\sin\phi=1$  (which means that all of the background can interfere with the R-signal, that is, all of it is in the same  $J^{PC}$  state as R; see Appendix B) and (ii)  $B_- = B$  (all of the background is in a charge asymmetric state). So:

$$\alpha_{max} = \Gamma_R \frac{|\bar{B}|}{|\bar{M}|} \quad (A-9)$$

Let  $\sigma_R$  ( $\sigma_B$ ) be the cross-sections associated with the R-signal (background), and  $\Delta m_R$  the  $3\pi$  inv. mass region over which R is observed (in general,  $\Delta m_R \gg \Gamma_R$ ); we then estimate:

$$\sigma_B = \int_{W = m_R - \frac{1}{2}\Delta m_R}^{m_R + \frac{1}{2}\Delta m_R} dF |\bar{B}|^2 \approx \int_{m_R - \frac{1}{2}\Delta m_R}^{m_R + \frac{1}{2}\Delta m_R} dW^{1/2} |\bar{B}|^2 = \Delta m_R |\bar{B}|^2 \quad (A-10)$$

$$\sigma_R = \int dF \frac{|\bar{M}|^2}{(W^{1/2} - m_R)^2 + (\Gamma_R/2)^2} = \int \frac{|\bar{M}|^2 dW^{1/2}}{(W^{1/2} - m_R)^2 + (\Gamma_R/2)^2} = \frac{2\eta}{\Gamma_R} |\bar{M}|^2 \quad (A-11)$$



so for  $\alpha_{\max}$  we estimate:

$$\alpha_{\max} = \left[ \frac{2\pi f_R}{\Delta m_R} \cdot \frac{\sigma_B}{\sigma_R} \right]^{1/2} \quad (\text{A-12}), \text{ Yuta - Okubo formula}$$

Note, that it is possible to have negligible asymmetry in the background, as it is experimentally observed 9), 10) and at the same time  $B \approx B_{\pm}$ , because:

$$|\bar{B}|^2 = |\bar{B}_+|^2 + |\bar{B}_-|^2 + 2 \operatorname{Re} \bar{B}_+^* \bar{B}_- \quad , \text{ so}$$

$$\alpha_B = \frac{2|\bar{B}_+||\bar{B}_-|}{|\bar{B}_+|^2 + |\bar{B}_-|^2} \cos \delta_B \quad (\text{A-13})$$

so  $\alpha_B$  can be small in the following cases:

$$(i) |\bar{B}_+| \gg |\bar{B}_-|, \quad (ii) |\bar{B}_+| \ll |\bar{B}_-|, \quad (iii) \cos \delta_B \ll 1$$

## APPENDIX B

### PARTIAL WAVE ANALYSIS OF A $2 \rightarrow 3$ PROCESS AND INTERFERING $2 \rightarrow 4$ AMPLITUDES .

Consider the process  $ab \rightarrow 123$ , where particles 1,2,3, are spinless; we start from relation (24) of reference 21), which for three spinless particles 1,2,3, in their centre of mass frame reads :

$$\begin{aligned}
 |PJM; wjm \lambda_1=0 \lambda_2=0; \lambda_3=0\rangle &= \frac{1}{4} \left[ \frac{Pq}{Ww} \right]^{1/2} \eta_j \eta_j \times \\
 \int \sin\theta d\theta d^j_{m_0}(\theta) \int \sin\Theta d\Theta d\Phi d\varphi \mathcal{D}_{Mm}^{J*}(\Phi, \Theta, \varphi) \times \\
 \mathcal{R}_{\Phi, \Theta, \varphi} |q_1 \nu_1=0; q_2 \nu_2=0; q_3 \lambda_3=0\rangle & \quad (B-1)
 \end{aligned}$$

$$|PJM; wjm \lambda_1=0 \lambda_2=0; \lambda_3=0\rangle \equiv |JM; jm\rangle \quad \text{is the ang.}$$

momentum state of the three spinless particles; J is the total ang. momentum, while j is the ang. momentum of the 1,2 system.

$\mathcal{R}_{\Phi, \Theta, \varphi} |q_1 \nu_1=0; q_2 \nu_2=0; q_3 \lambda_3=0\rangle \equiv |123\rangle$  is the most general state vector we may construct for the three particles 1,2,3. For the explanation of the meaning of all other symbols, see

reference 21). From (B-1), we get:

$$|123\rangle \propto \sum_{JM;jm} d_{m_0}^j(\theta) \mathcal{D}_{Mm}^J(\Phi, \Theta, \varphi) |JM;jm\rangle \quad (\text{B-2})$$

On the other hand we know how to construct the two-particle helicity states  $|ab\rangle$  (e.g. reference 22); we have ( $\mu = |\mu_a - \mu_b|$ ):

$$|ab\rangle \propto \sum_{J'M'} \mathcal{D}_{M'\mu}^{J'}(\varphi', \theta', -\varphi') |J'M'\mu_a \mu_b\rangle \quad (\text{B-3})$$

We now combine (B-2) and (B-3) ( $T_{123;ab} = \langle ab | T | 123 \rangle$ ),

putting the ab system on the z-axis ( $\mathcal{D}_{M'\mu}^{J'}(0,0,0) = \delta_{M'\mu}$ )

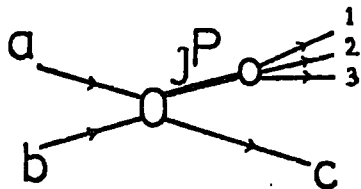
and using ang. momentum conservation ( $\langle J'M'\mu_a \mu_b | T | JM;jm \rangle =$   
 $= \delta_{MM'} \delta_{JJ'} T_{\mu_a \mu_b}^{JM;jm}$ ) , to get:

$$T_{123;ab} \propto \sum_{J;jm} d_{m_0}^j(\theta) \mathcal{D}_{\mu m}^J(\Phi, \Theta, \varphi) T_{\mu_a \mu_b}^{J;jm} \quad (\text{B-4})$$

which may serve as a "partial wave" analysis of a  $2 \rightarrow 3$  amplitude; note that in (B-4)  $\varphi$  is arbitrary, while from  $\theta, \Phi, \Theta$  only two are independent.

We may now show explicitly, that two interfering amplitudes

of the type



should necessarily have

particles 1,2,3, in the same  $J^P$  state, in order that their interference gives a non-vanishing contribution in the Dalitz plot distribution for the decay  $R \rightarrow 123$  (when in one of them the state  $J^P$  is resonant).

First, consider the  $2 \rightarrow 2$  problem, and suppose ( $\mu = \mu_a - \mu_b$ ,  $\mu' = \mu_c - \mu_d$ ,  $z = \cos \theta$ ,  $i = 1, 2$ )

$$T_i \propto \begin{array}{c} a \quad \quad c \\ \quad \searrow \quad \nearrow \\ \quad J_i \\ \quad \nearrow \quad \searrow \\ b \quad \quad d \end{array} \propto T_i^{J_i}(s) d_{\mu\mu'}^{J_i}(z) \quad (B-5)$$

Then for the interference term contributing to the dif. cross-section, which may be thought of as being partly equivalent to a Dalitz-plot distribution for the  $2 \rightarrow 3$  problem<sup>23)</sup>, we have:

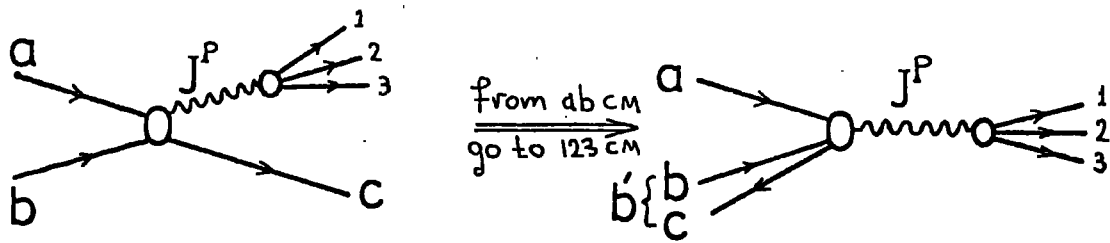
$$\frac{d\sigma^{(interf.)}}{dz} \propto 2 \operatorname{Re} T_1 T_2^* \propto T_1^{J_1}(s) T_2^{J_2}(s) d_{\mu\mu'}^{J_1} d_{\mu\mu'}^{J_2} \quad (B-6)$$

which in general does not vanish, while we have :

$$\sigma_{(s)}^{(interf.)} \propto \int_{J_1, J_2} T_1^{J_1}(s) T_2^{J_2}(s) \quad (B-7)$$

We now show that this is not the case for the interference term contributing to a Dalitz-plot distribution. We first reduce the  $2 \rightarrow 4$  problem to a  $2 \rightarrow 3$  problem; for, if the process  $ab \rightarrow c123$  is dominated by Regge exchanges in the  $b\bar{c}$  channel, and it is peripheral in  $t = (p_b - p_c)^2$ , the system  $(b\bar{c})$  may be considered as a quasi-

particle  $b'$ , with  $m_b^2 = t$



Indeed, in the  $\omega$  experiment, we have  $s_{ab} = 7.84 \text{ GeV}^2$ , while the dif. cross-section decreases approximately from  $2 \text{ mb/GeV}^2$  to  $.2 \text{ mb/GeV}^2$  in the interval  $0.0 \leq t \leq -0.6 \text{ GeV}^2$ , so the separation of  $a, b$  is much larger than that of  $b, \bar{c}$ . One thus may hope, that the extrapolation of the proper  $ab' \rightarrow 123$  amplitude to values  $m_b^2 \geq -.6 \text{ GeV}^2$  will not spoil its properties. If we now have (using (B-4) )

$$\equiv T_i \propto \sum_{j_i m_i} d_{m_i 0}^{j_i}(\theta) \mathcal{G}_{\mu m_i}^{J_i}(\Phi, \Theta, \Psi) T_i(s, x, y) \quad (\text{B-8})$$

( $i=1,2, \mu = \mu_a - \mu_b, s = (p_a + p_b)^2$ ), the interference integral on the Dalitz plot will be:

$$\frac{d\sigma}{dx dy} \stackrel{(\text{interf.})}{\propto} \delta_{J_1, J_2} \sum_{j_1 m_1} T_1(s, x, y) T_2(s, x, y) \quad (\text{B-9})$$

and it explicitly vanishes unless  $J_1 = J_2$ , Q.E.D.

We can now trivially make the above formalism to conserve parity. First, in constructing the  $|123\rangle$  states, we may use the relation :

$$\mathcal{D}_{Mm}^J = \sum_{\bar{m}\bar{m}'} \sum_{\hat{m}\hat{m}'} \langle j j' \bar{m} \bar{m}' | J m \rangle \langle j j' \hat{m} \hat{m}' | J M \rangle \mathcal{D}_{\hat{m}\bar{m}}^j \mathcal{D}_{\hat{m}'\bar{m}'}^{j'} \quad (\text{B-10})$$

and insert it to (B-2), in order to transform from a  $(j, J)$  representation to a  $(j, j')$  representation ( $j'$  is the ang. momentum of particle "3" with respect to the "12" system), which is identically parity conserving. On the other hand, we know<sup>22)</sup> how to construct parity eigenstates for the two-body  $ab'$  system in its centre of mass. So, we may construct parity conserving partial wave amplitudes (pcpwa), connecting states of definite  $j j'$  (and therefore of definite parity), of the 123 system with states of definite  $J^P$  of the  $ab'$  system. It is then clear, that in order that the interference integral be non-zero, the interfering states should have the same both  $j$  and  $j'$

$$(\mathcal{D}^J \rightarrow \mathcal{D}^j \mathcal{D}^{j'}) \text{ , that is the same parity.}$$

TABLE B-1 : Ang. mom.-parity of  $3\pi$  states

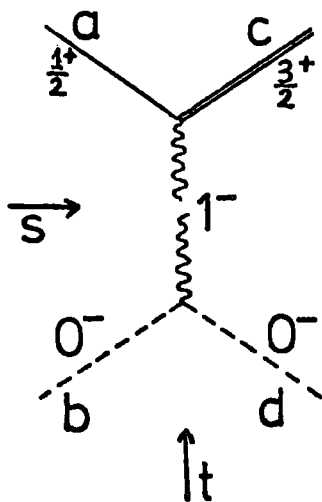
<div style="display: flex; justify-content: space-around; align-items: center;"> <div style="text-align: center;"> <math>\pi_1 \longleftarrow j \xrightarrow{(-1)^j} \pi_2</math>  <math>\uparrow j' \downarrow (-1)^{j'}</math>  <math>\pi_3</math> </div> <div style="text-align: center;"> <math>j+j' \leq 4</math>  <math> j-j'  \leq J \leq j+j'</math>  <math>P = (-1)^{j+j'+1}</math> </div> </div>					
$j \backslash j$	$0^+$	$1^-$	$2^+$	$3^-$	$4^+$
0	$0^-$	$1^+$	$2^-$	$3^+$	$4^-$
1	$1^+$	$0^- 1^- 2^-$	$1^+ 2^+ 3^+$	$2^- 3^- 4^-$	
2	$2^-$	$1^+ 2^+ 3^+$	$0^- 1^- 2^- 3^- 4^-$		
3	$3^+$	$2^- 3^- 4^-$			
4	$4^-$				

# APPENDIX C

## CALCULATION OF SOME FEYNMAN DIAGRAMS.

### C-1. Vector meson exchange in $0^{-\frac{1}{2}+} \rightarrow 0^{-\frac{3}{2}+}$

We calculate the vector meson exchange Born terms in a  $0^{-\frac{1}{2}+} \rightarrow 0^{-\frac{3}{2}+}$  process (e.g.  $\Delta$  production), using the couplings:



$$(M1) \quad \mathcal{L} = g \bar{\psi}^{\mu} \psi \varepsilon_{\mu\nu\lambda\tau} p_{\nu}^{\lambda} (p_{\rho} + p_{\sigma})^{\rho} A^{\tau} \quad (\text{III-1})$$

$$\mathcal{L} = g' (\phi_b \partial_{\rho} \phi_d - (\partial_{\rho} \phi_b) \phi_d) A^{\rho} \quad (\text{III-2})$$

FIG. C-1

(i) t-channel amplitudes

$$(0^{-}0^{-} \rightarrow \frac{1}{2}^{-}\frac{3}{2}^{+})$$

We arrange our momenta as in fig. C-2 -the



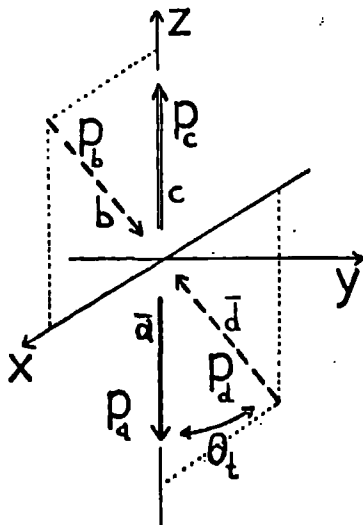


FIG. C-2

$\frac{3}{2}^+$  particle's momentum lies on the positive z-direction - hence, we have  $\lambda_c = s_c$ ,  
 $\lambda_a = -s_a$  ( $s_i$  are the spin-projections and  $\lambda_i$  are the helicities; in the main text we always label helicities by the name of the corresponding particle), so for  $\nu$  we will have to use expression

(D-1b) of Appendix D with  $\hat{\chi}_{\frac{1}{2}} = \begin{bmatrix} -1 \\ 0 \end{bmatrix}$ ,

$\hat{\chi}_{-\frac{1}{2}} = \begin{bmatrix} 0 \\ 1 \end{bmatrix}$ , so "effectively"

$s_a \equiv \lambda_a$ . Using (III-1,2), for the t-channel scattering amplitude we have: ( $k=p_a+p_c=p_b+p_d$ )

$$T_{\lambda_a \lambda_c}^{(t)} = -i g g' \bar{u}^{\mu}(p_c, \lambda_c) \nu(p_a, \lambda_a) \epsilon_{\mu\nu\lambda\tau} p_c^\nu k^\lambda \frac{\delta_{\tau\sigma} - \frac{k_\tau k_\sigma}{k^2}}{m_\nu^2 - t} (p_b - p_d)^\sigma \quad (C-1)$$

Now the term with  $\frac{k_\tau k_\sigma}{k^2}$  vanishes since it contains

$$\bar{u}^\mu \epsilon_{\mu\nu\lambda\tau} p_c^\nu k^\lambda k^\tau = 0 \quad (\text{see Appendix D-2}), \text{ and putting } q = p_b - p_d \quad (q = \vec{p}_b - \vec{p}_d = 2\vec{p}_b) \text{ we get:}$$

$$T_{\lambda_a \lambda_c}^{(t)} = \frac{-i g g'}{m_\nu^2 - t} \bar{u}^{\mu}(p_c, \lambda_c) \nu(p_a, \lambda_a) \epsilon_{\mu\nu\lambda\tau} p_c^\nu p_a^\lambda q^\tau \quad (III-3)$$

For the Schwinger - Rarita spinors, we have (e.g. reference 2), page 72 ) :

$$\bar{u}^{\mu}(\vec{p}_c, \frac{3}{2}) = \bar{u}(\vec{p}_c, \frac{1}{2}) \epsilon_{(+1)}^{\mu*} \quad (C-2a)$$

$$\bar{u}^{\mu}(\vec{p}_c, \frac{1}{2}) = \frac{1}{\sqrt{3}} \bar{u}(\vec{p}_c, -\frac{1}{2}) \epsilon_{(+1)}^{\mu*} + \sqrt{\frac{2}{3}} \bar{u}(\vec{p}_c, \frac{1}{2}) \epsilon_{(0)}^{\mu*} \quad (C-2b)$$

(The Clebsch-Gordan coefficient  $\frac{1}{\sqrt{3}}$  in (C-2b), is the  $\frac{1}{\sqrt{3}}$  which will finally appear in the Stodolsky -Sakurai relation ).

Since we have the  $\frac{3}{2}^+$  particle on the z-axis, we can put (see, e.g. reference 2), page 62 )

$$\epsilon_{(\pm 1)} = \frac{1}{\sqrt{2}} \begin{bmatrix} 0 \\ \mp 1 \\ -i \\ 0 \end{bmatrix}, \quad \epsilon_{(0)} = \frac{1}{M} \begin{bmatrix} P \\ 0 \\ 0 \\ E \end{bmatrix} \quad (C-3)$$

so, looking at Appendix D-2, and figure C-2, we have:

$$\epsilon_{(M)}^{\mu*} \epsilon_{\mu\nu\lambda\tau} p_c^\nu p_a^\lambda q^\tau = (E_c + E_a) \vec{p}_a \times \vec{q} \cdot \vec{\epsilon}_{(M)}^* =$$

$$= 2t^{1/2} |\vec{p}_a \times \vec{p}_b| \epsilon_{y(M)}^* = \begin{cases} = 0 & \text{if } M=0 \quad (C-4a) \\ = i\sqrt{2} t^{1/2} |\vec{p}_a| |\vec{p}_b| \sin \theta_t & \text{if } M=+1 \quad (C-4b) \end{cases}$$

$|\vec{p}_a|, |\vec{p}_c|, |\vec{p}_b|, |\vec{p}_d|$ , are the lengths of the t-channel CM

3-momenta, and  $\theta_t$  is the t-channel scattering angle. Now, (III-3)

reads :

$$T_{\lambda_a \frac{3}{2}}^{(t)} = \frac{\sqrt{2} g g' t^{1/2}}{m_v^2 - t} \bar{u}(p_c, \frac{1}{2}) v(p_a, \lambda_a) |\vec{P}_a| |\vec{P}_b| \sin \theta_t \quad (C-5a)$$

$$T_{\lambda_a \frac{1}{2}}^{(t)} = \frac{1}{\sqrt{3}} \frac{\sqrt{2} g g' t^{1/2}}{m_v^2 - t} \bar{u}(p_c, -\frac{1}{2}) v(p_a, \lambda_a) |\vec{P}_a| |\vec{P}_b| \sin \theta_t \quad (C-5b)$$

We now calculate  $\bar{u}v$ , looking at Appendix (D-1) :

$$\bar{u}(p_c, \pm \frac{1}{2}) v(p_a, \lambda_a) = \sqrt{\frac{(E_a + m_a)(E_c + m_c)}{4}} \left[ \chi_{\pm}^{\dagger} - \chi_{\pm}^{\dagger} \frac{\vec{\sigma} \cdot \vec{P}_c}{E_c + m_c} \right] \times$$

$$\begin{bmatrix} \frac{\vec{\sigma} \cdot \vec{P}_a}{E_a + m_a} \hat{\chi}_{\lambda_a} \\ \hat{\chi}_{\lambda_a} \end{bmatrix} = -\frac{1}{2} |\vec{P}_a| \frac{E_a + m_a + E_c + m_c}{(E_a + m_a)^{1/2} (E_c + m_c)^{1/2}} \left( \chi_{\pm}^{\dagger} \sigma_3 \hat{\chi}_{\lambda_a} \right) \quad (C-6)$$

Hat ( $\wedge$ ) denotes "antiparticle" Pauli spinor; we next define :

$$a_{\pm} = t - (m_b \pm m_d)^2, \quad b_{\pm} = t - (m_a \pm m_c)^2 \quad (C-7)$$

hence:

$$|\vec{P}_b| = \frac{1}{2t^{1/2}} \sqrt{a_+ a_-}, \quad |\vec{P}_a| = \frac{1}{2t^{1/2}} \sqrt{b_+ b_-} \quad (C-8)$$

Also have :

$$\frac{E_a + m_a + E_c + m_c}{(E_a + m_a)^{1/2} (E_c + m_c)^{1/2}} = \frac{2t^{1/2}}{\sqrt{b_+}} \quad (C-9)$$

$$\chi_+^\dagger \sigma_3 \hat{\chi}_+ = [1 \ 0] \begin{bmatrix} 1 & 0 \\ 0 & -1 \end{bmatrix} \begin{bmatrix} -1 \\ 0 \end{bmatrix} = -1 = \chi_-^\dagger \sigma_3 \hat{\chi}_- \quad (C-10a)$$

$$\chi_+^\dagger \sigma_3 \hat{\chi}_- = \chi_-^\dagger \sigma_3 \hat{\chi}_+ = 0 \quad (C-10b)$$

So, we end up with :

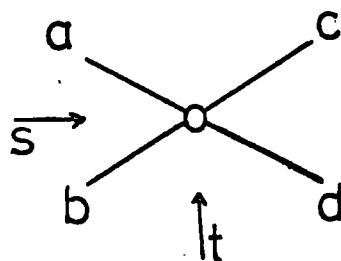
$$T_{-\frac{1}{2} \frac{3}{2}}^{(t)} = T_{\frac{1}{2} \frac{1}{2}}^{(t)} = 0$$

$$T_{\frac{1}{2} \frac{3}{2}}^{(t)} = \sqrt{3} T_{-\frac{1}{2} \frac{1}{2}}^{(t)} = \frac{gg'}{m_v^2 - t} \frac{\sin \theta_t}{4} b_+ \sqrt{\frac{a_+ a_- - b_-}{2t}} \quad (C-11)$$

$$= \frac{gg'}{m_v^2 - t} |\vec{p}_a| |\vec{p}_b| \sin \theta_t \cdot \frac{t^{1/2}}{\sqrt{2}} \sqrt{b_+}$$

$$= \frac{gg'}{2\sqrt{2}} \frac{\Phi(s,t)^{1/2}}{m_v^2 - t} \left[ (m_a + m_c)^2 - t \right]^{1/2} \quad (III-4,5)$$

remembering that for a process :



, we

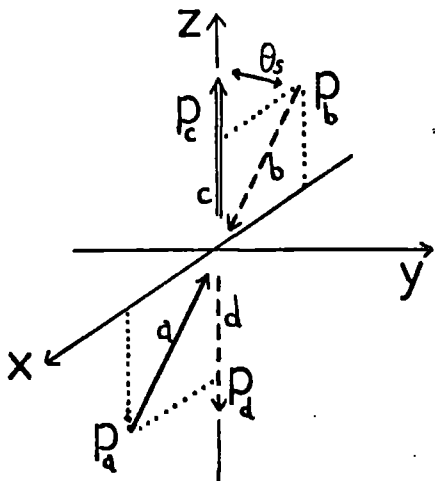
have (e.g. reference 22), page 175 ) :

$$4s p_{sab}^2 p_{s'cd}^2 \sin^2 \theta_s \equiv 4t p_{t'ac}^2 p_{t'bd}^2 \sin^2 \theta_t \equiv \phi(s,t) \quad (C-12)$$

(here, we have :  $|\vec{p}_a| \equiv p_{t'ac}$  ,  $|\vec{p}_b| \equiv p_{t'bd}$  )

(ii) s-channel amplitudes

(  $0^{-\frac{1}{2}+} \rightarrow 0^{-\frac{3}{2}+}$  )



Arranging our momenta as in figure C-3, and proceeding as in (i), we get :

FIG. C-3

$$T_{\lambda_a \lambda_c}^{(s)} = \frac{igg'}{m_v^2 - t} \bar{u}(p_c, \lambda_c) u(p_a, \lambda_a) \epsilon_{\mu\nu\lambda\tau} p_c^\nu p_a^\tau (p_b + p_d)^\mu \quad (C-13)$$

$$T_{\lambda_a \frac{3}{2}}^{(s)} = \frac{-\sqrt{2}gg's^{1/2}}{m_v^2 - t} \bar{u}(p_c, \frac{1}{2}) u(p_a, \lambda_a) |\vec{p}_d| |\vec{p}_a| \sin \theta \quad (C-14a)$$

$$T_{\lambda_a \frac{1}{2}}^{(s)} = \frac{-1}{\sqrt{3}} \frac{\sqrt{2} g g' s^{1/2}}{m_v^2 - t} \bar{u}(p_c, -\frac{1}{2}) u(p_a, \lambda_a) |\vec{p}_d| |\vec{p}_a| \sin \theta \quad (C-14b)$$

where now  $p_a, p_c, p_b, p_d$  are the s-channel CM momenta, and  $\theta \equiv \theta_s$  is the s-channel scattering angle.

We now calculate  $\bar{u}u$ , using (D-1a) and (D-2a), with:

$$\chi_{\frac{1}{2}} = \begin{bmatrix} 1 \\ 0 \end{bmatrix}, \quad \chi_{-\frac{1}{2}} = \begin{bmatrix} 0 \\ 1 \end{bmatrix} \quad (C-15a) \text{ for particle c}$$

$$\chi'_{\frac{1}{2}} = \begin{bmatrix} \cos \frac{\theta}{2} \\ \sin \frac{\theta}{2} \end{bmatrix}, \quad \chi'_{-\frac{1}{2}} = \begin{bmatrix} -\sin \frac{\theta}{2} \\ \cos \frac{\theta}{2} \end{bmatrix} \quad (C-15b) \text{ for particle a}$$

$$\bar{u}(p_c, \lambda_c) u(p_a, \lambda_a) = \sqrt{\frac{(E_c + m_c)(E_a + m_a)}{4}} \left[ \chi_{\lambda_c}^\dagger \quad -\chi_{\lambda_c}^\dagger \frac{\vec{\sigma} \cdot \vec{p}_c}{E_c + m_c} \right] \times$$

$$\begin{bmatrix} \chi'_{\lambda_a} \\ \frac{\vec{\sigma} \cdot \vec{p}_a}{E_a + m_a} \chi'_{\lambda_a} \end{bmatrix} = \sqrt{\frac{(E_c + m_c)(E_a + m_a)}{4}} B_{\lambda_c \lambda_a} \quad (C-16)$$

where, using:

$$\vec{\sigma} \cdot \vec{p}_c \vec{\sigma} \cdot \vec{p}_a \equiv \vec{p}_c \cdot \vec{p}_a + i \vec{p}_c \times \vec{p}_a \cdot \vec{\sigma} = |\vec{p}_a| |\vec{p}_c| \begin{bmatrix} \cos \theta & -\sin \theta \\ \sin \theta & \cos \theta \end{bmatrix} \quad (C-17)$$

we can put:

$$D \equiv \frac{|\vec{P}_a| |\vec{P}_c|}{(E_a + M_a)(E_c + M_c)} \quad (C-18)$$

$$B_{\lambda_c \lambda_a} \equiv \chi_{\lambda_c}^\dagger \chi'_{\lambda_a} - D \chi_{\lambda_c}^\dagger \begin{bmatrix} \cos \theta & -\sin \theta \\ \sin \theta & \cos \theta \end{bmatrix} \chi'_{\lambda_a} \quad (C-19)$$

Using (C-15), we find:

$$B_{\frac{1}{2} \frac{1}{2}} = +B_{-\frac{1}{2} -\frac{1}{2}} = (1 + D - 2D \cos \theta) \cos \frac{\theta}{2} \quad (C-20a)$$

$$B_{-\frac{1}{2} \frac{1}{2}} = -B_{\frac{1}{2} -\frac{1}{2}} = (1 - D - 2D \cos \theta) \sin \frac{\theta}{2} \quad (C-20b)$$

and the signs come out correctly, as expected from parity conservation.

Putting :

$$F = -g g' s^{1/2} |\vec{P}_a| |\vec{P}_c| \sqrt{\frac{(E_a + M_a)(E_c + M_c)}{2}} \quad (C-21)$$

we end up with :

$$T_{\frac{1}{2} \frac{3}{2}}^{(s)} = \sqrt{3} T_{-\frac{1}{2} \frac{1}{2}}^{(s)} = F \frac{\sin \theta}{m_v^2 - t} (1 + D - 2D \cos \theta) \cos \frac{\theta}{2} \quad (III-7a)$$

$$-T_{-\frac{1}{2} \frac{3}{2}}^{(s)} = \sqrt{3} T_{\frac{1}{2} \frac{1}{2}}^{(s)} = F \frac{\sin \theta}{m_v^2 - t} (1 - D - 2D \cos \theta) \sin \frac{\theta}{2} \quad (III-7b)$$

As a check of our results, we verify the relation

$$\sum |T^{(s)}|^2 = \sum |T^{(t)}|^2 \quad . \quad \text{From (III-4,5) we have:}$$

$$\sum |T^{(t)}|^2 = \frac{(gg')^2}{3} \frac{\phi(s,t)}{(m_v^2 - t)^2} \left[ (m_q + m_c)^2 - t \right] \quad (\text{C-22})$$

while from (III-7) we get:

$$\begin{aligned} \sum |T^{(s)}|^2 &= \frac{8F^2}{3} \frac{\sin^2 \theta_s}{(m_v^2 - t)^2} (1 + D^2 - 2D \cos \theta_s) = \\ &= \frac{(gg')^2}{3} \frac{\phi(s,t)}{(m_v^2 - t)^2} (E_q + m_q)(E_c + m_c)(1 + D^2 - 2D \cos \theta_s) \quad (\text{C-23}) \end{aligned}$$

where, we used (C-12). Substituting for  $\cos \theta_s$ ,

$$\cos \theta_s = \frac{s^2 + s(2t - \sum m_a^2) + (m_a^2 - m_b^2)(m_c^2 - m_d^2)}{4s|\vec{p}_a||\vec{p}_c|} \quad \begin{matrix} (\text{F-5}) \\ (\text{C-24}) \end{matrix}$$

we can verify, that:

$$(E_q + m_q)(E_c + m_c)(1 + D^2 - 2D \cos \theta_s) \equiv (m_q + m_c)^2 - t \quad , \quad \text{Q.E.D.}$$



C-2 Pseudoscalar meson exchange in  $0^-(1^-) \frac{1}{2}^+ \rightarrow 1^-(\frac{1}{2}^+)$

Here, we want to calculate the contribution of the pseudoscalar meson exchange Born term to the t-channel helicity amplitudes for  $0^-(\frac{1}{2}^+) \rightarrow 1^-(\frac{1}{2}^+)$  and  $1^-(\frac{1}{2}^+) \rightarrow 1^-(\frac{1}{2}^+)$  processes.

(1)  $0^-(\frac{1}{2}^+) \rightarrow 1^-(\frac{1}{2}^+)$

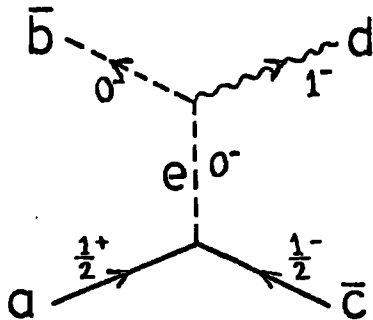


FIG. C-4

$$\mathcal{L} = g' \phi_e \phi_b p_b^\mu A_\mu^d \quad (\text{C-25})$$

$$\mathcal{L} = g \bar{\Psi} \gamma_5 \Psi \phi \quad (\text{III-14})$$

Putting our momenta as shown in figure C-5, again, we effectively have  $\lambda_1 = s_1$  everywhere. Lagrangian (C-25) is the same as (III-2), but now only one of the pseudoscalar mesons is external, and a term vanishes.

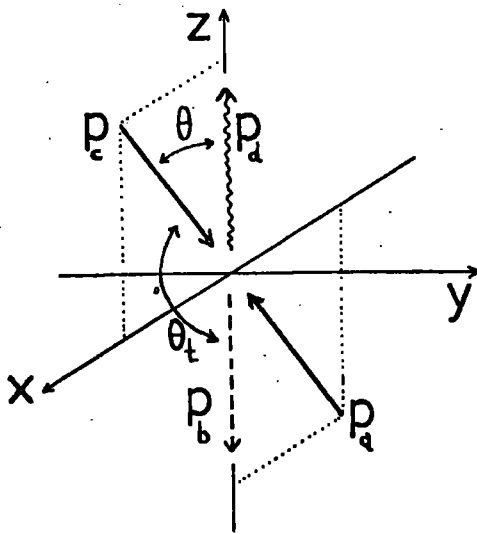


FIG. C-5

Couplings (C-25) and (III-14) lead to:

$$T_{\lambda_d; \lambda_q \lambda_c} = \bar{u}_{(p_c; \lambda_c)} \gamma_5 u_{(p_q; \lambda_q)} \frac{g g'}{m_\pi^2 - t} P_b^\mu \epsilon_{(\lambda_d)}^{\mu*} \quad (C-26)$$

and, clearly,  $T_{\pm 1; \lambda_a \lambda_c} = 0$ , since  $\epsilon_{(\pm 1)}^\mu$  has neither 0 nor 3 component - (C-3) - and  $\vec{p}_b$  is on the z-axis; on the other hand:

$$\begin{aligned} P_b^\mu \epsilon_{(0)}^{\mu*} &= [E_b; 00 - |\vec{p}_d|] \left[ \frac{|\vec{p}_d|}{m_d}; 00 \frac{E_d}{m_d} \right] = \frac{t^{1/2}}{m_d} |\vec{p}_d| = \\ &= \frac{\sqrt{a_+ a_-}}{2 m_d} \quad (C-27) \quad (\text{look at (C-7,8)}) \end{aligned}$$

We now calculate  $\bar{v} \gamma_5 u$  (see Appendix D-1; in our representation,

according to reference 58), we have  $\gamma_5 = i \gamma_0 \gamma_1 \gamma_2 \gamma_3 = \begin{pmatrix} 0 & I \\ I & 0 \end{pmatrix}$ ;

$\vec{p}_a = -\vec{p}_c = \vec{p}$ ,  $m_a = m_c = m$ ,  $E_a = E_c = E = \frac{t^{1/2}}{2}$  ) :

$$\begin{aligned} \bar{v}_{(p_c; \lambda_c)} \gamma_5 u_{(p_q; \lambda_q)} &= \frac{E+m}{2} \begin{bmatrix} -\hat{\chi}_{\lambda_c}^\dagger \frac{\vec{\sigma} \cdot \vec{p}}{E+m} & -\hat{\chi}_{\lambda_c}^\dagger \\ \hat{\chi}_{\lambda_c}^\dagger & \end{bmatrix} \begin{bmatrix} 0 & 1 \\ 1 & 0 \end{bmatrix} \begin{bmatrix} \chi_{\lambda_q} \\ \frac{\vec{\sigma} \cdot \vec{p}}{E+m} \chi_{\lambda_q} \end{bmatrix} = \\ &= -\frac{t^{1/2}}{2} \hat{\chi}_{\lambda_c}^\dagger \chi_{\lambda_q} = (-1)^{\lambda_q - \frac{1}{2}} \frac{t^{1/2}}{2} \delta_{\lambda_q \lambda_c} \quad (C-28) \end{aligned}$$

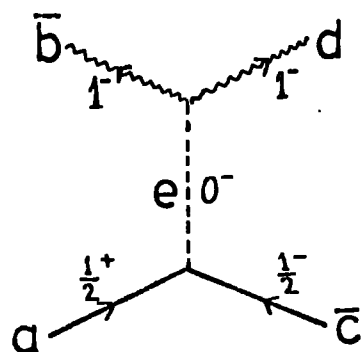
where we have found  $\hat{\chi}_{\lambda_c}^\dagger \chi_{\lambda_q}$  using the expressions for the Pauli spinors given in Appendix D-2, since it is invariant under rotations.

So, we end up with:

$$T_{\lambda_d; \lambda_q \lambda_c} = g g' \frac{t^{1/2}}{m_\pi^2 - t} \frac{\sqrt{a_+ a_-}}{4 m_d} (-1)^{\lambda_q - \frac{1}{2}} \delta_{\lambda_q \lambda_c} \delta_{\lambda_d 0} \quad (C-29)$$

It may be checked that these amplitudes obey the correct parity relations.

(ii)  $1^{-}\frac{1}{2}^{+} \rightarrow 1^{-}\frac{1}{2}^{+}$



$$\mathcal{L} = g' \phi \epsilon_{\kappa\lambda\mu\nu} P_b^\kappa P_d^\lambda A_b^\mu A_d^\nu \quad (\text{III-20})$$

$$\mathcal{L} = g \bar{\psi} \gamma_5 \psi \phi \quad (\text{III-14})$$

FIG. C-6

We again put everything as in figure C-5, but now particle b, which momentum lies on the negative z-direction, is an  $1^-$  particle, so we have to put  $\lambda_b = -s_b$ . We have :

$$\begin{aligned} T_{\lambda_b \lambda_d ; \lambda_a \lambda_c} &= \bar{v}(P_b, \lambda_b) \gamma_5 u(P_a, \lambda_a) \frac{g g'}{m_\pi^2 - t} \epsilon_{\kappa\lambda\mu\nu} P_b^\kappa P_d^\lambda \epsilon_b^{\mu*} \epsilon_d^{\nu*} = \\ &= \frac{g g'}{m_\pi^2 - t} \left[ (-1)^{\lambda_a - \frac{1}{2}} \delta_{\lambda_a \lambda_c} \frac{t^{1/2}}{2} \right] \left[ t^{1/2} \vec{P}_d \times \vec{\epsilon}_b^* \cdot \vec{\epsilon}_d^* \right] \quad (\text{C-30}) \end{aligned}$$

where we used (D-8) and (C-28). Now we can immediately see that

$$T_{00; \lambda_a \lambda_c} = T_{01; \lambda_a \lambda_c} = T_{10; \lambda_a \lambda_c} = 0 \text{ since } \vec{P}_d \text{ and } \vec{E}_{(0)} \text{ have}$$

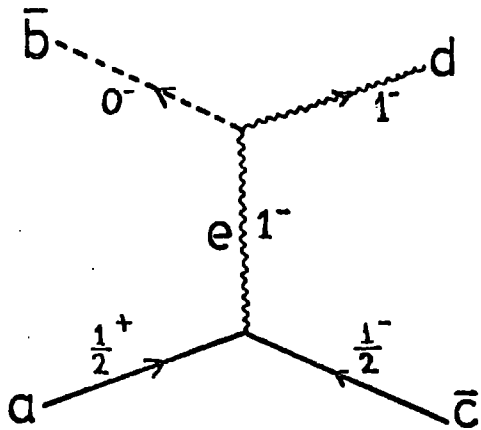
z-components only. Using (C-3) to calculate the triple product, we end up with :

$$T_{\lambda_b \lambda_d i \lambda_c \lambda_c} = gg' \frac{t}{m_\pi^2 - t} \frac{[4m_b^2 - t]^{1/2}}{4} (-1)^{\lambda_a - \frac{\lambda_d}{2}} \delta_{\lambda_a \lambda_c} \delta_{\lambda_b \lambda_d} S_{\lambda_a \lambda_1} \quad (C-31)$$

and these amplitudes obey the correct parity relations .

C-3 Vector meson exchange in  $0^{-}\frac{1}{2}^{+} \rightarrow 1^{-}\frac{1}{2}^{+}$

We calculate the t-channel Born helicity amplitudes for vector meson exchange in  $0^{-}\frac{1}{2}^{+} \rightarrow 1^{-}\frac{1}{2}^{+}$ , for two different  $\frac{1}{2}^{+}\frac{1}{2}^{+}1^{-}$  couplings, and for our standard  $1^{-}1^{-}0^{-}$  coupling :



$$\mathcal{L} = g A_e^\mu \epsilon_{\mu\nu\rho\sigma} P_b^\nu P_d^\rho A_d^\sigma \phi_b \quad (\text{III-20})$$

$$\mathcal{L} = g' \bar{\Psi} \Psi P_a^\mu A_e^\mu \quad (\text{III-21})$$

$$\mathcal{L} = g' \bar{\Psi} \gamma_\mu \Psi A_e^\mu \quad (\text{III-21a})$$

FIG. C-7

Our conventions are clarified in figure C-5; again everywhere we effectively have  $\lambda_1 = s_1$ .

(i) Use (III-21)

From (III-20) and (III-21) we get :

$$\begin{aligned} T_{\lambda_d; \lambda_a \lambda_c} &= -i g g' \bar{v}(p_c, \lambda_c) u(p_a, \lambda_a) P_a^\mu \frac{\delta_{\mu\nu} - \frac{k_\mu k_\nu}{k^2}}{m_V^2 - t} \epsilon_{\nu\rho\sigma\mu} P_b^\nu P_d^\rho \epsilon_{(\lambda_d)}^{\sigma*} = \\ &= \frac{-i g g'}{m_V^2 - t} \bar{v}(p_c, \lambda_c) u(p_a, \lambda_a) \epsilon_{\nu\rho\sigma\mu} P_b^\nu P_d^\rho P_a^\mu \epsilon_{(\lambda_d)}^{\sigma*} \quad (\text{C-32}) \end{aligned}$$

Now  $\bar{v}u$  is a scalar, and we evaluate it in a frame in which  $\vec{p}_a$  lies on the positive z-direction ( $\vec{p}_a = -\vec{p}_c$ ) so, we may use the expressions given in Appendix D-1 for the Pauli spinors. We immediately find :

$$\bar{v}_{(p_c, \lambda_c)} u_{(p_a, \lambda_a)} = -\hat{\chi}_{\lambda_c}^\dagger \vec{\sigma} \cdot \vec{p}_a \chi_{\lambda_a} = -|\vec{p}_a| \hat{\chi}_{\lambda_c}^\dagger \sigma_3 \chi_{\lambda_a} = |\vec{p}_a| \delta_{\lambda_a \lambda_c} \quad (C-33)$$

(look at (C-10) ).

Using (D-8), (C-32) now reads :

$$T_{\lambda_d \lambda_a \lambda_c} = \frac{-ig g'}{m_V^2 - t} \left( |\vec{p}_a| \delta_{\lambda_a \lambda_c} \right) t^{1/2} |\vec{p}_d| |\vec{p}_a| \sin \theta_t \epsilon_y^*(\lambda_d) \quad (C-34)$$

So we see that no helicity flip is allowed at the ac vertex, and that

$T_{0; \lambda_a \lambda_c} = 0$  since  $\vec{E}_{(0)}$  has only z-component in our frame ( but

$\epsilon_y^*(\pm 1) = +\frac{i}{\sqrt{2}}$  - (C-3) - ). Looking at (C-7,8) we end up with :

$$T_{\lambda_d \lambda_a \lambda_c} = \frac{g g'}{m_V^2 - t} \frac{\sin \theta_t}{8\sqrt{2}} (4m_a^2 - t) (q_+ q_-)^{1/2} \delta_{\lambda_a \lambda_c} \delta_{\lambda_d |1} \quad (C-35)$$

Parity relations check.

(ii) Use III-21a

Next, we couple (III-20) with (III-21a) to get :

$$\begin{aligned}
 T_{\lambda_d; \lambda_a \lambda_c} &= -ig g' \bar{v}(p_c, \lambda_c) \gamma_\mu u(p_a, \lambda_a) \frac{\delta_{\mu\nu} - \frac{k_\mu k_\nu}{m_V^2}}{m_V^2 - t} \epsilon_{\mu\nu\rho\sigma} P_b^\nu P_d^\rho \epsilon_{(\lambda_d)}^{\sigma*} = \\
 &= \frac{-ig g'}{m_V^2 - t} \epsilon_{\nu\rho\mu\sigma} P_b^\nu P_d^\rho \bar{v}(p_c, \lambda_c) \gamma_\mu u(p_a, \lambda_a) \epsilon_{(\lambda_d)}^{\sigma*} = \\
 &= \frac{-ig g'}{m_V^2 - t} t^{1/2} \vec{\epsilon}_{(\lambda_d)}^* \times \vec{P}_d \cdot \bar{v}(p_c, \lambda_c) \vec{\gamma} u(p_a, \lambda_a) = \\
 &= \frac{+ig g'}{m_V^2 - t} t^{1/2} |\vec{P}_d| \left\{ \epsilon_x^*(\lambda_d) \bar{v} \gamma_y u - \epsilon_y^*(\lambda_d) \bar{v} \gamma_x u \right\} \quad (C-36)
 \end{aligned}$$

Where we used (D-8), since  $\bar{v} \gamma_\mu u$  is a 4-vector. Again, we have  $T_{0; \lambda_a \lambda_c} = 0$ , since  $\vec{\epsilon}_{(0)}$  has only z-component, with the conventions on figure C-5; for the remaining amplitudes, we have :

$$T_{\pm 1; \lambda_a \lambda_c} = \frac{g g'}{m_V^2 - t} \frac{t^{1/2} |\vec{P}_d|}{\sqrt{2}} \bar{v}(p_c, \lambda_c) \gamma_\pm u(p_a, \lambda_a) \quad (C-37)$$

where we have used (C-3), and have defined the 3-vectors  $\vec{\alpha}_\pm = \begin{bmatrix} 1 \\ \mp i \\ 0 \end{bmatrix}$ ,

so that:

$$\gamma_\pm \equiv \gamma_x \mp i \gamma_y = \begin{bmatrix} 0 & \vec{\sigma} \cdot \vec{\alpha}_\pm \\ -\vec{\sigma} \cdot \vec{\alpha}_\pm & 0 \end{bmatrix} \quad (C-38)$$

Using the identity

$$\vec{\sigma} \cdot \vec{p} \vec{\sigma} \cdot \vec{\alpha} \vec{\sigma} \cdot \vec{p} = 2 \vec{\alpha} \cdot \vec{p} \vec{\sigma} \cdot \vec{p} - p^2 \vec{\sigma} \cdot \vec{\alpha} \quad (C-39)$$

and the expressions for  $\bar{v}, u$  in Appendix D-1 we find :

$$\bar{v}(p_c, \lambda_c) \gamma_{\pm} u(p_a, \lambda_a) = \frac{\sin \theta_t}{E_a + m_a} |\vec{p}_a|^2 \delta_{\lambda_a \lambda_c} + E_a \hat{\chi}_{\lambda_c}^{\dagger} \vec{\sigma} \cdot \vec{a}_{\pm} \chi_{\lambda_a} \quad (C-40)$$

To calculate  $\Gamma_{\lambda_a \lambda_c}^{\pm} \equiv \hat{\chi}_{\lambda_c}^{\dagger} \vec{\sigma} \cdot \vec{a}_{\pm} \chi_{\lambda_a}$ , we have to use the rotated Pauli spinors ( since this quantity is not a scalar ) :

$$\chi_{\frac{1}{2}} = \begin{bmatrix} \cos \frac{\theta}{2} \\ \sin \frac{\theta}{2} \end{bmatrix}, \quad \hat{\chi}_{\frac{1}{2}} = -\chi_{\frac{1}{2}}, \quad \chi_{-\frac{1}{2}} = \hat{\chi}_{-\frac{1}{2}} = \begin{bmatrix} -\sin \frac{\theta}{2} \\ \cos \frac{\theta}{2} \end{bmatrix} \quad (C-41)$$

and  $\vec{\sigma} \cdot \vec{a}_{\pm} = \begin{cases} \begin{bmatrix} 0 & 0 \\ 2 & 0 \\ 0 & 2 \\ 0 & 0 \end{bmatrix} \end{cases}$  ( for the definition of the angle  $\theta$ , see

figure C-5 :  $\theta = \pi - \theta_t$  ) ; we find :

$$\Gamma_{\frac{1}{2}\frac{1}{2}}^{+} = -\sin \theta, \quad \Gamma_{-\frac{1}{2}\frac{1}{2}}^{+} = 1 - \cos \theta, \quad \Gamma_{\frac{1}{2}-\frac{1}{2}}^{+} = 1 + \cos \theta, \quad \Gamma_{-\frac{1}{2}-\frac{1}{2}}^{+} = -\sin \theta \quad (C-42a)$$

$$\Gamma_{\frac{1}{2}\frac{1}{2}}^{-} = -\sin \theta, \quad \Gamma_{-\frac{1}{2}\frac{1}{2}}^{-} = -(1 - \cos \theta), \quad \Gamma_{\frac{1}{2}-\frac{1}{2}}^{-} = -(1 + \cos \theta), \quad \Gamma_{-\frac{1}{2}-\frac{1}{2}}^{-} = \sin \theta \quad (C-42b)$$

Already, these relations guarantee that our amplitudes do have the correct properties under parity transformation; putting together (C-42, 40, 37) , we end up with :

$$T_{1; \frac{1}{2}\frac{1}{2}} = \frac{-gg'}{m_v^2 - t} \frac{m_a t^{1/2} |\vec{p}_a|}{\sqrt{2}} \sin \theta_t = T_{1; -\frac{1}{2}-\frac{1}{2}} \quad (C-43a)$$

$$T_{1; -\frac{1}{2}\frac{1}{2}} = \frac{gg'}{m_v^2 - t} \frac{t |\vec{p}_a|}{\sqrt{2}} (1 + \cos \theta_t) \quad (C-43b)$$



$$T_{1; \frac{1}{2} - \frac{1}{2}} = \frac{gg'}{m_v^2 - t} \frac{t |\vec{P}_d|}{\sqrt{2}'} (1 - \cos \theta_t) \quad (\text{C-43c})$$

where :

$$|\vec{P}_d| = \frac{1}{2t} (a_+ a_-)^{1/2} \quad (\text{C-44})$$

# APPENDIX D

## SOME USEFUL RELATIONS

### D-1 Dirac spinors.

We have 58), 59) : ( $\vec{p}$  (E) is the 3-momentum (energy) of the Fermion of mass M,  $p = |\vec{p}|$ ,  $\gamma_0 = \begin{pmatrix} 1 & 0 \\ 0 & -1 \end{pmatrix}$  )

$$u(p,s) = N(p) \begin{bmatrix} \chi_s \\ \frac{\vec{\sigma} \cdot \vec{p}}{E+M} \chi_s \end{bmatrix} \quad (D-1a) \quad v(p,s) = N(p) \begin{bmatrix} \frac{\vec{\sigma} \cdot \vec{p}}{E+M} \hat{\chi}_s \\ \hat{\chi}_s \end{bmatrix} \quad (D-1b)$$

To get "up" ("down") state for a "particle", put :

$$\chi_{\frac{1}{2}} = \begin{bmatrix} 1 \\ 0 \end{bmatrix} \quad \left( \chi_{-\frac{1}{2}} = \begin{bmatrix} 0 \\ 1 \end{bmatrix} \right) ; \quad \hat{\chi}_{\frac{1}{2}} = \begin{bmatrix} 0 \\ 1 \end{bmatrix} \quad \left( \hat{\chi}_{-\frac{1}{2}} = \begin{bmatrix} -1 \\ 0 \end{bmatrix} \right) ;$$

$$\bar{u} = u^\dagger \gamma_0 =$$

$$= N(p) \left[ \chi_s^\dagger \quad -\chi_s^\dagger \frac{\vec{\sigma} \cdot \vec{p}}{E+M} \right] \quad (D-2a)$$

To get "up" ("down") state for an "antiparticle", put :

$$\bar{v} = v^\dagger \gamma_0 =$$

$$= N(p) \left[ \hat{\chi}_s^\dagger \frac{\vec{\sigma} \cdot \vec{p}}{E+M} \quad -\hat{\chi}_s^\dagger \right] \quad (D-2b)$$

Normalization

$$(\vec{\sigma} \cdot \vec{p} \vec{\sigma} \cdot \vec{p} = p^2)$$

$$\sum_s \bar{u}(p,s) u(p,s) = N_{(p)}^2 \left( \frac{4M}{E+M} \right) \quad (D-3a)$$

$$\sum_s \bar{v}(p,s) v(p,s) = - N_{(p)}^2 \left( \frac{4M}{E+M} \right) \quad (D-3b)$$

So, if we want to normalize to  $2M$ ,

$$\sum_s \bar{u}(p,s) u(p,s) = - \sum_s \bar{v}(p,s) v(p,s) = 2M \quad (D-4)$$

we have to choose :

$$N_{(p)} = \sqrt{\frac{E+M}{2}} \quad (D-5)$$

$$\left( \bar{u}u = \frac{M}{E} u^+u \right)$$

D-2 An identity

We want to evaluate

$$S = \epsilon_{\kappa\mu\lambda\nu} P_a^\kappa P_c^\mu P_b^\lambda \epsilon^\nu \quad (D-6)$$

where  $\epsilon_{\kappa\mu\lambda\nu}$  is the fully antisymmetric tensor of fourth rank,  $p_a$  and  $p_c$  are 4-momenta (and we are in the a-c centre of mass frame), and  $p_b, \epsilon$  may be any 4-vectors. First, observe that

$$\begin{aligned} \epsilon_{\kappa\mu\lambda\nu} P_a^\kappa P_c^\mu P_b^\lambda \epsilon^\nu &= \frac{1}{2} (\epsilon_{\kappa\mu\lambda\nu} - \epsilon_{\mu\kappa\lambda\nu}) P_a^\kappa P_c^\mu P_b^\lambda \epsilon^\nu = \\ &= \frac{1}{2} \epsilon_{\kappa\mu\lambda\nu} P_a^\kappa P_c^\mu P_b^\lambda \epsilon^\nu - \frac{1}{2} \epsilon_{\mu\kappa\lambda\nu} P_a^\mu P_c^\kappa P_b^\lambda \epsilon^\nu = 0 \end{aligned} \quad (D-7)$$

Now write:

$$S = \epsilon_{\kappa\mu\lambda\nu} P_a^\kappa P_c^\mu P_b^\lambda \epsilon^\nu + \epsilon_{\kappa\mu\lambda\nu} P_a^\kappa P_c^\mu P_b^\lambda \epsilon^\nu + \sum_{\lambda \neq 0, \nu \neq 0} \epsilon_{\kappa\mu\lambda\nu} P_a^\kappa P_c^\mu P_b^\lambda \epsilon^\nu = S_1 + S_2 + S'$$

hence, in  $S_1(S_2)$  neither  $\kappa$ , nor  $\mu$  can be equal to zero, so we can put

$p_a^1 = -p_c^1$ , so  $S_1 = S_2 = 0$ , according to (D-7). On the other hand, in

$S'$ , one of the  $\kappa, \mu$  must be equal to zero, so write:

$$\begin{aligned} S = S' &= \epsilon_{0\mu\lambda\nu} P_a^0 P_c^\mu P_b^\lambda \epsilon^\nu + \epsilon_{\kappa 0\lambda\nu} P_a^\kappa P_c^0 P_b^\lambda \epsilon^\nu = \\ &= E_a \left[ \epsilon_{0\mu\lambda\nu} P_c^\mu P_b^\lambda \epsilon^\nu \right] + E_c \left[ -\epsilon_{0\kappa\lambda\nu} (-P_c)^\kappa P_b^\lambda \epsilon^\nu \right] \end{aligned}$$

so:  $(E_a + E_c = t^{\frac{1}{2}})$

$$\epsilon_{\mu\nu\lambda\sigma} p_a^\mu p_c^\nu p_b^\lambda \epsilon^\sigma = \begin{cases} 0 & \text{if } a = c \\ t^{\frac{1}{2}} \vec{p}_c \times \vec{p}_b \cdot \vec{\epsilon} & \text{in a-c CM frame.} \end{cases} \quad (\text{D-8})$$

D-3 Isospin conservation in KN scattering

Consider a process of the type  $KN \rightarrow K'N$ , where  $K' = K, K^*, K^{**}, \dots$ . For the "elastic" and cex channels we have ( fig. D-1 ) :

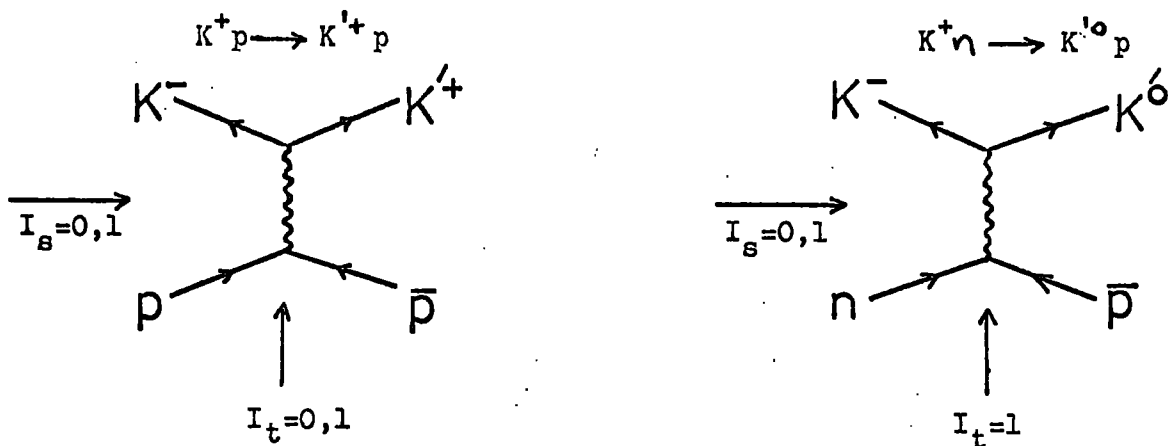


FIG. D-1

$$|p\bar{p}\rangle = 2^{-\frac{1}{2}} ( |10\rangle + |00\rangle ) \quad |n\bar{p}\rangle = |1-1\rangle \quad (D-9a)$$

$$|K^-K'^+\rangle = 2^{-\frac{1}{2}} ( |10\rangle + |00\rangle ) \quad |K^-K'^0\rangle = |1-1\rangle \quad (D-9b)$$

So, for the t-channel "elastic" and charge exchange amplitudes, we have :

$$T_{el}^{(t)} = \frac{1}{2}T^{I_t=1} + \frac{1}{2}T^{I_t=0} \quad ; \quad T_{cex}^{(t)} = T^{I_t=1} \quad (D-10)$$

Hence, for elastic  $KN \rightarrow KN$  scattering, we have :

$$T_{cex}^{(t)} = \rho - A_2 \quad (D-11a)$$

$$T_{el}^{(t)} = \frac{1}{2}(\rho - A_2) + \frac{1}{2}(\omega - f) + \frac{1}{2}P \quad (D-11b)$$

while for  $KN \rightarrow K^*N$  :

$$T_{\text{cox}}^{(t)} = \pi + \rho - A_2 \quad (\text{D-12a})$$

$$T_{\text{el}}^{(t)} = \frac{1}{2}\pi + \frac{1}{2}(\rho - A_2) + \frac{1}{2}(\omega - f) \quad (\text{D-12b})$$

For the s-channel amplitudes, we have (e.g. reference 60), page 240 ) :

$$T_{\text{cox}}^{I_s=0} = T_{\text{el}}^{(s)} - 2T_{\text{cox}}^{(s)} \quad (\text{D-13a})$$

$$T_{\text{el}}^{I_s=1} = T_{\text{el}}^{(s)} \quad (\text{D-13b})$$

TABLE D-1 Isospin decomposition of the  $K\Delta$  system:  $\frac{3}{2} \otimes \frac{1}{2} = 2+1$

	$ 1-1\rangle$	$ 10\rangle$	$ 11\rangle$	$ 2-2\rangle$	$ 2-1\rangle$	$ 20\rangle$	$ 21\rangle$	$ 22\rangle$	
$ \frac{3}{2} - \frac{3}{2}\rangle  \frac{1}{2} - \frac{1}{2}\rangle$				1					$ \Delta^-\rangle  K^0\rangle$
$ \frac{3}{2} - \frac{3}{2}\rangle  \frac{1}{2} \frac{1}{2}\rangle$	$-\frac{\sqrt{3}}{2}$				$\frac{1}{2}$				$ \Delta^-\rangle  K^+\rangle$
$ \frac{3}{2} - \frac{1}{2}\rangle  \frac{1}{2} - \frac{1}{2}\rangle$	$\frac{1}{2}$				$\frac{\sqrt{3}}{2}$				$ \Delta^0\rangle  K^0\rangle$
$ \frac{3}{2} - \frac{1}{2}\rangle  \frac{1}{2} \frac{1}{2}\rangle$		$-\frac{\sqrt{2}}{2}$				$\frac{\sqrt{2}}{2}$			$ \Delta^0\rangle  K^+\rangle$
$ \frac{3}{2} \frac{1}{2}\rangle  \frac{1}{2} - \frac{1}{2}\rangle$		$\frac{\sqrt{2}}{2}$				$\frac{\sqrt{2}}{2}$			$ \Delta^+\rangle  K^0\rangle$
$ \frac{3}{2} \frac{1}{2}\rangle  \frac{1}{2} \frac{1}{2}\rangle$			$-\frac{1}{2}$				$\frac{\sqrt{3}}{2}$		$ \Delta^+\rangle  K^+\rangle$
$ \frac{3}{2} \frac{3}{2}\rangle  \frac{1}{2} - \frac{1}{2}\rangle$			$\frac{\sqrt{3}}{2}$				$\frac{1}{2}$		$ \Delta^{++}\rangle  K^0\rangle$
$ \frac{3}{2} \frac{3}{2}\rangle  \frac{1}{2} \frac{1}{2}\rangle$								1	$ \Delta^{++}\rangle  K^+\rangle$



# APPENDIX E

## CROSSING RELATIONS AND PARTIAL WAVE AMPLITUDES FOR THE $KN \rightarrow K^*N$ AND $K^*N \rightarrow K^*N$ PROCESSES .

In this Appendix we outline the algebraic calculation required in chapter IV . We start with the t-channel amplitudes  $\Pi_0$  and  $\Pi_{11}^*$  for  $KN \rightarrow K^*N$  and  $K^*N \rightarrow K^*N$  respectively, cross them into the s-channel, construct the s-channel parity conserving partial wave amplitudes (pcpwa) , and interpret their real parts as K-matrix elements by removing their explicit threshold behaviour.

### s-channel amplitudes:

Notation :

$$( \mu = m_K, m = m_N, M = m_{K^*} )$$

$$\bar{N}'N \rightarrow K^*\bar{K} \quad ( \Pi_0 ) \quad \Longrightarrow \quad KN \rightarrow K^*N' \quad ( T_{KN';N} )$$

$$\bar{N}_2N_1 \rightarrow K_2^*\bar{K}_1^* \quad ( \Pi_{11}^* ) \quad \Longrightarrow \quad K_1^*N_1 \rightarrow K_2^*N_2 \quad ( T_{K_2N_2; K_1N_1} )$$

We shall use the sign conventions of reference 22), according to

reference 82). The crossing relation (F-9,10) of Appendix F gives :

$$T_{kN';jN} = (-1)^{1+N+N'} d_{0k}^1(\omega_k) M_{N'N}^{\frac{1}{2}} \mathcal{T}_0 \quad (\text{E-1a})$$

$$T_{k_2 N_2; k_1 N_1} = (-1)^{1+N_1+N_2} M_{N_2 N_1}^{\frac{1}{2}} M_{k_2 k_1}^1 \mathcal{T}_{11}^* \quad (\text{E-1b})$$

where the matrix  $M_{ba}^s$  is given by :

$$M_{ba}^s = d_{sb}^s(\omega_b) d_{sq}^s(\omega_q) - d_{-sb}^s(\omega_b) d_{-sq}^s(\omega_q) \quad (\text{E-2})$$

$\omega_a, \omega_b$  are the crossing angles of particles a,b with helicities a,b.

It is now straightforward (although lengthy) to find the limits of the crossing angles, (F-11) as the  $K^*N$  threshold is approached ( $q \rightarrow 0$ ,  $\sqrt{s} \rightarrow 1.83 \text{ GeV}$ ) :  $(x = \cos \theta_s)$

$$\cos \omega_N = \frac{(s+m^2-\mu^2)t - 2m^2(M^2-\mu^2)}{2\sqrt{s}p\sqrt{-t} (4m^2-t)^{1/2}} \longrightarrow -1 \quad (\text{E-3a})$$

$$\cos \omega_{N'} = \frac{-(s+m^2-M^2)t - 2m^2(M^2-\mu^2)}{2\sqrt{s}q\sqrt{-t} (4m^2-t)^{1/2}} \longrightarrow -x \quad (\text{E-3b})$$

$$\cos \omega_K = \frac{(s+M^2-m^2)(t+M^2-\mu^2) - 2M^2(M^2-\mu^2)}{2\sqrt{s}q\sqrt{q_+q_-}} \longrightarrow +x \quad (\text{E-3c})$$

$$\sin \omega_N \longrightarrow 0, \quad \sin \omega_{N'} \longrightarrow -\sqrt{1-x^2}, \quad \sin \omega_K \longrightarrow +\sqrt{1-x^2} \quad (\text{E-3d})$$

$$\cos \omega_{K_1} = -\cos \omega_{K_2} = \frac{(s+M^2-m^2)(-t)^{1/2}}{2\sqrt{s}q(4M^2-t)^{1/2}} \longrightarrow +\sqrt{\frac{1-x}{2}} \quad (\text{E-4a})$$

$$\cos \omega_{N_1} = -\cos \omega_{N_2} = -\frac{(s+m^2-M^2)(-t)^{1/2}}{2\sqrt{s}q(4m^2-t)^{1/2}} \longrightarrow -\sqrt{\frac{1-x}{2}} \quad (\text{E-4b})$$

$$\sin \omega_{N_1} = \sin \omega_{N_2} \longrightarrow -\sqrt{\frac{1+x}{2}} \quad (\text{E-4c})$$

$$\sin \omega_{K_1} = \sin \omega_{K_2} \longrightarrow +\sqrt{\frac{1+x}{2}} \quad (\text{E-4d})$$

Using (E-4), from the crossing relations (E-1,2) we find:

$$T_{0\frac{1}{2};\frac{1}{2}} = \cos \omega_K \cos \frac{\omega_N + \omega_{N'}}{2} \Pi_0 \longrightarrow x \sqrt{\frac{1+x}{2}} \Pi_0 \quad (\text{E-5a})$$

$$T_{0\frac{1}{2};-\frac{1}{2}} = \cos \omega_K \sin \frac{\omega_N + \omega_{N'}}{2} \Pi_0 \longrightarrow x \sqrt{\frac{1-x}{2}} \Pi_0 \quad (\text{E-5b})$$

$$T_{\pm 1\frac{1}{2};\frac{1}{2}} = \pm \frac{\sin \omega_K}{\sqrt{2}} \cos \frac{\omega_N + \omega_{N'}}{2} \Pi_0 \longrightarrow \pm \sqrt{\frac{1-x^2}{2}} \sqrt{\frac{1+x}{2}} \Pi_0 \quad (\text{E-5c})$$

$$T_{\pm 1\frac{1}{2};-\frac{1}{2}} = \pm \frac{\sin \omega_K}{\sqrt{2}} \sin \frac{\omega_N + \omega_{N'}}{2} \Pi_0 \longrightarrow \pm \sqrt{\frac{1-x^2}{2}} \sqrt{\frac{1-x}{2}} \Pi_0 \quad (\text{E-5d})$$

$$T_{\pm 1\frac{1}{2};0-\frac{1}{2}} = -\frac{\sin \omega_{K_1}}{\sqrt{2}} \sin \frac{\omega_{N_1} + \omega_{N_2}}{2} \Pi_{11}^* \longrightarrow \frac{1}{\sqrt{2}} \sqrt{\frac{1+x}{2}} \Pi_{11}^* \quad (\text{E-6a})$$

$$T_{\pm 1/2; \mp 1 - 1/2} = \pm \cos \omega_{k_2} \sin \eta \frac{\omega_{N_1} + \omega_{N_2}}{2} \Pi_{11}^* \rightarrow \pm \sqrt{\frac{1-x}{2}} \Pi_{11}^* \quad (\text{E-6b})$$

All other amplitudes for  $K^*N \rightarrow K^*N$  vanish (only nucleon flip amplitudes survive).

We next expand  $\Pi_0$  and  $\Pi_{11}^*$  amplitudes to lowest order in  $q$  and take their real parts ( $\Pi_{11}^*$  is already real to first order in  $q$ ):

$$\text{Re} \Pi_0 = A + B p q x \quad (\text{E-7a})$$

$$\Pi_{11}^* = C q^2 (1-x) \quad (\text{E-7b})$$

where :

$$A = \frac{-3\beta S_0^{\alpha_0 \alpha'}}{(m+M)^2 \alpha_0 \alpha'} \frac{1 + \cos \pi \alpha_0 \alpha'}{2} \quad , \quad \alpha_0 = m^2 \frac{M^2 - \mu^2}{M+M} \quad (\text{E-8})$$

$$B = \frac{-3\beta S_0^{\alpha_0 \alpha'}}{(m+M)^2 \alpha_0 \alpha'} \alpha' \left[ \pi \sin \pi \alpha_0 \alpha' + 2(1 + \cos \pi \alpha_0 \alpha') \right] g \frac{m+M}{\sqrt{S_0}} \quad (\text{E-9})$$

$$C = \frac{-24\beta}{M^2 - \mu^2} \quad (\text{E-10})$$

pcpwa as K-matrix elements

We next partial wave project - (F-18) - amplitudes (E-5),

and find the corresponding pcwa from (F-23) which for our processes reads :

$$T_{KN';N}^{J\pm} = T_{KN';N}^J \pm (-1)^{J+\frac{1}{2}} T_{KN';-N}^J \quad (\text{E-11a})$$

$$T_{K_2N_2;K_1N_1}^{J\pm} = T_{K_2N_2;K_1N_1}^J \pm (-1)^{J-\frac{1}{2}} T_{K_2N_2;-K_1-N_1}^J \quad (\text{E-11b})$$

We interpret these pcwa as K-matrix elements after removing their explicit threshold factors :

$$\text{Re}T_0^{\frac{1}{2}\pm} = \text{Re}\left[T_{0\frac{1}{2};\frac{1}{2}}^{\frac{1}{2}} \mp T_{0\frac{1}{2};-\frac{1}{2}}^{\frac{1}{2}}\right] = \begin{cases} \frac{B}{24\eta(m+M)} \rho q & ; k_0^{\frac{1}{2}+} = \frac{B}{24\eta(m+M)} \quad (\text{E-12a}) \\ \frac{A}{24\eta(m+M)} & ; k_0^{\frac{1}{2}-} = \frac{A}{24\eta(m+M)} \quad (\text{E-12b}) \end{cases}$$

$$\text{Re}T_1^{\frac{1}{2}\pm} = \text{Re}\left[T_{1\frac{1}{2};\frac{1}{2}}^{\frac{1}{2}} \mp T_{1\frac{1}{2};-\frac{1}{2}}^{\frac{1}{2}}\right] = \begin{cases} 0 & ; k_1^{\frac{1}{2}+} = 0 \quad (\text{E-12c}) \\ \frac{A}{12\sqrt{2}\eta(m+M)} & ; k_1^{\frac{1}{2}-} = \frac{A}{12\sqrt{2}\eta(m+M)} \quad (\text{E-12d}) \end{cases}$$

$$T_{11}^{\frac{1}{2}\pm} = \pm T_{1\frac{1}{2};-1-\frac{1}{2}}^{\frac{1}{2}} = \pm \frac{C}{12\eta(m+M)} q^2 ; \begin{cases} k_{11}^{\frac{1}{2}+} = \frac{C}{12\eta(m+M)} \quad (\text{E-13a}) \\ k_{11}^{\frac{1}{2}-} = 0 \quad (\text{E-13b}) \end{cases}$$

$$T_{10}^{\frac{1}{2}\pm} = T_{01}^{\frac{1}{2}\pm} = \pm T_{1\frac{1}{2};0-\frac{1}{2}}^{\frac{1}{2}} = \pm \frac{C}{24\sqrt{2}\eta(m+M)} q^2 ; \begin{cases} k_{10}^{\frac{1}{2}+} = k_{01}^{\frac{1}{2}+} = \frac{C}{24\sqrt{2}\eta(m+M)} \quad (\text{E-13c}) \\ k_{10}^{\frac{1}{2}-} = k_{01}^{\frac{1}{2}-} = 0 \quad (\text{E-13d}) \end{cases}$$

$$T_{00}^{\frac{1}{2}\pm} = 0 \quad ; \quad k_{00}^{\frac{1}{2}\pm} = 0 \quad (\text{E-13e})$$

$$\text{Re}T_{-1}^{\frac{3}{2}\pm} = \text{Re}\left[T_{-1\frac{1}{2}j\frac{1}{2}}^{\frac{3}{2}} \pm T_{-1\frac{1}{2}j-\frac{1}{2}}^{\frac{3}{2}}\right] = \begin{cases} \frac{BPq}{120\sqrt{6}\pi(m+M)} & ; \quad k_{-1}^{\frac{3}{2}+} = \frac{B}{120\sqrt{6}\pi(m+M)} \quad (\text{E-14a}) \\ \frac{A}{24\sqrt{6}\pi(m+M)} & ; \quad k_{-1}^{\frac{3}{2}-} = \frac{A}{24\sqrt{6}\pi(m+M)} \quad (\text{E-14b}) \end{cases}$$

$$\text{Re}T_0^{\frac{3}{2}\pm} = \text{Re}\left[T_{0\frac{1}{2}j\frac{1}{2}}^{\frac{3}{2}} \pm T_{0\frac{1}{2}j-\frac{1}{2}}^{\frac{3}{2}}\right] = \begin{cases} \frac{BPq}{60\pi(m+M)} & ; \quad k_{0}^{\frac{3}{2}+} = \frac{B}{60\pi(m+M)} \quad (\text{E-14c}) \\ \frac{A}{24\pi(m+M)} & ; \quad k_{0}^{\frac{3}{2}-} = \frac{A}{24\pi(m+M)} \quad (\text{E-14d}) \end{cases}$$

$$\text{Re}T_1^{\frac{3}{2}\pm} = \text{Re}\left[T_{1\frac{1}{2}j\frac{1}{2}}^{\frac{3}{2}} \pm T_{1\frac{1}{2}j-\frac{1}{2}}^{\frac{3}{2}}\right] = \begin{cases} \frac{BPq}{40\sqrt{2}\pi(m+M)} & ; \quad k_{1}^{\frac{3}{2}+} = \frac{B}{40\sqrt{2}\pi(m+M)} \quad (\text{E-14e}) \\ \frac{A}{24\sqrt{2}\pi(m+M)} & ; \quad k_{1}^{\frac{3}{2}-} = \frac{A}{24\sqrt{2}\pi(m+M)} \quad (\text{E-14f}) \end{cases}$$

$$T_{11}^{\frac{3}{2}\pm} = \mp T_{1\frac{1}{2}j-1-\frac{1}{2}}^{\frac{3}{2}} = \pm \frac{Cq^2}{48\pi(m+M)} \quad ; \quad \begin{cases} k_{11}^{\frac{3}{2}+} = \frac{C}{48\pi(m+M)} \quad (\text{E-15a}) \\ k_{11}^{\frac{3}{2}-} = 0 \quad (\text{E-15b}) \end{cases}$$

$$T_{10}^{\frac{3}{2}\pm} = T_{01}^{\frac{3}{2}\pm} = \mp T_{1\frac{1}{2}j0-\frac{1}{2}}^{\frac{3}{2}} = \pm \frac{Cq^2}{48\sqrt{2}\pi(m+M)} \quad ; \quad \begin{cases} k_{10}^{\frac{3}{2}+} = k_{01}^{\frac{3}{2}+} = \frac{C}{48\sqrt{2}\pi(m+M)} \quad (\text{E-15c}) \\ k_{10}^{\frac{3}{2}-} = k_{01}^{\frac{3}{2}-} = 0 \quad (\text{E-15d}) \end{cases}$$

$$T_{-10}^{\frac{3}{2}\pm} = T_{0-1}^{\frac{3}{2}\pm} = \mp T_{H\frac{1}{2}; 0-\frac{1}{2}}^{\frac{3}{2}} = \mp \frac{Cg^2}{48\sqrt{6}(\eta+\eta)} ; \begin{cases} k_{-10}^{\frac{3}{2}\pm} = k_{0-1}^{\frac{3}{2}\pm} = \frac{-C}{48\sqrt{6}\eta(\eta+\eta)} & \text{(E-15e)} \\ k_{-10}^{\frac{3}{2}\pm} = k_{0-1}^{\frac{3}{2}\pm} = 0 & \text{(E-15f)} \end{cases}$$

$$T_{-1-1}^{\frac{3}{2}\pm} = \mp T_{-1\frac{1}{2}; 1-\frac{1}{2}}^{\frac{3}{2}} = \mp \frac{Cg^2}{16\eta(\eta+\eta)} ; \begin{cases} k_{-1-1}^{\frac{3}{2}\pm} = \frac{-C}{16\eta(\eta+\eta)} & \text{(E-15g)} \\ k_{-1-1}^{\frac{3}{2}\pm} = 0 & \text{(E-15h)} \end{cases}$$

To finish with this tedious listing of formulas, we write down the full K-matrices for  $J^P = \frac{1}{2}^{\pm}, \frac{3}{2}^{\pm}$ :

$$K_{\frac{1}{2}^{\pm}} = \begin{bmatrix} K_{\frac{1}{2}^{\pm}} & K_{0^{\pm}} & K_{1^{\pm}} \\ K_{0^{\pm}} & K_{\frac{1}{2}^{\pm}} & K_{\frac{1}{2}^{\pm}} \\ K_{1^{\pm}} & K_{\frac{1}{2}^{\pm}} & K_{\frac{1}{2}^{\pm}} \end{bmatrix}$$

$$K_{\frac{3}{2}^{\pm}} = \begin{bmatrix} K_{\frac{3}{2}^{\pm}} & K_{-1^{\pm}} & K_{0^{\pm}} & K_{1^{\pm}} \\ K_{-1^{\pm}} & K_{\frac{3}{2}^{\pm}} & K_{-1^{\pm}} & K_{\frac{3}{2}^{\pm}} \\ K_{0^{\pm}} & K_{\frac{3}{2}^{\pm}} & K_{00^{\pm}} & K_{01^{\pm}} \\ K_{1^{\pm}} & K_{\frac{3}{2}^{\pm}} & K_{10^{\pm}} & K_{\frac{3}{2}^{\pm}} \end{bmatrix}$$

# APPENDIX F

## NOTATION AND NORMALIZATION CONVENTIONS

With reference to figure F-1, where each particle of mass  $m_a$ , etc. carries 4-momentum  $p_a$ , etc, we define the usual Mandelstam invariants by :

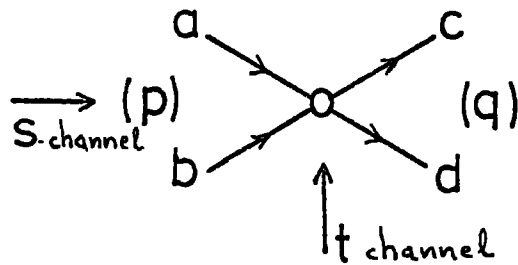


FIG. F-1

$$s = (p_a + p_b)^2, \quad t = (p_a - p_c)^2, \quad u = (p_a - p_d)^2 \quad (F-1)$$

Conservation of 4-momentum,

$$p_a + p_b = p_c + p_d \quad (F-2)$$

requires that these are related by :

$$s + t + u = \sum_a m_a^2 \quad (F-3)$$

The s-channel centre of mass 3-momentum and scattering angle are given by :



$$P_{sab}^2 = \frac{1}{4s} \left[ s - (m_a + m_b)^2 \right] \left[ s - (m_a - m_b)^2 \right] \quad (F-4)$$

$$\cos \theta_s = \frac{s^2 + s \left( 2t - \sum_a m_a^2 \right) + (m_a^2 - m_b^2)(m_c^2 - m_d^2)}{4s P_{sab} P_{scd}} \quad (F-5)$$

(similarly for all other particles/channels). We usually put :

$$p = P_{sab} , q = P_{scd} \quad (F-6)$$

The physical regions for scattering are bounded by  $-1 \leq \cos \theta_s \leq +1$  etc , and the boundary is given by the equation : (  $\Phi(s,t)$  is the Kibble function )

$$\begin{aligned} \Phi(s,t) = & stu - s(m_a^2 - m_c^2)(m_b^2 - m_d^2) - t(m_a^2 - m_b^2)(m_c^2 - m_d^2) - \\ & - (m_a^2 m_d^2 - m_b^2 m_c^2)(m_a^2 + m_d^2 - m_b^2 - m_c^2) \equiv 0 \quad (F-7) \end{aligned}$$

We denote an s(t) -channel centre of mass helicity amplitude by :

$$T_{cd;ab}^{(s)} = \langle cd | T | ab \rangle \quad (F-8a)$$

$$T_{c\bar{a};d\bar{b}}^{(t)} = \langle c\bar{a} | T | d\bar{b} \rangle \quad (F-8b)$$

where the T-matrix is defined by (I-3), and  $|ab\rangle$ , etc is the usual Jacob and Wick helicity state. Lorentz invariance requires these amplitudes to be functions of the Mandelstam invariants only. Crossing symmetry requires that s-channel and t-channel amplitudes should be one and the same analytic function of their variables, when the helicities are measured from the same frame. The crossing

matrix rotates the helicities from e.g. the t-channel centre of mass to the s-channel centre of mass, so we have <sup>82)</sup> :

$$T_{cd;ab}^{(s)}(s,t) = \sum_{a',b',c',d'} M_{cd;ab||c'a';d'b'} T_{c'a';d'b'}^{(t)}(s,t) \quad (F-9)$$

where for the crossing matrix M we have :

$$M_{cd;ab||c'a';d'b'} = (-1)^{b'-b+d'-d} d_{a_q}^{s_a}(\omega_a) d_{b_b}^{s_b}(\omega_b) d_{c_c}^{s_c}(\omega_c) d_{d_d}^{s_d}(\omega_d) \quad (F-10)$$

where  $s_a$ , etc are the spins of particles a, etc, and the crossing angles  $\omega_a$ , etc are given by :

$$\cos \omega_a = \frac{-(s+m_a^2-m_b^2)(t+m_a^2-m_c^2) - 2m_a^2(m_b^2-m_d^2-m_q^2+m_c^2)}{4\sqrt{s t} P_{sab} P_{tac}} \quad (F-11)$$

etc (by cyclic permutation) .

Throughout this work we normalize our amplitudes according to reference 2); also, our unit is always the 1GeV ( unless otherwise is explicitly stated ) . The dif. cross-section, and density matrix elements for the decay of particle "4" (in the t-channel helicity frame ) are given by :

$$\frac{d\sigma}{dt} = \frac{1}{64\pi p^2 s} \frac{1}{(2s_a+1)(2s_b+1)} N \quad (F-12)$$

$$N \rho_{mm'} = \sum_{a,b,c} T_{bm;ac}^{(t)} T_{bm';ac}^{(t)*} \quad (F-13)$$

where, because of the orthogonality of the crossing matrix (F-10), we have :

$$N = \sum_{a,b,c,d} |T_{cd;ab}^{(s)}(s,t)|^2 = \sum_{a,b,c,d} |T_{ca;db}^{(t)}(s,t)|^2 \quad (F-14)$$

The total cross-section for the process  $ab \rightarrow X$  (anything, at sufficiently low energies, in most of the cases, it may be well approximated by quasi-two particle states) is defined by :

$$\sigma_T(ab) = \sum_X \int dt \frac{d\sigma(ab \rightarrow X)}{dt} \quad (F-15)$$

and the unitarity relation (I-2), leads to the optical theorem, which in our normalization reads :

$$\sigma_T(ab) = \frac{1}{(2s_a+1)(2s_b+1)} \cdot \frac{1}{2qs^{1/2}} \cdot \sum_{a,b} \Im T_{ab;ab}(s,t=0) \quad (F-16)$$

The scattering amplitude may be expressed in terms of a partial wave series :

$$T_{cd;ab}^{(s)}(s,t) = 8\pi s^{1/2} \sum_J (2J+1) d_{\lambda\lambda'}^J(x) T_{cd;ab}^J(s) \quad (F-17)$$

$$(x = \cos \theta_s, \lambda = a-b \quad \lambda' = c-d)$$

where  $J$  is the total angular momentum, and since it is conserved, the partial wave amplitudes (p.w.a.)

$$T_{cd;ab}^J(s) = \frac{1}{16\pi s^{1/2}} \int_{-1}^{+1} dx d_{\lambda\lambda'}^J(x) T_{cd;ab}^{(s)}(s,t) \quad (F-18)$$

express the probability for scattering with a particular angular momentum J .

In terms of p.w.a. , the unitarity relation (I-2) reads :

$$\Im T_{cd;ab}^J = \sum_{i \equiv xy} \rho_i \sum_{x,y} T_{xy;ab}^J T_{xy;cd}^{J*} \quad (F-19)$$

(only two- particle intermediate states have been taken into account in the probability sum implied by (I-2) )

The optical theorem (F-16) may now be written as

$$\sigma_T(ab) = \frac{1}{(2s_a+1)(2s_b+1)} \frac{4\pi}{P} \sum_J (2J+1) \sum_{a,b} \Im T_{ab;ab}^J \quad (F-20)$$

We may make our amplitudes identically unitary, by parametrizing the p.w.a. as :

$$T^J = \frac{1}{P} \frac{e^{2i\delta_J} - 1}{2i} \quad (F-21)$$

or more generally :

$$\text{( defn. of } K^J \text{ matrix ) } \quad T^J = K^J (1 - i\rho K^J)^{-1} \quad (F-22)$$

where  $\delta_J$  (  $K^J$  ) are real, holomorphic functions of s.  $\rho = \begin{pmatrix} P \\ \rho \end{pmatrix}$

is the diagonal matrix formed by the intermediate two-particle channels momenta.

The partial wave amplitudes defined by (F-18), do not connect states of definite parity. We may define the parity conserving partial wave amplitudes (pcpwa) as linear combinations of p.w.a. (  $\eta_a$  etc. is the intrinsic parity of particle a etc. ) :

$$T_{cd;ab}^{J\pm} = T_{cd;ab}^J \pm \eta_a \eta_b (-1)^{J-S_a-S_b} T_{cd;-a-b}^J \quad (\text{F-23})$$

These amplitudes connect states of definite angular momentum and parity. It is an immediate consequence of analyticity that at the ab and cd thresholds ( $p \rightarrow 0$  and  $q \rightarrow 0$  respectively), the pcwa should behave like :

$$T_{cd;ab}^{J\pm} \propto p^{\ell} q^{\ell'} \quad (\text{F-24})$$

where  $\ell$  and  $\ell'$  are the lowest orbital ang. momenta, consistent with parity conservation, possible in the ab and cd channels respectively.

## REFERENCES

- 1) J.H. Christenson et al., Phys. Rev. Letters 13 , 138 (1964).
- 2) H. Pilkuhn, The Interactions of Hadrons, (North-Holland Publ. Co., Amsterdam, 1967).
- 3) T.D. Lee and L. Wolfenstein, Phys. Rev. 138, B1490 (1965).
- 4) L.B. Okun, Soviet J. Nucl. Phys. 1 , 670 (1965)  
J. Prentki and M. Veltman, Phys. Letters 15 (1965) 88.
- 5) J. Bernstein, G. Feinberg, and T.D. Lee, Phys. Rev. 139 , B1650 (1965).  
S. Barshay, Phys. Letters 17 , (1965) 78.
- 6) e.g. G. Goldhaber, in Experimental meson Spectroscopy edited by C. Baltay and A.H. Rosenfeld (Columbia Univ. press, New York, 1970) p. 59.
- 7) R. Friedberg, T.D. Lee, and M. Schwartz, unpublished.
- 8) T.D. Lee, Phys. Rev. 139 , B1415 (1965).
- 9) M. Gormley et al., Phys. Rev. Letters 21 , 402 (1968).
- 10) M.R. Jane et al., RHEL preprint RPP/H/123 (1973). Also,  
J.G. Layter et al., Phys. Rev. Letters 29 , 316 (1972).
- 11) H. Yuta and S. Okubo, Phys. Rev. Letters 21 , 781 (1968).
- 12) M. Gormley et al., Phys. Rev. Letters 22 , 108 (1969).
- 13) K. Taggart, Phys. Rev. D2 , 1960 (1970).
- 14) G. Goldhaber, in the Proc. of the workshop on Particle

Physics at intermediate energies, Ed. R.D. Field Jr, UCRL 20655 (June 1971).

- 15) G.S. Abrams et al., Phys. Rev. D4 , 653 (1971).
- 16) S.M. Flatté et al., Phys. Rev. 145 , 1050 (1966).
- 17) G.S. Abrams, G. Goldhaber, and B.H. Hall, Phys. Rev. D4 , 647 (1971).
- 18) W.A. Simmons and S.F. Tuan, Phys. Rev. D4 , 663 (1971).
- 19) A.S. Goldhaber, G.C. Fox, and C. Quigg, Phys. Letters 30B (1969) 249.
- 20) H.I. Miettinen, Private communication.
- 21) G.C. Wick, Annals of Phys. 18 , 65 (1962).
- 22) A.D. Martin and T.D. Spearman, Elementary Particle Theory, (North-Holland Publ. Co., Amsterdam, 1970).
- 23) G.A. Ringland, Private communication.
- 24) G.S. Abrams et al., Phys. Rev. Letters 25 , 617 (1970).
- 25) P.L. Bastien et al., Phys. Rev. D3 , 2047 (1971).
- 26) J.P. Ader, M. Capdeville, G. Cohen-Tannoudji and Ph. Salin, Nuovo Cimento A56 , 952 (1968).
- 27) R.D. Mathews, Nucl. Phys. B11 , (1969) 339.
- 28) e.g. reference 2), page 142 .
- 29) E.L. Berger, Private communication.

- 30) D. Morgan, RHEL preprint RPP/T/27 , 1972 .
- 31) H. Pilkuhn et al., Nucl. Phys. B65 (1973) 460.
- 32) S.D.P. Vlassopoulos , Durham preprint (May 1974).
- 33) M. Kramer and U. Maor, Nucl. Phys. B13 (1969) 651.
- 34) G.V. Dass and C.D. Froggat, Nucl. Phys. B10 (1969) 151.  
M. Markytan, Nucl. Phys. B10 (1969) 193 .
- 35) P.D.B. Collins, Phys. Reports 10 (1971) 103.
- 36) L. Stodolsky and J.J. Sakurai, Phys. Rev. Letters 11 ,  
90 (1963).  
L. Stodolsky, Phys. Rev. 134 , B1099 (1964).
- 37) D. Griffiths and R.J. Jabbur, Nucl. Phys. B11 (1969) 7 .
- 38) G.S. Abrams and U. Maor , Phys. Rev. Letters 25 , 621 (1970).
- 39) A.H. Mueller, Phys. Rev. D2 , 2963 (1970).
- 40) S.C. Loken et al., Phys. Rev. D6 , 2346 (1972).
- 41) A. Berthon et al., CERN preprint, CERN/D.Ph.II/PHYS 73-7 .
- 42) C. Fu et al., Nucl. Phys. B28 (1971) 528.
- 43) D.V. Nanopoulos and S.D.P. Vlassopoulos , CERN preprint,  
TH-1842 (February 1974), to be published in Nuovo Cimento Letters.
- 44) R. Barloutaud et al., Phys. Letters 38B (1972) 257.
- 45) J.C. Berlinghieri et al., Nucl. Phys. 8B (1968) 333 .
- 46) V.G. Lind et al., Nucl. Phys. B14 (1969) 1.



- 47) K.W.J. Barnham et al., Nucl. Phys. B28 (1971) 171.
- 48) D.D. Carmony et al., Nucl. Phys. B12 (1969) 9 .
- 49) W. De Baere et al., Nuovo Cimento A51 (1967) 401 .
- 50) J.M. Brunet et al., Nucl. Phys. B37 (1971) 114 .
- 51) Y.W. Kang, Phys. Rev. 176 (1968) 1587 .
- 52) C. Michael, Nucl. Phys. B57 (1973) 292 .
- 53) R.L. Eisner, CERN preprint, CERN/D.PH.II/PHYS. 73-9 (1973).
- 54) A. Firestone et al., Phys. Rev. Letters 25 , 958 (1970).
- 55) P. Astbury et al., Phys. Letters 23 (1966) 396.
- 56) K.J. Folley et al., Phys. Rev. Letters 11 , 503 (1963).
- 57) M. Borghini et al., Phys. Letters 31B (1970) 405.  
M. Borghini et al., Phys. Letters 36B (1971) 497.
- 58) J.D. Bjorken and S.D. Drell, "Relativistic Quantum Mechanics",  
Vol. 1, Mc Graw-Hill, (1964).
- 59) J. Bernstein, "Elementary Particles and their currents" ,  
W.H. Freeman and Co., (1968).
- 60) W.S.C. Williams, "An Introduction to Elementary Particles",  
Academic Press, (1971).
- 61) D.G. Sutherland, Private Communication.
- 62) R.C. Johnson and S.D.P. Vlassopoulos, CERN preprint TH-1861,  
(April 1974), to appear in Phys. Letters.

- 63) J.D. Dowell, "The Search for the  $Z^*$ 's" , in the Proceedings of the XVI International Conference on High Energy Physics, Chicago, Batavia (1972).
- 64) Particle Data Group, Rev. Mod. Phys. 45 No.2, S1, (1973) page 134.
- 65) Particle Data Group, "A compilation of  $K^+N$  reactions" , UCRL-20000  $K^+N$  (September 1969).
- 66) R. Aaron, R.D. Amado, and R.R. Silbar, Phys. Rev. Letters 26 , 407 (1971).
- 67) R. Aaron, M. Rich, W.L. Hogan and Y.N. Srivastava, Phys. Rev. D7 , 1401 (1973).
- 68) R. Aaron and R.D. Amado, Phys. Rev. Letters 27 , 1316 (1971).
- 69) N. Hedegaard-Jensen, H. Nielsen and G.C. Oades, Phys. Letters 46B (1973) 385.
- 70) G. Giacomelli et al., (BGRT Collaboration), "Phase shift analysis of  $K^+N \rightarrow KN$  scattering in the  $I = 0$  state up to 1.5 GeV/c " , CERN preprint (August 1973), to appear in Nuclear Physics.
- 71) B.C. Wilson et al. (BGRT Collaboration), Nucl. Phys. B42 (1972) 445.
- 72) H. Harari, Phys. Rev. Letters 20 , 1395 (1968) .  
P.G.O. Freund, Phys. Rev. Letters 20 , 235 (1968).
- 73) H. Harari, Lectures at the Scottish Universities Summer School in Physics (1973), to be published.
- 74) C. Lovelace, in F. Loeffler and E. Malamud (Eds.)

"Proceedings of the Conference on  $\pi\pi$  and  $K\pi$  interactions"  
(May 1969), Argonne-Purdue Preprint, unpublished.

- 75) C. Lovelace, Nucl. Phys. B12 (1969) 253.
- 76) F. Schrempp, Phys. Letters 29B (1969) 598.  
F. Schrempp, Nucl. Phys. B41 (1972) 557.
- 77) R. Dolen, D. Horn, and C. Schmid, Phys. Rev. 166,  
1768 (1968).
- 78) W. Drechsler, Phys. Rev. D2, 364 (1970).
- 79) A.W. Reid and D.G. Sutherland, "Models for the Pomeron  
and low energy  $K^+p$  scattering", Glasgow Preprint (June 1973),  
unpublished.
- 80) D. Cline, J. Matos and D.D. Reeder, Phys. Rev. Letters  
23, 1318 (1969).
- 81) B. Sakita and K.C. Wali, Phys. Rev. 139, B1355 (1965).
- 82) T.L. Trueman and G.C. Wick, Ann. Phys. 26, 332 (1964).

